OFFICE OF CIVILIAN RADIOACTIVE WASTE MANAGEMENT

1. QA: QA

ANALYSIS/MODEL COVER SHEET

Complete Only Applicable Items

2. ☒ Analysis — Check all that apply	3. ☒ Model — Check all that apply
Type of Analysis: ☐ Engineering; ☒ Performance Assessment; ☐ Scientific	Type of Model: ☒ Conceptual Model; ☒ Abstraction Model; ☒ Mathematical Model; ☐ System Model; ☒ Process Model
Intended Use of Analysis: ☐ Input to Calculation; ☒ Input to another Analysis or Model; ☐ Input to Technical Document; ☐ Input to other Technical Products	Intended Use of Model: ☐ Input to Calculation; ☒ Input to another Model or Analysis; ☐ Input to Technical Document; ☐ Input to other Technical Products
Describe use: Input to EBS Physical and Chemical Environment Model	Describe use: Input to EBS Physical and Chemical Environment Model

4. Title:

In-Drift Precipitates/Salts Analysis

5. Document Identifier (including Rev. No. and Change No., if applicable):

ANL-EBS-MD-000045 Rev. 00

6. Total Attachments:	7. Attachment Numbers - No. of Pages in Each:
1	I-21

	Printed Name	Signature	Date
8. Originator	Paul Mariner	Robert MacKinnon for PM	4/14/00
9. Checker	Pat Brady	Robert MacKinnon for PB	4/14/00
10. Lead/Supervisor	James Nowak	Robert MacKinnon for JN	4/14/00
11. Responsible Manager	Robert MacKinnon	Robert MacKinnon for	4/14/00

12. Remarks:

This analysis produces a model that predicts the evaporative evolution of average J-13 well water and its precipitates as a function of relative humidity, temperature, fugacity of carbon dioxide, incoming seepage rate, and relative evaporation rate. The model uses a thermodynamic database developed within the analysis that is TBV. However, it produces results of acceptable accuracy for pH, ionic strength, and Cl molality when compared to results of laboratory evaporation experiments.

Application of this model to the drift environment for a given time period may require updated values for inputs. While the results contained herein can be applied to a wide range of temperatures, carbon dioxide fugacities, and relative evaporation rates, updated calculations would need to be performed for applications having different compositions of incoming seepage.

This analysis also presents a model developed to predict the composition of condensed water vapor underneath the drip shield. This model produces lookup tables that are a function of temperature and carbon dioxide fugacity.

WM-11 NF03
Add: Manny Comar
Paper Copy

INFORMATION COPY
LAS VEGAS DOCUMENT CONTROL

Enclosure 1

OFFICE OF CIVILIAN RADIOACTIVE WASTE MANAGEMENT
ANALYSIS/MODEL REVISION RECORD

Complete Only Applicable Items

2. Analysis or Model Title:

In-Drift Precipitates/Salts Analysis

3. Document Identifier (including Rev. No. and Change No., if applicable):

ANL-EBS-MD-000045 REV 00

4. Revision/Change No.	5. Description of Revision/Change
00	Initial Issue

DISCLAIMER

This contractor document was prepared for the U.S. Department of Energy (DOE), but has not undergone programmatic, policy, or publication review, and is provided for information only. The document provides preliminary information that may change based on new information or analysis, and represents a conservative treatment of parameters and assumptions to be used specifically for Total System Performance Assessment analyses. The document is a preliminary lower level contractor document and is not intended for publication or wide distribution.

Although this document has undergone technical reviews at the contractor organization, it has not undergone a DOE policy review. Therefore, the views and opinions of authors expressed may not state or reflect those of the DOE. However, in the interest of the rapid transfer of information, we are providing this document for your information per your request.

CONTENTS

Page

1. PURPOSE 10

2. QUALITY ASSURANCE 10

3. COMPUTER SOFTWARE AND MODEL USAGE 11
   3.1 COMPUTER SOFTWARE 11
   3.2 MODELS 11

4. INPUTS 11
   4.1 DATA AND PARAMETERS 11
      4.1.1 Thermodynamic Constants and Salt Properties 11
      4.1.2 Experimental Data Used for Model Validation 12
      4.1.3 Model Input Parameters 16
   4.2 CRITERIA 18
      4.2.1 NRC Evolution of Near Field Environment IRSR Criteria 18
         4.2.1.1 Data and Model Justification Acceptance Criteria 19
         4.2.1.2 Data Uncertainty and Verification Acceptance Criteria 19
         4.2.1.3 Model Uncertainty Acceptance Criteria 20
         4.2.1.4 Model Verification Acceptance Criteria 20
      4.2.2 Features, Events and Processes (FEPs) 21
   4.3 CODES AND STANDARDS 21
      4.3.1 Codes 21
      4.3.2 Standards 21

5. ASSUMPTIONS 21
   5.1 PROCESSES MODELED 21
   5.2 GENERAL ASSUMPTIONS 22
      5.2.1 Standard State of Water or Brine 22
      5.2.2 Redox Conditions 22
      5.2.3 Equilibrium Conditions 22
      5.2.4 Relative Humidity vs. Time 23
   5.3 ION INTERACTION 23
   5.4 MINERALS AND GASES 28
   5.5 SALT STABILITY AT LOW RELATIVE HUMIDITY 31
   5.6 CONDENSED WATER MODEL 34

6. MODEL 34
   6.1 REVIEW OF SALTS/PRECIPITATES PROCESSES 34
      6.1.1 Evaporation, Relative Humidity, and Salt Precipitation 34
      6.1.2 Formation and Chemistry of Brines and Salt Precipitates 35
      6.1.3 Potential Brines and Salt Precipitates at Yucca Mountain 37
      6.1.4 Precipitates/Salts Model Developed for the TSPA-VA 39
         6.1.4.1 Salt Precipitation Results 39

6.1.4.2 Salt Dissolution Results 40
6.2 CONCEPTUAL MODEL 41
6.3 MODEL DESIGN 42
6.3.1 Input Parameters and Boundary Conditions 43
6.3.1.1 Seepage Water Composition 43
6.3.1.2 Time Period Modeled 43
6.3.1.3 Locations Modeled 43
6.3.1.4 Temperature and Gas Composition 43
6.3.1.5 Relative Evaporation Rate 43
6.3.2 Model Output 43
6.3.3 Model Limitations 44
6.3.4 Condensed Water Model 44
6.4 MODEL IMPLEMENTATION 44
6.4.1 Low Relative Humidity Model 45
6.4.2 High Relative Humidity Model 47
6.4.2.1 Simple Evaporation 48
6.4.2.2 Evaporation with Solid-Centered Flow-Through 48
6.4.3 Condensed Water Model 49
6.5 MODEL VALIDATION 49
6.5.1 HRH Model Validation 50
6.5.1.1 Evaporation of Average J-13 Well Water at 85°C 50
6.5.1.2 Evaporation of 100x Average J-13 Well Water at 90°C and 85 Percent Relative Humidity 55
6.5.1.3 Evaporation of Topopah Spring Tuff Pore Water at 75°C 59
6.5.1.4 Evaporation of Pure Salt Solutions 62
6.5.2 LRH Model Validation 63
6.6 MODEL RESULTS 64
6.6.1 High Relative Humidity Model Results 65
6.6.1.1 Evaporation of Average J-13 Well Water 65
6.6.1.2 Results of Evaporation with a Constant Incoming Seepage 69
6.6.2 Low Relative Humidity Model Results 74
6.6.3 Precipitates/Salts Model Lookup Tables 78
6.6.4 Condensed Water Composition and Lookup Tables 82

7. CONCLUSIONS 84
7.1 MODEL AND RESULTS 85
7.2 ABSTRACTION 87
7.3 VALIDATION, UNCERTAINTY, AND LIMITATIONS 88
7.4 TBVs 89
7.5 FEPs 90

8. REFERENCES 91
8.1 DOCUMENTS 91
8.2 DATA, LISTED BY TRACKING NUMBER 95
8.2.1 INPUT DATA 95
8.2.2 DEVELOPED DATA 95

8.3 CODES, STANDARDS, REGULATIONS, PROCEDURES, AND SOFTWARE 96

ATTACHMENTS 97

FIGURES

Page

Figure 1. Previous Predictions of Relative Humidity and Temperature on the Waste Package Surface Over Time. 18

Figure 2. pH and Ionic Strength Predictions vs. J-13 Evaporation Data from Rosenberg et al. (1999a, evap4) 52

Figure 3. Na, CO_3, and F Predictions vs. J-13 Evaporation Data from Rosenberg et al. (1999a, evap4) 52

Figure 4. Cl and K Predictions vs. J-13 Evaporation Data from Rosenberg et al. (1999a, evap4) 53

Figure 5. NO_3, SO_4, and Si Predictions vs. J-13 Evaporation Data from Rosenberg et al. (1999a, evap4) 53

Figure 6. Ca and Mg Predictions vs. J-13 Evaporation Data from Rosenberg et al. (1999a, evap4) 54

Figure 7. Mineral Precipitation Predictions for J-13 Evaporation Experiment of Rosenberg et al. (1999a, evap4) 54

Figure 8. pH and Ionic Strength Predictions for 100x J-13 Evaporation Experiment by CRWMS M&O (2000, Batch 1) 55

Figure 9. Na and F Predictions vs. 100x J-13 Evaporation Data from CRWMS M&O (2000, Batch 1) 56

Figure 10. Cl and K Predictions vs. 100x J-13 Evaporation Data from CRWMS M&O (2000, Batch 1) 57

Figure 11. NO_3, SO_4, and CO_3 Predictions vs. 100x J-13 Evaporation Data from CRWMS M&O (2000, Batch 1) 57

Figure 12. Ca and Mg Predictions vs. 100x J-13 Evaporation Data from CRWMS M&O (2000, Batch 1) 58

Figure 13. Mineral Precipitation Predictions for 100x J-13 Evaporation Experiment of CRWMS M&O (2000, Batch 1) 58

Figure 14. pH and Ionic Strength Predictions vs. Topopah Spring Tuff Pore Water Evaporation Data from Rosenberg et al. (1999b, evap3) 60

Figure 15. Na, Mg, and NO_3 Predictions vs. Topopah Spring Tuff Pore Water Evaporation Data from Rosenberg et al. (1999b, evap3) 60

Figure 16. Cl, Ca, and K Predictions vs. Topopah Spring Tuff Pore Water Evaporation Data from Rosenberg et al. (1999b, evap3) 61

Figure 17. SO_4, CO_3, Si, and F Predictions vs. Topopah Spring Tuff Pore Water Evaporation Data from Rosenberg et al. (1999b, evap3) 61

Figure 18. Mineral Precipitation Predictions for Topopah Spring Tuff Pore Water Evaporation Experiment of Rosenberg et al. (1999b, evap3) 62

Figure 19. pH and Ionic Strength Predictions from Simple Evaporation of Average J-13 Well Water at 95°C and f_{CO2} of 10^{-3} 66

Figure 20. Cl, CO_3, K, and Na Predictions from Simple Evaporation of Average J-13 Well Water at 95°C and f_{CO2} of 10^{-3} 66

Figure 21. NO_3, SO_4, Si, and F Predictions from Simple Evaporation of Average J-13 Well Water at 95°C and f_{CO2} of 10^{-3} 67

Figure 22. Ca, Mg, and Al Predictions from Simple Evaporation of Average J-13 Well Water at 95°C and f_{CO2} of 10^{-3} 67

Figure 23. Fe Predictions from Simple Evaporation of Average J-13 Well Water at 95°C and f_{CO2} of 10^{-3} 68

Figure 24. Mineral Precipitation Predictions from Simple Evaporation of Average J-13 Well Water at 95°C and f_{CO2} of 10^{-3} 68

Figure 25. Cl Concentration Predictions vs. Pore Volume for $R^{es} = 0.99$, $T = 95$°C, $f_{CO2} = 10^{-3}$, $C^s = 0.0002$ molal, and Initial $C = 0.6$ molal 70

Figure 26. J-13 Steady State pH vs. ($1-R^{es}$) and Temperature ($f_{CO2} = 10^{-1}$) 70

Figure 27. J-13 Steady State pH vs. ($1-R^{es}$) and Temperature ($f_{CO2} = 10^{-3}$) 71

Figure 28. J-13 Steady State pH vs. ($1-R^{es}$) and Temperature ($f_{CO2} = 10^{-6}$) 71

Figure 29. J-13 Steady State Cl vs. ($1-R^{es}$) and Temperature (identical for $f_{CO2} = 10^{-1}$, 10^{-3}, and 10^{-6}) 72

Figure 30. J-13 Steady State Ionic Strength vs. ($1-R^{es}$) and Temperature ($f_{CO2} = 10^{-1}$) 72

Figure 31. J-13 Steady State Ionic Strength vs. (1-R^{es}) and Temperature (f_{CO2} = 10^{-3}) 73

Figure 32. J-13 Steady State Ionic Strength vs. (1-R^{es}) and Temperature (f_{CO2} = 10^{-6}) 73

Figure 33. Cumulative Moles of Incoming Seepage Dissolved Solids vs. Time (J-13, Q^s = 1 L/yr, f_{CO2} = 10^{-3}) 75

Figure 34. Fraction of Moles Dissolved Within Reactor vs. Time (J-13, Q^s = 1 L/yr, f_{CO2} = 10^{-3}) 75

Figure 35. Dissolved Concentration vs. Time (J-13, Q^s = 1 L/yr, f_{CO2} = 10^{-3}) 76

Figure 36. Total Moles in Reactor vs. Time (J-13, Q^s = 1 L/yr, f_{CO2} = 10^{-3}) 76

Figure 37. Total Dissolved Moles in Reactor vs. Time (J-13, Q^s = 1 L/yr, f_{CO2} = 10^{-3}) 77

Figure 38. Cumulative Mass of Water and Dissolved Ions in Generated Brine vs. Time (J-13, Q^s = 1 L/yr, f_{CO2} = 10^{-3}) 77

Figure 39. Predicted pH of Condensed Water for a Range of Temperatures (T) and Fugacities of Carbon Dioxide (f_{CO2}). 83

Figure 40. Predicted Ionic Strength of Condensed Water for a Range of Temperatures (T) and Fugacities of Carbon Dioxide (f_{CO2}). 83

TABLES

Page

Table 1. Aqueous Solubilities of Sodium and Potassium Salts at 100°C. Values from Solubilities Listed in the Handbook of Chemistry and Physics (Weast and Astle 1981, pp. B-131 to B-137 and B-146 to B-150), Unless Otherwise Indicated 12

Table 2. Equilibrium Relative Humidity for Saturated Aqueous Solutions in Contact With an Excess of Solid-Phase Sodium and Potassium Salts (Dean 1992, p. 11.6) 13

Table 3. Water Chemistry Data From Experimental J-13 Well Water Evaporation (Rosenberg et al. 1999a, p. 17) 14

Table 4. pH Data From Experimental J-13 Well Water Evaporation (Rosenberg et al. 1999a, p. 19) 14

Table 5. Water Chemistry Data From Experimental J-13 Well Water Evaporation (CRWMS M&O 2000, p. 4-17 and p. 6-16) 15

Table 6. Water Chemistry Data From Topopah Spring Pore Water Evaporation Experiment (Rosenberg et al. 1999b, p. 17) 16

Table 7. Average Composition of Water from Well J-13 (Harrar et al. 1990) 17

Table 8. FEPs Applicable to the Precipitates/Salts Analysis 21

Table 9. Aqueous Species in the PT4 Database and the Origins of Their Pitzer Coefficients 25

Table 10. Cation-Anion Pairs Added to the PT4 Database 25

Table 11. Anion-Anion Pairs Added to the PT4 Database 25

Table 12. Cation-Neutral and Anion-Neutral Species Pairs Added to the PT4 Database 25

Table 13. Anion-Anion-Cation Interaction Parameters Added to the PT4 Database 26

Table 14. Aqueous Species in the PT4 Database and the Source of Their Thermodynamic Data 27

Table 15. Minerals Included in PT4 Database 29

Table 16. Minerals in the PT4 Database that are Suppressed for the Precipitates/Salts Model Lookup Table Calculations 31

Table 17. Comparison of Handbook Aqueous Solubilities of Sodium and Potassium Salts at 100°C With Values Calculated Using the EQ3/6 HRH Model. 63

Table 18. Lookup Table for Average J-13 Well Water Seepage at $f_{CO2} = 10^{-1}$ 79

Table 19. Lookup Table for Average J-13 Well Water Seepage at $f_{CO2} = 10^{-3}$ 80

Table 20. Lookup Table for Average J-13 Well Water Seepage at $f_{CO2} = 10^{-6}$ 81

Table 21. Lookup Table for Condensed Water Model 84

Table 22. FEPs and the AMR Conclusions 90

ACRONYMS AND ABBREVIATIONS

100x	concentration factor of 100
ACC	accession number
AMR	Analyses/Model Report
C_i	concentration of component i
CHV	data0.chv, a thermodynamic database of EQ3/6 version 7.2b
COM	data0.com, a thermodynamic database of EQ3/6 version 7.2b
DOE	Department of Energy
DTN	Data Tracking Number
EBS	Engineered Barrier System
f_{co2}	carbon dioxide fugacity
FEP	Features, Events, and Processes
gm	gram
HMW	data0.hmw, a thermodynamic database of EQ3/6 version 7.2b
HRH	high relative humidity
I	ionic strength
IRSR	Issue Resolution Status Report
ITN	Input Tracking Number
kg	kilogram
KTI	key technical issues
L	liter
LLNL	Lawrence Livermore National Laboratory
LRH	low relative humidity
mg	milligram
mL	milliliter
molal	moles per liter
NFE	Near Field Environment
NRC	Nuclear Regulatory Commission
PAO	Performance Assessment Operations
PIT	data0.pit, a thermodynamic database of EQ3/6 version 7.2b
PT4	data0.pt4, a thermodynamic database developed in this AMR for EQ3/6
Q^e	evaporation rate
Q^s	incoming seepage rate
QA	Quality Assurance
R^{es}	relative evaporation rate
RH	relative humidity
T	temperature
TBD	Technical Basis Document
TBV	to be verified
TH	thermohydrologic
THC	thermohydrological-chemical
TIC	Technical Information Center number
TSPA-VA	Total System Performance Assessment - Viability Assessment
XRD	X-Ray Diffraction

1. PURPOSE

As directed by a written development plan (CRWMS M&O 1999a), an analysis of the effects of salts and precipitates on the repository chemical environment is to be developed and documented in an Analyses/Model Report (AMR). The purpose of this analysis is to assist Performance Assessment Operations (PAO) and the Engineered Barrier Performance Department in modeling the geochemical environment within a repository drift, thus allowing PAO to provide a more detailed and complete in-drift geochemical model abstraction and to answer the key technical issues (KTI) raised in the NRC Issue Resolution Status Report (IRSR) for the Evolution of the Near Field Environment (NFE) Revision 2 (NRC 1999).

The scope of this document is to develop a model of the processes that govern salt precipitation and dissolution and resulting water composition in the Engineered Barrier System (EBS). This model is developed to serve as a basis for the in-drift geochemical modeling work performed by PAO and is to be used in subsequent PAO analyses including the EBS physical and chemical model abstraction effort. However, the concepts may also apply to some near and far field geochemical processes and can have conceptual application within the unsaturated zone and saturated zone transport modeling efforts.

The intended use of the model developed in this report is to estimate, within an appropriate level of confidence, the pH, chloride concentration, and ionic strength of water on the drip shield or other location within the drift during the post-closure period. These estimates are based on evaporative processes that are subject to a broad range of potential environmental conditions. An additional intended use is to estimate the environmental conditions required for complete vaporization of water. The presence and composition of liquid water in the drift (i.e., pH, chloride concentration, and ionic strength) are potentially important to corrosion and radionuclide transport calculations performed by PAO.

2. QUALITY ASSURANCE

The Quality Assurance (QA) program applies to the development of this AMR. The PAO responsible manager has evaluated the technical document development activity in accordance with QAP-2-0, *Conduct of Activities.* The QAP-2-0 activity evaluation has determined that the preparation and review of this technical document is subject to *Quality Assurance Requirements and Description* (QARD) requirements (DOE 2000). Preparation of this analysis did not require the classification of items in accordance with QAP-2-3, *Classification of Permanent Items.* This activity is not a field activity. Therefore, an evaluation in accordance with NLP-2-0, *Determination of Importance Evaluations*, was not required.

This document and its conclusions may be affected by technical product input information that requires confirmation. Any changes to the document or its conclusions that may occur as a result of completing the confirmation activities will be reflected in subsequent revisions. The status of the input information quality may be confirmed by review of the Document Input Reference System database.

3. COMPUTER SOFTWARE AND MODEL USAGE

3.1 COMPUTER SOFTWARE

The software used in this analysis include:

- EQ3/6 v7.2b [STN: 10075-7.2bLV-00, Wolery 1992a and 1992b, Wolery and Daveler 1992, CRWMS M&O 1999e] with the solid-centered flow-through addendum [CSCI: URCL-MA-110662 V7.2b, MI: 30084-M04-001 (Addendum Only), CRWMS M&O 1998a]. The software was obtained from Configuration Management and installed on an IBM-compatible computer. It is appropriate for the application and is used only within the range of validation in accordance with AP-SI.1Q, *Software Management*. No macros or software routines were developed for, or used by, this software.

- MathSoft Mathcad7 Professional, a commercially available software package for technical calculations. This software was used to perform and display the routine algebraic calculations developed in Section 6.4.1. These equations and all calculations are checkable by hand and are shown in Attachment I. No macros or software routines were developed for, or used by, this software.

- Microsoft Excel 97, a commercially available spreadsheet software package. This software was used to tabulate and chart results. No macros or software routines were developed for, or used by, this software.

3.2 MODELS

The previous precipitates/salts analysis used for performance assessment near-field geochemical analysis is documented in chapter 4 of the Total System Performance Assessment-Viability Assessment (TSPA-VA) Analyses Technical Basis Document (TBD) (CRWMS M&O 1998b). The model and analysis developed in the current document supersedes those presented in the TBD.

4. INPUTS

4.1 DATA AND PARAMETERS

The Precipitates/Salts analysis requires the following types of input: 1) relevant thermodynamic properties of potentially important ground-water constituents, 2) experimental data used for model validation, and 3) values for model input parameters. These inputs are described in the following subsections.

4.1.1 Thermodynamic Constants and Salt Properties

The thermodynamic data used in the model simulations are generally from the databases in GEMBOCHS.V2-EQ8-DATA0.PIT.R2 generated by GEMBOCHS.V2-JEWEL.SRC.R3 02-aug-1995 16:19:24. These databases include the PIT and COM databases (DTN: MO9911SPATHD62.002) that comes with the EQ3/6 v7.2b software package [CSCI: URCL-

MA-110662 V7.2b, Wolery 1992a and 1992b, Wolery and Daveler 1992]. These databases are unqualified and therefore designated as TBV (TBV-3916). Database development for this AMR is discussed in Section 5.

The aqueous solubilities of various binary Na and K salts at 100°C are presented in Table 1. Each value represents the maximum amount of the specified salt that can be dissolved into pure water at the given temperature. These values are useful for model validation.

Table 2 lists handbook values of the equilibrium relative humidity of saturated aqueous solutions in contact with an excess of solid-phase sodium and potassium salts. These values represent the maximum relative humidity at which a salt is stable at the given temperature. The equilibrium relative humidity of many of these salts and others are plotted versus temperature in CRWMS M&O (2000, p. 6-12). These values are useful for estimating whether a particular salt is stable when subjected to a given relative humidity and temperature.

Table 1. Aqueous Solubilities of Sodium and Potassium Salts at 100°C. Values from Solubilities Listed in the Handbook of Chemistry and Physics (Weast and Astle 1981, pp. B-131 to B-137 and B-146 to B-150), Unless Otherwise Indicated

Salt	Molecular Weight (gm/mole)	Aqueous Solubility at 100°C (gm/100 mL)	Aqueous Solubility at 100°C (molal)
NaCl	58.4	39.1	6.70
KCl	74.6	56.7	7.60
$Na_2CO_3 \cdot H_2O$	124.0	52.08	4.2
K_2CO_3	138.2	156	11.3
NaF	42.0	5.08[a]	1.21[a]
KF	58.1	150[b]	26[b]
Na_2SO_4	142.0	42.7	3.01
K_2SO_4	174.3	24.1	1.38
$NaNO_3$	85.0	180.	21.2
KNO_3	101.1	247	24.4

TIC: 240580 (accepted data)

[a]Dean 1992, p. 5.20 (TIC: 239897, accepted data)

[b]at 80°C, Dean 1992, p. 5.17 (TIC: 239897, accepted data)

4.1.2 Experimental Data Used for Model Validation

Three sources of experimental data from Lawrence Livermore National Laboratory (LLNL) are relevant to this model. They are Rosenberg et al. (1999a and 1999b) and CRWMS M&O (2000). These data are used only as a reference for model validation. They were not used to develop or calibrate the model.

Table 2. Equilibrium Relative Humidity for Saturated Aqueous Solutions in Contact With an Excess of Solid-Phase Sodium and Potassium Salts (Dean 1992, p. 11.6)

Salt	Equilibrium Relative Humidity (%)	Temperature of Measurement (ºC)
NaCl	76.4	80
KCl	79.5	80
$Na_2CO_3 \cdot 10H_2O$	87[a]	24.5
$K_2CO_3 \cdot 2H_2O$	42	40
NaF	96.6[a]	100
KF	22.9[a]	100
$Na_2SO_4 \cdot 10H_2O$	93[a]	20
K_2SO_4	96	60
$NaNO_3$	65.5	80
KNO_3	82	60
KNO_3, $NaNO_3$, and NaCl	30.49[a]	16.39

TIC: 239897 (accepted data)

[a] Weast and Astle 1981, p. E-44 (TIC: 240580, accepted data)

In each of these reports, experimental data are reported for the evaporation of synthetic J-13 well water in a beaker that was open to the atmosphere and maintained at a constant elevated temperature. In the Rosenberg et al. (1999a) experiment named evap1, synthetic average J-13 well water was evaporated without contact with tuff or other non-precipitated rock material. The experiment began with 30 liters of synthetic average J-13 well water with a measured composition as shown in Table 3. The water did not include Al or Fe. A peristaltic pump was used to pump this water into a 1-liter pyrex beaker at a constant rate while a hot plate was used to maintain a water temperature of 85°C to evaporate the water. Water samples were collected after the 30 liters had been evaporated to approximately 30 mL. Results of this experiment are included in Table 3. The solids that had accumulated at this stage were identified by x-ray diffraction (XRD) to be amorphous silica, aragonite, and calcite. Analysis of solids after complete evaporation indicated the additional presence of halite, niter, thermonatrite, and possibly gypsum, anhydrite, and hectorite.

In another Rosenberg et al. (1999a) experiment (named evap4), the pH of the evaporating water was monitored. The experiment used the same J-13 starting solution as evap1. The data are presented in Table 4 as a function of concentration factor. The concentration factor is the ratio of the initial water mass divided by the water mass at the time of analysis.

Table 3. Water Chemistry Data From Experimental J-13 Well Water Evaporation (Rosenberg et al. 1999a, p. 17)

Constituent	Units	Synthetic J-13 Well Water	Evaporated Synthetic J-13 Well Water (Concentration Factor: 956x)
Ca	mg/kg	6.4	29.86
Mg	mg/kg	2.2	0.14
Na	mg/kg	46	44082
K	mg/kg	5.3	4792
SiO_2	mg/kg	11.3	18008
NO_3	mg/kg	8.0	5532
HCO_3	mg/kg	108	24878
Cl	mg/kg	6.9	4835
F	mg/kg	2.2	1550
SO_4	mg/kg	18.1	12926
pH	pH	7.84	nr[a]

(CRWMS M&O 1999c)
[a] not reported

Table 4. pH Data From Experimental J-13 Well Water Evaporation (Rosenberg et al. 1999a, p. 19)

Concentration Factor	pH
1.00	8.46
1.00	8.65
1.05	9.04
1.29	9.43
1.60	9.58
2.41	9.67
6.08	9.67
6.37	9.77
7.59	9.79
11.6	9.95
12.6	10.00
15.3	10.03
20.9	10.08
25.2	10.09
34.4	10.12
52.1	10.18
104.	10.18
157.	10.18

(CRWMS M&O 1999c)

In a similar evaporation experiment reported in CRWMS M&O (2000, p. 6-16) (called Batch 1), a synthetic 100-times concentrated (100x) average J-13 well water was dripped through a column of heated tuff into a teflon beaker. The beaker was open to the atmosphere and maintained at a constant temperature of 90°C and relative humidity of 85 percent. The starting and final solution compositions are displayed in Table 5. The recipe for the synthetic 100x J-13 well water did not include Si, Al, or Fe, likely because these components have limited solubility or are minor constituents (Al and Fe). A 100x concentration of these components cannot be prepared without making adjustments, such as raising the pH to an unrealistic value. A true 100x J-13 water can only be realistically derived by evaporating unconcentrated J-13 in a container open to a fixed fugacity of carbon dioxide and allowing supersaturated minerals to precipitate from solution during the process (as was done in Rosenberg et al. (1999a)).

Synthetic Topopah Spring tuff pore water was evaporated in an experiment reported in Rosenberg et al. (1999b). The experiment, named evap3, was performed following the same procedures as in Rosenberg et al. (1999a) presented earlier. The only difference was the starting water composition. Both the starting and final solutions are presented in Table 6. Rosenberg et al. (1999b, p. 2) determined by mass ratio that the final solution had an approximate concentration factor of 1243 ± 10 percent. XRD analysis at this concentration factor detected gypsum. After complete evaporation, tachyhydrite was also detected.

Table 5. Water Chemistry Data From Experimental J-13 Well Water Evaporation (CRWMS M&O 2000, p. 4-17 and p. 6-16)

Constituent	Units	Synthetic 100x J-13 Well Water	Evaporated Synthetic 100x J-13 Well Water
Ca	mg/L	5	36
Mg	mg/L	2	0
Na	mg/L	4032	76314
K	mg/L	513	10832
NO_3	mg/L	732	14085
CO_3	mg/L as HCO_3	4142	54614
Cl	mg/L	730	14419
F	mg/L	208	3630
SO_4	mg/L	1632	29783
pH	pH	nr[a]	nr

DTN: LL000202905924.117 (Table S00134_002)

[a] not reported

Table 6. Water Chemistry Data From Topopah Spring Pore Water Evaporation Experiment (Rosenberg et al. 1999b, p. 17)

Constituent	Units	Synthetic Pore Water	Evaporated Synthetic Pore Water (Concentration Factor: 1243x)
Ca	mg/kg	57.2	15629
Mg	mg/kg	11.7	5478
Na	mg/kg	8.2	5961
K	mg/kg	4.2	2779
SiO_2	mg/kg	9.8	513
NO_3	mg/kg	11.0	nm[a]
HCO_3	mg/kg	16.2	< 35
Cl	mg/kg	78.0	53084
F	mg/kg	2.3	< 577
SO_4	mg/kg	81.7	2077
pH	pH	7.68	6-6.5[b]

(CRWMS M&O 1999d)
[a] not measured
[b] estimate from pH paper

4.1.3 Model Input Parameters

The Precipitates/Salts model input parameters are:

- Concentration or activity of each modeled component i in the incoming seepage (C_i^s) [units: mass/volume, moles/mass, or moles/volume]
- Temperature (T) [units: degrees Celcius]
- Relative humidity (RH) [units: nondimensional or percentage]
- Fugacity of carbon dioxide (f_{CO2}) [units: nondimensional]
- Seepage rate (Q^s) [units: mass/time or volume/time]
- Relative evaporation rate (R^{es}) [units: nondimensional], defined below

The modeled incoming seepage includes the following components: Na, K, Ca, Mg, Cl, F, CO_3, SO_4, NO_3, SiO_2, Fe(III), Al, H, and H_2O. In the Precipitates/Salts analysis, representative water from well J-13 is used as the incoming seepage. The specific composition used originates from the data in Harrar et al. (1990, p 4.2) and is displayed in Table 7. The Precipitates/Salts Model is intended to incorporate seepage composition data from thermohydrological-chemical (THC) modeling when they become available.

Table 7. Average Composition of Water from Well J-13 (Harrar et al. 1990)

Constituent	Average J-13 Concentration[a] (mg/L)	Average J-13 Concentration[a] (molal)
Ca	12.9	3.23E-4
Mg	2.0	8.2E-5
Na	45.8	1.99E-3
K	5.0	1.3E-4
SiO_2	61.0	1.02E-3
NO_3	8.8	1.4E-4
CO_3	128.9[b]	2.15E-3
Cl	7.1	2.0E-4
F	2.2	1.2E-4
SO_4	18.4	1.92E-4
Fe	~0.030	5.4E-7
Al	~0.030	1.1E-6
pH	7.4	7.4

DTN: LL980711104242.054

[a] Approximations marked "~" are estimates based on few data.

[b] mg/L as HCO_3

The model is designed for constant temperatures (T) in the range of ambient (~20°C) to approximately boiling (~95°C), relative humidity (RH) between 0 and 100 percent, and fugacities of carbon dioxide (f_{CO2}) between 10^{-10} and 10^{-1}. However, the actual values used in the analyses described in this document do not completely cover the entire design ranges. In the analyses, T was varied between four values (95°C, 75°C, 45°C, and 25°C) to develop a response surface that is intended to cover the range of values anticipated. The f_{CO2} values used in the model predictions are 10^{-1}, 10^{-3}, and 10^{-6}.

RH as a function of time was taken from the values reported in chapter 3 of the TBD for the waste package surface (CRWMS M&O 1998c). These values, displayed in Figure 1, are from a simulation in which no backfill is used in the drift, unlike the current design; however, they provide approximations of the values and trends expected in the drift. They are used as a reference only and not as direct input so they are not required to be qualified. Instead, they are used to justify an assumption regarding the general trends of RH as a function of time in the potential repository, i.e., that except for early times, RH increases as a function of time until it levels off.

The relative evaporation rate (or flux) (R^{es}) is defined in this AMR by the equation:

$$R^{es} = \frac{Q^e}{Q^s} \qquad \text{(Eq. 1)}$$

where Q^e is the steady state evaporation flux and Q^s is the incoming seepage rate (or flux). The model is designed for a range of R^{es} from 0 to 1. The values used in this analysis are: 0, 0.1, 0.5, 0.9, 0.99, and 0.999. These values are used to generate a lookup table that is intended to cover the range of values anticipated.

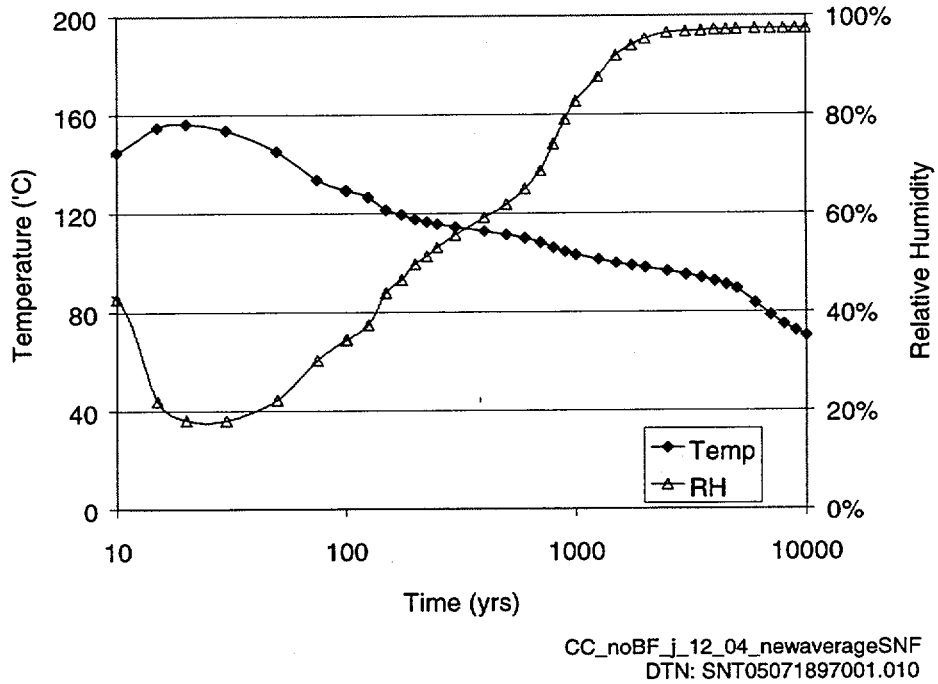

Figure 1. Previous Predictions of Relative Humidity and Temperature on the Waste Package Surface Over Time.

4.2 CRITERIA

Section 4.2.1 provides a summary of the applicable Nuclear Regulatory Commission (NRC) review and acceptance criteria outlined in its Issue Resolution Status Report (IRSR) that apply to model development. A listing of the project features, events, and processes (FEPs) that potentially apply to this AMR are provided in Section 4.2.2.

4.2.1 NRC Evolution of Near Field Environment IRSR Criteria

The wording for the IRSR criteria listed below is generally taken from Section 4.3.1 of NRC (1999). These criteria apply to subissues 4.1 (coupled thermohydrological-chemical (THC) effects on seepage and flow), 4.2 (waste package chemical environment), 4.3 (chemical environment for radionuclide release), 4.4 (effects of THC processes on radionuclide transport through engineered and natural barriers) and 4.5 (coupled THC processes affecting potential nuclear criticality in the near field).

4.2.1.1 Data and Model Justification Acceptance Criteria

1. Consider both temporal and spatial variations in conditions affecting coupled thermohydrological-chemical (THC) effects on the chemical environment for radionuclide release. [NRC (1999), Sections 4.1.1, 4.2.1, 4.3.1, 4.4.1, and 4.5.1]

2. Consider site characteristics in establishing initial and boundary conditions for conceptual models and simulations of coupled processes that may affect the chemical environment for radionuclide release. [NRC (1999), Sections 4.1.1, 4.2.1, 4.3.1, 4.4.1, and 4.5.1]

3. Collect sufficient data on the characteristics of the natural system and engineered materials, such as the type, quantity, and reactivity of material, in establishing initial and boundary conditions for conceptual models and simulations of THC coupled processes that affect the chemical environment for radionuclide release. [NRC (1999), Sections 4.1.1, 4.2.1, 4.3.1, 4.4.1, and 4.5.1]

4. Use sensitivity and uncertainty analyses (including consideration of alternative conceptual models) to determine whether additional new data are needed to better define ranges of input parameters. [NRC (1999), Sections 4.1.1, 4.2.1, 4.3.1, and 4.4.1]

5. If the testing program for coupled THC processes on the chemical environment for radionuclide release from the engineered barrier system is not complete at the time of license application, or if sensitivity and uncertainty analysis indicate the additional data are needed, identify specific plans to acquire the necessary information as part of the performance confirmation program. [NRC (1999), Sections 4.1.1, 4.2.1, 4.3.1, and 4.4.1]

4.2.1.2 Data Uncertainty and Verification Acceptance Criteria

1. Use reasonable or conservative ranges of parameters or functional relations to determine effects of coupled THC processes on the chemical environment for radionuclide release. Parameter values, assumed ranges, probability distributions, and bounding assumptions must be technically defensible and reasonably account for uncertainties. [NRC (1999), Sections 4.1.1, 4.2.1, 4.3.1, 4.4.1, and 4.5.1]

2. Consider uncertainty in data due to both temporal and spatial variations in conditions affecting coupled THC effects on the chemical environment for radionuclide release. [NRC (1999), Sections 4.1.1, 4.2.1, 4.3.1, 4.4.1, and 4.5.1]

3. Properly consider in the evaluation of coupled THC processes the uncertainties in the characteristics of the natural system and engineered materials, such as the type, quantity, and reactivity of material, in establishing initial and boundary conditions for conceptual models and simulations of THC coupled processes that affect the chemical environment for radionuclide release. [NRC (1999), Sections 4.1.1, 4.2.1, 4.3.1, 4.4.1, and 4.5.1]

4. Use available data to ensure consistency in the initial conditions, boundary conditions, and computational domain used in sensitivity analysis involving coupled THC effects on the chemical environment for radionuclide release. [NRC (1999), Sections 4.1.1, 4.2.1, 4.3.1, 4.4.1, and 4.5.1]

5. Assess in the performance confirmation program whether the natural system and engineered materials are functioning as intended and anticipated with regard to coupled THC effects on the chemical environment for radionuclide release from the EBS. [NRC (1999), Sections 4.1.1, 4.2.1, 4.3.1, and 4.4.1]

4.2.1.3 Model Uncertainty Acceptance Criteria

1. Use appropriate models, tests, and analyses that are sensitive to the THC couplings under consideration for both natural and engineering systems as described in the following examples. The effects of THC coupled processes that may occur in the natural setting or due to interactions with engineered materials or their alteration products include (i) thermohydrologic (TH) effects on gas and water chemistry; (ii) hydrothermally driven geochemical reactions, such as zeolitization of volcanic glass; (iii) dehydration of hydrous phases liberating moisture; (iv) effects of microbial processes; and (v) changes in water chemistry that may result from interactions between cementitious, or WP, materials and groundwater, which, in turn, may affect the chemical environment for radionuclide release. [NRC (1999); Sections 4.1.1, 4.2.1, 4.3.1, and 4.4.1]

2. Investigate alternative modeling approaches consistent with available data and current scientific understanding, and appropriately consider their results and limitations. [NRC (1999), Sections 4.1.1, 4.2.1, 4.3.1, 4.4.1, and 4.5.1]

3. Provide a reasonable description of the mathematical models included in its analyses of coupled THC effects on the chemical environment for radionuclide release. The description should include a discussion of alternative modeling approaches not considered in its final analysis and the limitations and uncertainties of the chosen model. [NRC (1999), Sections 4.1.1, 4.2.1, 4.3.1, 4.4.1, and 4.5.1]

4.2.1.4 Model Verification Acceptance Criteria

1. The mathematical models for coupled THC effects on the chemical environment for radionuclide release must be consistent with conceptual models based on inferences about the near-field environment, field data and natural alteration observed at the site, and expected engineered materials. [NRC (1999), Sections 4.1.1, 4.2.1, 4.3.1, 4.4.1, and 4.5.1]

2. Appropriately adopt accepted and well-documented procedures to construct and test the numerical models used to simulate coupled THC effects on the chemical environment for radionuclide release. [NRC (1999), Sections 4.1.1, 4.2.1, 4.3.1, 4.4.1, and 4.5.1]

3. Abstracted models for coupled THC effects on the chemical environment for radionuclide release must be based on the same assumptions and approximations shown to be appropriate for closely analogous natural or experimental systems. Abstracted model results are verified through comparison to outputs of detailed process models and empirical observations. Abstracted model results are compared with different mathematical models to judge robustness of results. [NRC (1999), Sections 4.1.1, 4.2.1, 4.3.1, 4.4.1, and 4.5.1]

4.2.2 Features, Events and Processes (FEPs)

Table 8 lists the Yucca Mountain Project FEPs (CRWMS M&O 1999b) that are discussed in this document..

Table 8. FEPs Applicable to the Precipitates/Salts Analysis

YMP FEP Number	NEA Category	FEP Name
2.1.04.02.00	2.1.04au	Physical and chemical properties of backfill
2.1.04.03.00	2.1.04r	Erosion or dissolution of backfill
2.1.04.05.00	2.1.04b	Backfill evolution
2.2.08.04.00	2.2.08c	Redissolution of precipitates directs more corrosive fluids to containers

ACC: MOL.19991214.0518, MOL.19991214.0519

Any resolution of these FEPs is discussed in Section 7.5.

4.3 CODES AND STANDARDS

4.3.1 Codes

This AMR was prepared to comply with the DOE interim guidance (Dyer 1999) which directs the use of the proposed NRC high-level waste rule, 10 CFR Part 63. Subparts of this proposed rule that are applicable to data include Subpart B, Section 15 (Site Characterization) and Subpart E, Section 114 (Requirements for Performance Assessment). The Subpart applicable to models is also outlined in Subpart E Section 114.

4.3.2 Standards

ASTM C 1174-97 *Standard Practice for Prediction of the Long-Term Behavior of Materials, Including Waste Forms, Used in Engineered Barrier Systems (EBS) for Geological Disposal of High-Level Radioactive Waste* was used as guidance in the preparation of this analysis.

5. ASSUMPTIONS

5.1 PROCESSES MODELED

The processes modeled by the Precipitates/Salts model are:

- Vaporization of incoming seepage water,
- Precipitation of dissolved solids resulting from vaporization, and
- Dissolution of precipitates.

The Precipitates/Salts model does not simulate interaction with potential materials within the drift, such as tuff, grout, or waste package materials. It is composed of two sub-models. An

EQ3/6 Pitzer model is used to predict equilibrium aqueous chemistry, precipitation, and dissolution when the relative humidity is above 85 percent. Below 85 percent, a Low Relative Humidity (LRH) salts model is used.

A model for the composition of condensed water vapor underneath the drip shield is included in this AMR to investigate the effects of temperature and carbon dioxide fugacity.

5.2 GENERAL ASSUMPTIONS

5.2.1 Standard State of Water or Brine

As discussed in Section 6, a brine at standard state has an equilibrium relative humidity that is equivalent to the activity of water in the brine. Standard state in this sense implies that the brine has a flat interface with the air and that the behavior of the water molecule (H_2O) is not influenced by solid surfaces. Non-standard state effects due to interface curvature and adsorption would tend to decrease equilibrium relative humidity values and allow for stable brine solutions at lower relative humidity values than standard state brines.

For the Precipitates/Salts Model, non-standard state water is not considered. Only dissolved salts are considered to affect liquid-vapor equilibrium. The small amounts of water held in double layers and adsorbed to solid surfaces are assumed to have negligible roles in radionuclide transport and waste package corrosion. Although water held by the surface tension effects of capillary binding are likely more important than water in double layers or adsorbed to solids, even capillary forces under very dry conditions (in the range of negative 500 meters water pressure head) have a limited effect on H_2O activity in solution (Walton 1994, p. 3481). The assumption of standard state water (Assumption 5.2.1) will not affect the uncertainty in the model and is therefore not designated TBV. This assumption is used throughout.

5.2.2 Redox Conditions

The redox conditions within the drift are assumed to be oxidizing at all times (Assumption 5.2.2). No reduced chemical species or redox reactions are included in the model. For the elements with multiple oxidation states (C, S, N, and Fe), the oxidation states in this model are C(IV), S(VI), N(V), and Fe(III). Thus, total concentrations of these elements in the model are not distributed among other oxidation states. Reducing conditions would preclude use of this model; therefore, the assumption of oxidizing conditions is not TBV. This assumption is used throughout.

5.2.3 Equilibrium Conditions

The model assumes equilibrium chemical conditions (Assumption 5.2.3). Chemical reactions are assumed to occur rapidly compared to anticipated seepage and evaporation rates. However, several slow-forming minerals are not allowed to precipitate (see Section 5.4). The assumption of equilibrium conditions will not affect the uncertainty in the model and is therefore not designated TBV. This assumption is used throughout.

5.2.4 Relative Humidity vs. Time

Figure 1 shows the general trend of how *RH* changes over time. Basically, *RH* decreases to low values shortly after emplacement of high temperature waste containers and as the containers cool over time, *RH* begins to rise until it levels off in the long term below but near 100 percent. The Precipitates/Salts model uses an approximation that *RH* rises to 50 percent at about 200 years and to 85 percent at about 1100 years (Assumption 5.2.4.1). Although *RH* at a given location may reach these values at different times, the assumption is that these are reasonable approximations for the times at which these values are achieved. Uncertainty in the timing will not affect the results of this model. The Precipitates/Salts model requires only an estimate of the timing of these relative humidity values as a seed to generate the results which are independent of time. Thus, the timing of these relative humidity values cancels out in the final results.

The second assumption about relative humidity and time is that relative humidity rises from 50 percent to 85 percent linearly with the logarithm of time (Assumption 5.2.4.2). This approximation is based on the predictions shown in Figure 1 (DTN: SNT05071897001.010) and more recent predictions (DTN: SN0001T0872799.006). This assumption is used to develop lookup tables that are independent of time. It is also a reasonable simplifying approximation for predictions that themselves have a degree of uncertainty. Therefore, this assumption is not TBV.

5.3 ION INTERACTION

Modeling the behavior of electrolytes in concentrated aqueous solutions typically requires the use of Pitzer ion-interaction equations. These semi-empirical equations, documented in the EQ3NR manual (Wolery 1992b, pp. 44-64), are used to estimate activity coefficients that correct for non-ideal electrolyte behavior in saline waters. The code EQ3/6 (version 7.2b) has the option of using Pitzer equations and includes two Pitzer-based thermodynamic databases. The Pitzer option extends the working range of the model calculations from a maximum ionic strength of 1 molal (using the B-dot equation) to 6 molal (Pitzer and Kim 1974, p. 5701) or possibly to 10 or 15 molal or higher (Clegg and Whitfield 1991, p. 295).

The two Pitzer databases included with EQ3/6 version 7.2b are the HMW and PIT databases (DTN: MO9911SPATHD62.002). The HMW database, based on the work of Harvie et al. (1984), is an internally consistent database with 9 elements and 17 aqueous species. Of the aqueous species, two contain sulfur (HSO_4^- and SO_4^{-2}), three contain magnesium (Mg^{+2}, $MgCO_3$ (aq), $MgOH^+$), five contain carbon (CO_3^{-2}, HCO_3^-, $CaCO_3$ (aq), $MgCO_3$ (aq), CO_2 (aq)), two contain calcium (Ca^{+2} and $CaCO_3$ (aq)), and five contain hydrogen or hydroxide (H^+, OH^-, HCO_3^-, HSO_4^-, $MgOH^+$). The remaining ions are Cl^-, K^+, and Na^+. Unfortunately, many elements important to the Precipitates/Salts model are not included in the HMW database, including Al, Fe, Si, F, and N. An additional limitation is that the HMW database is only applicable to water at 25°C.

The PIT database contains a much larger set of aqueous species than the HMW database and allows simulation temperatures spanning the range applicable to the Precipitates/Salts model. It does not include any carbon or silica species. However, the Pitzer coefficients for common

aqueous species in the PIT and HMW databases are either identical or nearly identical. In addition, the equilibrium coefficients for the common aqueous and mineral species are nearly identical. The differences are presumably because of modifications required for internal consistency within the HMW database.

The EQ3/6 Pitzer model was developed to predict aqueous reactions that include species that neither the HMW nor PIT database contain. Specifically, it was designed to predict the interactions of Na, K, Ca, Mg, Cl, F, CO_3, SO_4, NO_3, SiO_2, Fe(III), Al, H, and H_2O at low and high ionic strength and temperatures ranging from 20°C to 95°C. To do this, a new database called PT4 was developed based on assumptions analogous to those used by Reardon (1990) in his extension of a Pitzer model for cement pore water (Assumption 5.3.1). Reardon (1990) used the aqueous Pitzer coefficient data of Harvie et al. (1984) (i.e., the HMW data) but added aqueous species for silica ($H_3SiO_4^-$, $H_2SiO_4^{2-}$, and SiO_2 (aq) [also called $H_4SiO_4^0$]), ferric iron ($Fe(OH)_4^-$), and aluminum ($Al(OH)_4^-$) [also called AlO_2^-]. The Pitzer coefficients for $H_3SiO_4^-$, $Fe(OH)_4^-$, and $Al(OH)_4^-$ were assumed by Reardon to be identical to those of HSO_4^-, while the coefficients for $H_2SiO_4^{2-}$ were assumed to be identical to those for SO_4^{2-}. The Pitzer coefficients for SiO_2 (aq) (or $H_4SiO_4^0$) were assumed to be analogous to those for CO_2 (aq) (or $H_2CO_3^0$). The model was successfully used to predict the sequence of phase transformations involved when concrete is attacked by sulfur dioxide (Reardon 1990, p. 188). The same Pitzer coefficient analogies were assumed to be reasonable for the development of the PT4 database.

The developed PT4 database (DTN: MO9912SPAPT4PD.001) is a modification of the PIT database. Like the database developed by Reardon (1990), the PT4 database is not optimized for peak performance, and the modifications are not calibrated to additional laboratory data (although they may be validated by them). Instead, the modifications are based on analogies and simplifying assumptions to estimate ion interaction so that predictions of hydrogeochemical evolution can be made. The PT4 database was developed for the EQ3/6 salts model simply to satisfy model validation criteria that permit a fairly broad range of uncertainty (Section 6.5.1). Thus, validation of such a database does not need to be held to the same high standards as a universal Pitzer database that is inversely generated from a complete data set.

The Pitzer coefficients for the aqueous species in PT4 are the same as in the PIT and HMW databases. Aqueous species in the HMW database that are not in the original PIT database (i.e., carbonates species) were added to the PT4 database with the same Pitzer coefficients as in the HMW database (Assumption 5.3.2). The four anions and one neutral species that Reardon (1990) added by analogy were added to PT4 with the same binary and mixing coefficients that Reardon (1990) used (Assumption 5.3.3). F^- and NO_3^- basis species were already established in PT4 because they came with the PIT database. These species and the origin of their Pitzer coefficients are listed in Table 9.

Additional tables summarize the aqueous species with Pitzer parameters that were added to the PIT database to generate the PT4 database. Table 10 shows which cation-anion pairs were added that have specified cation-anion β^0, β^1, β^2, and C^ϕ interaction parameters in the Pitzer equations.

Table 11 shows which anion-anion pairs were added that have specified θ interaction parameters. Because the added species having Pitzer parameters were either anionic or neutral, no cation-cation interaction parameters were added. Table 12 shows which cation-neutral species and

anion-neutral species pairs were added that have λ interaction parameters, and Table 13 shows which anion-anion-cation combinations were added that have specified ψ interaction parameters.

Table 9. Aqueous Species in the PT4 Database and the Origins of Their Pitzer Coefficients

PT4 Database Aqueous Species With Pitzer Coefficients	Pitzer Interaction Coefficients Assumption
Al^{3+}, Ca^{+2}, $CaCO_3$ (aq), Cl^-, CO_2 (aq), CO_3^{2-}, F^-, H^+, HCO_3^-, HSO_4^-, K^+, Mg^{2+}, $MgCO_3$ (aq), $MgOH^+$, Na^+, NO_3^-, OH^-, SO_4^{2-}	Equivalent to coefficients in the PIT and/or HMW databases
SiO_2 (aq)	Equivalent to coefficients involving CO_2 (aq) in HMW
$Al(OH)_4^-$, $Fe(OH)_4^-$, and $H_3SiO_4^-$	Equivalent to coefficients involving HSO_4^- in HMW
$H_2SiO_4^{2-}$	Equivalent to coefficients involving SO_4^{2-} in HMW

DTN: MO9912SPAPT4PD.001

Table 10. Cation-Anion Pairs Added to the PT4 Database

Anion	Cation
HCO_3^-	Ca^{+2}, K^+, Mg^{2+}, Na^+
CO_3^{2-},	K^+, Na^+
$H_3SiO_4^-$, $H_2SiO_4^2$, $Al(OH)_4^-$, $Fe(OH)_4^-$, HSO_4^-	Ca^{+2}, H^+, K^+, Mg^{2+}, Na^+
Cl^-	$MgOH^+$
SO_4^{2-}	H^+
OH^-	Ca^{2+}

DTN: MO9912SPAPT4PD.001

Table 11. Anion-Anion Pairs Added to the PT4 Database

Anion	Anion
HCO_3^-	Cl^-, CO_3^{2-}, SO_4^{2-}
CO_3^{2-}	Cl^-, HCO_3^-, OH^-, SO_4^{2-}
$H_3SiO_4^-$, $Al(OH)_4^-$, $Fe(OH)_4^-$	Cl^-

DTN: MO9912SPAPT4PD.001

Table 12. Cation-Neutral and Anion-Neutral Species Pairs Added to the PT4 Database

Neutral Species	Cation or Anion
SiO_2 (aq)	Ca^{+2}, K^+, Mg^{2+}, Na^+, Cl^-, SO_4^{2-}
CO_2 (aq)	Ca^{+2}, K^+, Mg^{2+}, Na^+, Cl^-,

	SO_4^{2-}

DTN: MO9912SPAPT4PD.001

Table 13. Anion-Anion-Cation Interaction Parameters Added to the PT4 Database

Anion	Anion	Cation
HCO_3^-	Cl^-, SO_4^{2-}, $H_2SiO_4^{2-}$	Mg^{2+}, Na^+
HCO_3^-	CO_3^{2-}	K^+, Na^+
CO_3^{2-}	Cl^-, SO_4^{2-}, OH^-, $H_2SiO_4^{2-}$	K^+, Na^+
$H_3SiO_4^-$	Cl^-	Na^+, H^+
$H_3SiO_4^-$	SO_4^{2-}, $H_2SiO_4^{2-}$	K^+, Na^+, Mg^{2+}
$H_2SiO_4^{2-}$	Cl^-	Ca^{2+}, Mg^{2+}, Na^+
$H_2SiO_4^{2-}$	OH^-	K^+, Na^+
$Al(OH)_4^-$, $Fe(OH)_4^-$	Cl^-	H^+, Na^+
$Al(OH)_4^-$, $Fe(OH)_4^-$	SO_4^{2-}, $H_2SiO_4^{2-}$	K^+, Mg^{2+}, Na^+

DTN: MO9912SPAPT4PD.001

For the PT4 database to claim a temperature range of up to 100°C, temperature derivatives of the cation-anion parameters had to be known or estimated. For those that were not available in the PIT database it was assumed for the purposes of the Precipitates/Salt analysis that a median value of the known values could be used (Assumption 5.3.4). Thirty values from the PIT database were used to determine the median values for the $d\beta^0/dT$, $d\beta^1/dT$, $d\beta^2/dT$, and dC^ϕ/dT derivatives. These values, which were 0.000605, 0.00248, -0.385, and -0.0000930, respectively, were assigned to the non-zero cation-anion parameter coefficients added to PT4. The actual temperature derivatives may be much different. How this simplifying assumption affects the accuracy of the model results is not directly investigated; however, the database as a whole is validated based on model validation criteria in Section 6.5.1.

EQ3/6 uses ion activity products of basis species to calculate mineral saturation indices. The basis species used in the PT4 database include: Al^{3+}, Ca^{+2}, Cl^-, F^-, Fe^{3+}, H_2O, H^+, HCO_3^-, K^+, Mg^{2+}, Na^+, NO_3^-, SiO_2 (aq), and SO_4^{2-}. These species are the same basis species included in the COM database. They are also the same basis species included in the PIT and HMW databases for those elements that these databases have in common with this list. This is convenient because minerals defined in the COM, PIT, and HMW databases can be pulled into the PT4 database without having to redefine the reaction and recalculate the equilibrium constants.

Although Al^{3+} and Fe^{2+} are the basis species for Al and Fe in PT4, the Precipitates/Salts model utilizes the basis-switching option in the EQ3/6 input files to switch these basis species to $Al(OH)_4^-$ and $Fe(OH)_4^-$. $Al(OH)_4^-$ and $Fe(OH)_4^-$ are the predominant or major Al and Fe(III) species in the alkaline pH range of most of the Precipitate/Salts analyses and thus will improve code numerics and reduce the number of iterations required for convergence.

At this point it is important to recall that the objective is to develop a database (PT4) that simulates the interactions of Na, K, Ca, Mg, Cl, F, CO_3, SO_4, NO_3, SiO_2, Fe(III), Al, H, and H_2O at low and high ionic strength and temperatures ranging from 20°C to 95°C. At low ionic

strength, Pitzer interactions are not important. Thus, it is desirable at low ionic strength to have the database act like the COM database in which ion pairing is the dominant control on equilibrium calculations. To make this happen, aqueous species that are potentially important to basis species equilibrium activity calculations must be defined in the PT4 database. Without them, the mineral saturation indices, which are defined in terms of the basis species equilibrium activities, will be inflated, and calculated elemental solubilities may be low.

For example, if Al^{3+} and $Al(OH)_4^-$ were the only possible aqueous species for Al in a dilute alkaline solution, then for a given total concentration of Al, the equilibrium activity of Al^{3+} would be too high and would cause saturation indices of Al minerals to be too high. For the aluminum system, there are a number of other hydrolysis products (e.g., $AlOH^{2+}$, $Al(OH)_2^+$, and $Al(OH)_3$ (aq)) and other potentially important complexes (e.g., AlF_4^-, AlF_3 (aq), AlF_2^+, AlF^{2+}, $AlSO_4^+$, and $Al(SO_4)_2^-$ according to the COM database) that could account for a considerable portion of the total dissolved Al concentration. Because the hydrolysis products are thermodynamically more favored than Al^{3+} for dilute alkaline solutions, then including them would considerably reduce the calculated activity of Al^{3+}. In turn, this would considerably reduce the calculated saturation indices of Al minerals and, hence, considerably increase the calculated solubility of Al in solution. According to the Al-F and Al-SO_4 ion pairing data in the COM database, the Al solubility could be further increased by the presence of a high concentration of F or SO_4. Thus, it is important to consider all potentially important aqueous species when calculating saturation indices, at least when Pitzer equations do not account for all ion interactions.

Table 14 lists the aqueous species in the PT4 database. This table also shows the sources of the thermodynamic data for these species. No Pitzer coefficients are available for the aqueous species added to improve solubility calculations. Therefore, no Pitzer coefficients (or coefficients of zero) were given to these aqueous species in the PT4 database.

Validation of the PT4 database is demonstrated for the intended use in Section 6.5. The assumptions used to develop the database are implicit in this designation. These assumptions do not affect calculations in dilute solutions.

Table 14. Aqueous Species in the PT4 Database and the Source of Their Thermodynamic Data

PT4 Database Species Type	List of Species in Type	Source of Thermodynamic Data [a]
Basis Species	Al^{3+}, Ca^{+2}, Cl^-, F^-, Fe^{2+}, H^+, H_2O, HCO_3^-, K^+, Mg^{2+}, Na^+, NO_3^-, SiO_2 (aq), SO_4^{2-}	PIT and/or COM database
Aqueous Species with Pitzer Coefficients	Al^{3+}, $Al(OH)_4^-$, Ca^{+2}, $CaCO_3$ (aq), Cl^-, CO_2 (aq), CO_3^{2-}, F^-, $Fe(OH)_4^-$, H^+, $H_2SiO_4^{2-}$, $H_3SiO_4^-$, HCO_3^-, HSO_4^-, K^+, Mg^{2+}, $MgCO_3$ (aq), $MgOH^+$, Na^+, NO_3^-, OH^-, SO_4^{2-}	PIT and/or COM database
Aqueous Hydrolysis Products Added to Improve Solubility Calculations for Al and Fe(III) in Alkaline Solutions	$Al(OH)^{2+}$, $Al(OH)_2^+$, $Al(OH)_3$ (aq), $Fe(OH)_2^+$, $Fe(OH)_3$ (aq), $Fe(OH)^{2+}$	COM database
Other Aqueous Complexes Added to Improve Various Solubility Calculations	AlF_2^+, AlF^{2+}, AlF_3 (aq), AlF_4^-, $AlSO_4^+$, $Al(SO_4)_2^-$, CaF^+, $CaNO_3^+$, $FeCl_2^+$, $FeCl^{2+}$, $FeCl_4^-$, FeF^{2+}, FeF_2^+, $FeNO_3^{2+}$, $FeSO_4^+$, MgF^+	COM database
	$MgOH^+$	CHV database

DTN: MO9912SPAPT4PD.001

[a] All sources from databases in EQ3/6 version 7.2b software package (DTN: MO9911SPATHD62.002)

5.4 MINERALS AND GASES

The PT4 database contains all minerals and gases originally within the PIT database plus CO_2 (g) and a number of carbonates, silicates, and other minerals that were not present in the PIT database. The additional gas and mineral phases were added because of their potential importance in the aqueous system to be modeled.

Table 15 lists minerals included in the PT4 database, the source of the thermodynamic data, and where they occur in natural settings. The added reaction data from the COM database were copied directly from the COM database. For the additional minerals that were not in any of the EQ3/6 databases, equilibrium constants were calculated from Gibbs free energies according to the relationships described in Stumm and Morgan (1996, pp. 41-44). The Gibbs free energies (MO9912SPAGIBFE.000) are handbook values and therefore are accepted data. Because the PIT database itself is not internally consistent, the addition of these minerals is assumed not to threaten database consistency (Assumption 5.4.1). These minerals are included in the PT4 database because of their potential to precipitate.

Minerals that would likely either form very slowly or not form at all under the expected conditions within the drift are prevented from precipitating in the model when their calculated saturation indices exceed zero. Table 16 lists the minerals in the PT4 database that were suppressed in the analyses presented in this AMR and the reasons for their suppression (Assumption 5.4.2). This assumption is not TBV because it is investigated in a calculation described in the next paragraph. The only suppressed minerals that became supersaturated in the calculations used to develop the Precipitates/Salts model lookup table calculations (Table 18, Table 19, and Table 20) were quartz, maximum microcline, K-feldspar, albite, albite low, tridymite, diaspore, and dolomite.

There is evidence that albite low may precipitate authigenically at low temperatures (Fishman et al. 1995). In the EQ3/6 calculations, albite low precipitates if allowed to do so (DTN: MO0003MWDMIN45.011). However, the effects on the Precipitates/Salts model output (Table 18, Table 19, and Table 20) are negligible, primarily because Al is a minor constituent of the incoming seepage and albite low is a minor component of the precipitating mineral assemblage. This was determined by a separate set of EQ3/6 calculations in which albite low was allowed to precipitate (DTN: MO0003MWDMIN45.011).

Table 15. Minerals Included in PT4 Database

Mineral	Chemical Formula	Data Source	Occurrence
Alunite	$KAl_3(OH)_6(SO_4)_2$	PIT[a]	Hydrothermal mineral, sulfuric acid solution acts upon K-rich feldspar[d]
Analcime	$Na_{3.96}Al_{0.96}Si_{2.04}O_6{:}H_2O$	COM[b]	T-Zeolite Rock forming or hydrothermal weathering of Basalt, authigenic product of saline lakes [d, e, f]
Anhydrite	$CaSO_4{:}2H_2O$	PIT	Evaporite, late stage (caprock), some amygdaloidal cavities in basalt[d]
Aphthitalite	$NaK_3(SO_4)_2$	PIT	Evaporite, non marine [e]
Aragonite	$CaCO_3$	COM	Carbonate-less stable at low T than Calcite, hydrothermal , associated with gypsum & iron ore[d]
Brucite	$Mg(OH)_2$	PIT	Chlorite schists, Metamorphic, Alteration product of periclase & serpentine[d]
Burkeite	$Na_6CO_3(SO_4)_2$	COM	Evaporite, major mineral in Na-Cl-CO_3-SO_4 brine[e]
Calcite	$CaCO_3$	COM	Common chemical sedimentary mineral[d]
Carnallite	$KMgCl_3{:}6H_2O$	PIT	Marine evaporite usually massive to granular crystals[d]
Carobbite	KF	Data[c]	Evaporite
Chalcedony	SiO_2	COM	Low temperature amorphous form of quartz, hydrothermal[d]
Clinoptilolite-hy-K Clinoptilolite-hy–Na	$(Na,K)_{3.47}Al_{3.45}Fe_{0.017}Si_{14.53}O_{36}$	COM	Zeolite [e,f]
Clinoptilolite-K Clinoptilolite –Na	$(Na,K)_{3.47}Al_{3.45}Fe_{0.017}Si_{14.53}O_{36}{:}$ $10.92H_2O$	COM	Zeolite from devitrified tuff [e,f]
Dolomite	$CaMg(CO_3)_2$	COM	T Carbonate, often marine[d]
Epsomite	$MgSO_4{:}7H_2O$	PIT	Lake bed deposits, efflorescence on cave walls, Mg-sulfate spring waters [d,e]
Fluorite	CaF_2	PIT	T Usually hydrothermal veins [d]
Gaylussite	$CaNa_2(CO_3)_2{:}5H_2O$	COM	Rare hydrous carbonate – evaporite[d]
Goethite	FeOOH	COM	common weathering product of iron bearing minerals, also inorganic/biogenic precipitate[d]
Glauberite	$Na_2Ca(SO_4)_2$	PIT	Saline lakes with Na-Ca-SO_4 brines[e]
Gregoryite	K_2CO_3	Data[c]	Evaporite, mineral name unofficial (IMA)
Gypsum	$CaSO_4$	PIT	Common sulfate, evaporite[d]
Halite	NaCl	PIT	Evaporite, major salt in closed basins[d]
Hematite	Fe_2O_3	COM	T hydrothermal iron oxide, wide distribution[d]
Kaolinite	$Al_2Si_2O_5(OH)_4$	COM	T Clay-Phyllosilicate Mica group, secondary mineral, feldspar alteration[d]
Mirabalite	$Na_2SO_4{:}10H_2O$	PIT	Evaporite, Ca-SO_4 brine[e]
Montmor-Ca	$Ca_{0.165}Mg_{0.33}\ Al_{1.67}$ $Si_4O_{10}(OH)_2$	COM	Smectite clay, altered volcanic ash[d]
Montmor-K Montmor-Na	$(Na,K)_{0.33}Mg_{0.33}\ Al_{1.67}$ $Si_4O_{10}(OH)_2$ Montmorillonite	COM	Smectite clay, altered volcanic ash[d]
Montmor-Mg	$Mg_{0.495}Al_{1.67}\ Si_4O_{10}(OH)_2$	COM	Smectite clay, altered volcanic ash[d]
Mordenite	$Ca_{0.2895}Na_{0.361}Al_{0.94}Si_{5.06}O_{12}{:}$ $3.468H_2O$	COM	T-Zeolite, basaltic setting, above water table[f]

Nahcolite	$NaHCO_3$	COM	Evaporite[e]
Natron	$Na_2CO_3{:}10H_2O$	COM	Soda, unstable at atmospheric conditions, changes to thermonatrite[e]
Niter	KNO_3	PIT	Evaporite[g]
Nontronite-Ca Nontronite-Mg	$(Ca, Mg)_{0.165}Fe_2Al_{0.33}Si_{3.67}H_2O_{12}$	COM	Smectite clay[d]
Nontronite-K Nontronite-Na Nontronite-H	$(Na,K, H)_{0.33}Fe_2Al_{0.33}Si_{3.67}H_2O_{12}$	COM	Smectite clay[d]
Quartz	SiO_2	COM	T Rock forming or hydrothermal[d]
Sellaite	MgF_2	PIT	Evaporite[g]
Sepiolite	$Mg_4Si_6O_{15}(OH)_2{:}6\ H_2O$	COM	Associated with serpentine. May ppt. from alkaline saline water in arid environments[e]
Siderite	$FeCO_3$	COM	Found in clay ironstone[d]
Soda Niter	$NaNO_3$	Data[c]	Common in arid regions with caliche, also called nitratite[d,g]
Sylvite	KCl	PIT	Evaporite – late precipitate[d]
Tachyhydrite	$CaCl_2 2MgCl_2 12H_2O$	PIT	Major mineral in Ca-Mg-Na-Cl brine[e]
Thenardite	Na_2SO_4	PIT	Nonmarine evaporite[e]
Thermonatrite	$Na_2CO_3{:}H_2O$	COM	Dry lakes, stable form or natron[e]
Trona	$Na_3CO_3HCO_3{:}2H_2O$	Data[c]	Evaporite, lake deposits[d,e]
Trona-K	$K_2NaH(CO_3)_2{:}2H_2O$	COM	Evaporite, lake deposits
Villiaumite	NaF	Data[c]	Rare evaporite[g]

DTN: MO9912SPAPT4PD.001

[a]Mineral found in PIT database (DTN: MO9911SPATHD62.002)

[b]Mineral added from COM database (DTN: MO9911SPATHD62.002)

[c]DTN: MO9912SPAGIBFE.000

[d]Klein and Hurlbut 1999

[e]Eugster and Hardie 1978

[f]Murphy and Pabalan 1994

[g]Sonnenfeld 1984, pp. 149, 459

Table 16. Minerals in the PT4 Database that are Suppressed for the Precipitates/Salts Model Lookup Table Calculations

Mineral	Chemical Formula	Data Source	Reason for Suppression
Albite high	$NaAlSi_3O_8$	COM[b]	Rock forming sodium plagioclase[d]
Albite low [c]	$NaAlSi_3O_8$	COM	Rock forming sodium plagioclase [d,f]
Albite	$NaAlSi_3O_8$	COM	Rock forming sodium plagioclase [d,f]
Corundum	Al_2O_3	PIT	Accessory mineral in metamorphic rocks or rock forming in silica deficient igneous rocks[d]
Cristobalite(alpha)	SiO_2	COM	Rock forming mineral, Below 268ºC, low temp form [d,f]
Cristobalite(beta)	SiO_2	COM	Rock forming mineral, High temp 1470 to 1728ºC, above 268ºC at 1 atm [d]
Diaspore	$AlHO_2$	PIT	Major constituent in bauxite, associated with corundum in emery rock, in dolomite and chlorite schist[d]
Dolomite	$CaMg(CO_3)_2$	COM	T Carbonate, often marine[d]
Hercynite	$FeAl_2O_4$	PIT	Similar to spinel associated with corundum[d]
Ice	H_2O	PIT	Temperature too high
Illite	$K_{0.6}Mg_{0.25}Al_{0.5}Si_{3.5}O_{10}(OH)_2$	COM	General term for mica-like minerals, clay, alkali deficient, common in shales[d]
K-Feldspar	$KAlSi_3O_8$	COM	Rock forming potassium feldspar [d,f]
Maximum Microcline	$KAlSi_3O_8$	COM	Rock forming potassium feldspar[d]
Spinel	Al_2MgO_4	PIT	Common high temperature mineral, contact metamorphism of argillaceous rocks poor in silica. Or accessory in mafic igneous rocks[d]
Tridymite	SiO_2	COM	Rock forming, stable 870°C to 1470°C [d,f]

DTN: MO0003MWDTAB45.013

[a]Mineral found in PIT database (DTN: MO9911SPATHD62.002)

[b]Mineral added from COM database (DTN: MO9911SPATHD62.002)

[c]See text in this section about suppressing albite low.

[d]Klein and Hurlbut 1999

[f]Murphy and Pabalan 1994

5.5 SALT STABILITY AT LOW RELATIVE HUMIDITY

Several simplifying assumptions were used in the development of the Low Relative Humidity (LRH) salts model. Simplifying assumptions are necessary because the chemical evolution and dissolution of salt assemblages in natural evaporite systems are not well-understood or easily predicted. Because of procedural requirements, these assumptions are included before the importance of relative humidity is discussed and the model is presented in Section 6. Potential confusion may be reduced by reading Section 6 first. The assumptions presented below affect the model development in Section 6.4.1 and the results in Sections 6.6.2 and 6.6.3.

The LRH salts model covers the time period in which the relative humidity is less than 85 percent. Above 85 percent, the EQ3/6 Pitzer model is used. Due to a lack of data for the most current EBS design, the TH model results plotted in Figure 1 are used to approximate the time

required for *RH* to rise to 85 percent. According to these data, it will rise to 85 percent after about 1100 years (Assumption 5.2.4.1, above).

The LRH salts model assumes a constant seepage rate (Q^s) and constant seepage composition (Assumption 5.5.1). However, because abstractions may be used to divide the modeling period into a sequence of time periods having constant conditions, these assumptions are not TBV.

The dissolved solids in the seepage composition are restricted to Na, K, NO_3, SO_4, Cl, and CO_3 (Assumption 5.5.2). According to the EQ3/6 Pitzer model results (Section 6), these components are the most soluble in evaporated J-13 well water. The other components are almost entirely precipitated at lower ionic strengths in evaporated J-13 well water (Section 6). Thus, the assumption that other components need not be considered in this submodel will not considerably affect the conclusions. Therefore, this assumption is not TBV.

The model begins by precipitating all dissolved solids in incoming seepage. Boiling temperatures and a relative humidity below 50 percent are predicted to occur for many years within the drift (Figure 1). These conditions are predicted to result in dry conditions. The precipitated salts are considered to accumulate in a "reactor" which can be any location between the seepage entry point and the waste package. Two of the most likely positions for such a reactor are atop the drip shield and within a specific portion of the backfill above the drip shield. In this simple model, a storage capacity is not considered. There is no limit to the amount of salt that accumulates in the reactor, and the mass of brine that drains out of the reactor at the end of the time increment is equivalent to the mass of brine produced within the time increment.

The previous Precipitates/Salts model (CRWMS M&O 1998b) suggests that sodium and potassium nitrate may be the last salts to precipitate because of 1) their high solubility, 2) the EQ3/6-predicted evaporative evolution of J-13 well water, and 3) the hygroscopic nature of the nitrate salts. CRWMS M&O (2000, p. 6-12) shows that the equilibrium relative humidity of sodium nitrate under boiling conditions (~120°C according to Saxton et al. 1928, V. 3, p. 326) is approximately 50 percent. Because the early TH results indicate that the temperature falls to approximately 120°C when the *RH* rises to about 50 percent (Figure 1), it is assumed that nitrate salts accumulate until the *RH* in the reactor rises to 50 percent (Assumption 5.5.3). This is not an unreasonable assumption based on the relationship between salts, brine stability, and relative humidity (Section 6.1). This assumption is conservative and is therefore not TBV.

The amount of brine produced in the LRH model is controlled by the effective solubilities of the dissolved salts and the assumed fraction of moles of these salts in the reactor that are allowed to dissolve as a function of time. For the nitrate salts, the entire amount of accumulated nitrate salts are allowed to dissolve as soon as the *RH* reaches 50 percent (Assumption 5.5.3, above). For the remaining salts, the fraction of moles that have accumulated in the reactor that dissolve within a time increment is approximated as a function of time. Specifically, this fraction is assumed to increase exponentially from zero to one as time increases from a *RH* of 50 percent to 85 percent (Assumption 5.5.4). Thus, at 85 percent *RH*, all accumulated salts are dissolved. A more analytical approach would be to predict dissolved concentrations as a function of *RH* and to deplete the solid phases accordingly by mass balance, but such an approach would be based on poorly understood salt interactions in concentrated brines of evaporite systems. The simplified approach taken in the LRH salts model at least ensures that the concentrations and dissolution of

non-nitrate salts generally increase with increasing *RH*, as would be expected, and that all of these soluble salts will be dissolved by the time *RH* reaches 85 percent. At the same time, this simplified approach conserves mass, maintains charge balance, and estimates the amount of water in the produced brine as a function of time. Furthermore, this assumption provides reasonably conservative results for the intended use and is therefore not TBV.

The amount of water in the brine generated during each time increment is controlled by the amount of dissolved salts in the reactor during the time increment and the assumed effective solubilities of the salts. It is assumed that the mass of water (m_j^w) in the generated brine at time increment j can be estimated from the following equation:

$$m_j^w = \sum_a \frac{M_{a,j}^d}{S_a} \qquad \text{(Eq. 2)}$$

where $M_{a,j}^d$ and S_a are, respectively, the dissolved moles of anion a at time increment j and effective solubility (molal) of anion a in the reactor (Assumption 5.5.5). This equation, which represents the summation of the contributions of each dissolved salt to the total mass of water in the reactor, is supported by the literature (Kinsman 1976, p. 274). Again, however, predicting the effective solubilities of salts in a mixed, high temperature, J-13 salt system is not possible with a high degree of certainty. Therefore, the actual values of the effective solubilities are assumed to be 24.4 molal for nitrate salts (based on the pure phase solubility of KNO_3, presented in Table 1) and approximately 3 to 4 molal for the non-nitrate salts (Assumption 5.5.6). The 3 to 4 molal range for the non-nitrate salts is chosen to provide a good fit between the LRH salts model and the EQ3/6 Pitzer model at 85 percent relative humidity. This range is reasonable because it is within the range of the solubilities listed in Table 1 for pure Cl, CO_3, and SO_4 salts. This simplifying assumption does not affect the uncertainty in the model and is therefore not designated TBV.

Two additional assumptions for the LRH salts model involve the treatment of carbonate. First, the carbonate in the LRH salts model is assumed to be "soluble" carbonate (Assumption 5.5.7). The "soluble" carbonate is determined from the EQ3/6 Pitzer model results of evaporated J-13 water to a water activity of about 0.85. For evaporated J-13 water, this water activity occurs at an ionic strength of approximately 10 molal. According to the EQ3/6 results, a considerable amount of carbonate precipitates with Ca and Mg, but carbonate continues to concentrate. At a water activity of approximately 0.85, the remaining carbonate is considered "soluble" because the only salts it can form are K or Na salts. This reasonable assumption does not affect the uncertainty in the model and is therefore not designated TBV.

The second assumption involves estimating carbonate exchange with the atmosphere. The LRH salts model cannot be used to directly equilibrate the carbonate with the partial pressure of carbon dioxide. However, the amount of dissolved and precipitated carbonate can be constrained by charge balance. To achieve the 0.85 activity of water end point, the carbonate concentration in the incoming seepage is adjusted to achieve a Na:CO_3 ratio equivalent to the ratio of the EQ3/6 model results at 0.85 activity of water (Assumption 5.5.8). This reasonable assumption does not affect the uncertainty in the model and is therefore not designated TBV.

The final assumptions involve charge balance. Because of the assumptions regarding the treatment of carbonate and the inability of the LRH salts model to calculate and track pH, the model will inevitably use an incoming seepage that is not perfectly charge balanced. The model, however, is designed to mitigate the effects of the charge balance error by maintaining the charge imbalance throughout the calculation. Na concentrations and moles in each phase and each time increment are calculated by charge balance in the LRH salts model in a manner that maintains any original charge imbalance (Assumption 5.5.9). The valency of the carbonate is assumed to be between 1 and 2 depending on the pH calculated by the EQ3/6 Pitzer model for evaporated seepage (Assumption 5.5.10). For example, for a pH around 10, a valency of 1.33 is chosen to reflect an average valency of two parts HCO_3^- and one part CO_3^{2-}. For pH of about 9 or below and 11 and above, valencies of 1 and 2 are chosen, respectively. This reasonable assumption is not TBV because it does not affect the uncertainty in the model.

5.6 CONDENSED WATER MODEL

A model to predict the pH and ionic strength of condensed water underneath the drip shield or on other unreactive surfaces in the drift is also developed in this AMR. The only assumption required for this model is that the composition of the condensed water can be predicted based on equilibrium between pure water and the fugacity of carbon dioxide at a given temperature (Assumption 5.6). This assumption implies that the water does not react with dust, salts, or other material that would provide an additional source of ions. This model and its output are developed for downstream users who accept this assumption. Therefore, this assumption is not TBV.

6. MODEL

6.1 REVIEW OF SALTS/PRECIPITATES PROCESSES

6.1.1 Evaporation, Relative Humidity, and Salt Precipitation

Within a drift environment, water exists in two phases, liquid and vapor. Because these two phases are in contact with one another throughout time (except in the event that all liquid water vaporizes), Brownian motion causes water molecules to exchange constantly between the two phases. According to the Maxwell-Boltzmann law, a fraction of the molecules in one phase has the energy required to make the transformation to the other phase, and vice versa, for as long as both phases exist (Mahan 1975, pp. 131-139).

Under equilibrium conditions, there is no net movement of water molecules from one phase to the other, i.e., the non-zero evaporation rate equals the non-zero condensation rate. For liquid water to be in equilibrium with the vapor phase, the partial pressure of water vapor must equal the saturation vapor pressure of the liquid water at the conditions of the system.

Relative humidity is the ratio, expressed in percent, of the measured water vapor pressure and the saturated water vapor pressure at the same temperature and total pressure. This definition applies to water in its standard state. In porous media or on solid surfaces, there are other mechanisms that decrease the saturation water vapor pressure of the liquid, such as capillary binding of water by surface tension, osmotic binding of water in double layers, and direct adhesion of water

molecules to solid surfaces by London-van der Waals forces (Koorevaar et al. 1983, p. 63). For the current Precipitates/Salts model, it is assumed that these effects are negligible (Assumption 5.2.1).

Dissolved salts in water also decrease the saturation water vapor pressure because they reduce the chemical activity of water in the solution. The chemical activity of the water molecule, which is proportional to the mole fraction of water in the aqueous solution, is equivalent to the equilibrium relative humidity of the solution (Kinsman 1976, p. 274). As a result, brines reach liquid-vapor equilibrium, and thus stability, at relative humidity values below 100 percent. This effect on brine stability is considered in the Precipitates/Salts model.

Because the relative humidity within the potential drift is expected to be below 100 percent for many years during the pre- and post-closure periods, dilute ground water is not expected to be at liquid-vapor equilibrium within the drift during this time. For any dilute ground water that resides or flows into the drift during this period, there is a net transfer of liquid water to the vapor phase which results in increasing concentrations of dissolved salts in the remaining liquid water. If the vaporization rate is rapid compared to the flux of liquid water flowing into the drift, brines will develop within the drift. In addition, if the relative humidity is sufficiently low, dissolved salts will precipitate until either a more stable brine develops or dry conditions result.

6.1.2 Formation and Chemistry of Brines and Salt Precipitates

As water evaporates from solution, dissolved solids concentrate until they become supersaturated with respect to a solid phase whereupon, assuming conditions are favorable and precipitation is rapid, the solid phase will precipitate. If the solid phase is a binary salt and the concentrations of the two reactants (multiplied by their stoichiometric coefficients) are not equal, then the reactant having the lower relative concentration (multiplied by its stoichiometric coefficient) will become depleted in solution while the other reactant will continue to concentrate within the solution (Eugster and Hardie 1978, pp. 243-7, Eugster and Jones 1979, pp. 614-629). This mechanism is known as a chemical divide (Drever 1988, p. 235-6). A chemical divide determines which reactant concentrations are predominantly controlled by the solubility of a precipitating phase (i.e., those that become depleted in solution) and which reactant concentrations are only partially controlled by a precipitating phase (i.e., those that continue to concentrate in solution despite partial precipitation).

The chemical divide during evaporative precipitation is demonstrated by thermodynamic calculations and studies of saline lakes and sabkhas. Garrels and Mackenzie (1967) thermodynamically simulated the evaporative evolution of Sierra Nevada spring water into a strongly alkaline sodium carbonate brine observed in natural saline lakes in the western United States. In these calculations, calcite precipitated first, depleting the aqueous calcium concentration. Calcite precipitation is an important evolutionary step because the chemical divide for calcium and carbonate will determine whether the evaporating water will become carbonate poor or carbonate rich (Eugster and Hardie 1978, pp. 244). In this case, the water became carbonate rich. Next in the calculations, precipitation of sepiolite depleted the magnesium concentration. Continued evaporation resulted in a sodium carbonate brine with a pH near 10.

Studies of saline lakes in the western United States show that alkaline sodium carbonate brines, such as the brine derived by Garrels and Mackenzie (1967), are common (Eugster and Hardie 1978, p. 240). Many of these same alkaline brines occur in volcanic terrain and have high silica content (Jones et al. 1967). These waters are also enriched in chloride, sulfate, and to some extent potassium. Although potassium is a highly soluble salt, studies of naturally occurring brines indicate that it is largely removed during evaporative precipitation. The likely mechanisms for this removal are ion exchange reactions on clay minerals, silicate gels, and volcanic glass (Eugster and Hardie 1978, pp. 246).

In the late stage of evaporation, the highly soluble components precipitate. In carbonate-rich brines, these salts include, but are not limited to, Na, Cl, SO_4, CO_3, and SiO_2 (Eugster and Hardie 1978, p. 244). The predominant dissolved solids in carbonate-poor brines, such as brines resulting from the evaporation of sea water, are Na, Ca, Mg, Cl, and SO_4 (Eugster and Hardie 1978, p. 244). Other dissolved solids that have been observed to become enriched in some brines include F, Br, Sr, PO_4, and B (Eugster and Hardie 1978, p. 239-241). NO_3, although it is highly soluble, is not mentioned (and perhaps not investigated) in these studies.

The sequence of salt precipitation by evaporation depends on the chemistry of the solution and the environment. The relative and total concentrations of the dissolved salt species and the solubilities of the solid salt phases determine when a dissolved species becomes supersaturated, when it begins to precipitate, which other species precipitate with it, and which species continue to concentrate in the remaining solution.

The aqueous solubilities of various combinations of binary Na and K salts at 100°C are presented in Table 1. Each value represents the maximum amount of the specified salt that can be dissolved into pure water at the given temperature. These handbook values are useful in assessing semi-quantitatively the relative solubilities of different salts in an aqueous solution containing many different dissolved solids. For example, Table 1 indicates that sulfate salts and sodium fluoride are some of the least soluble of these salts.

In naturally occurring brines, high sulfate concentrations are attributed to the dissolution of gypsum in geologic strata or the oxidation of sulfides such as pyrite which are widespread in the western United States (Eugster and Hardie 1978, pp. 243). In a carbonate-poor (calcium-rich) brine, such as a brine derived from the evaporation of sea water, sulfate precipitates as gypsum or anhydrite before halite precipitates (Kinsman 1976, p. 275). In carbonate-rich alkaline brines, sulfate precipitates as a sodium salt (Eugster and Hardie 1978, pp. 246). Based on the data in Table 1, sulfate salts would be expected to precipitate due to evaporation prior to halite or other more soluble salts, given approximately equal concentrations of sulfate and chloride in the solution.

Another indication of the likely sequence of salt precipitation is evident in the comparison of hygroscopic properties, i.e., the abilities of different brines or salts to absorb water from the air. Table 2 lists literature values of the equilibrium relative humidity of aqueous solutions saturated with a given salt. Lower values in this table imply lower chemical activities of H_2O (see previous section) and therefore higher salt solubilities. This relationship is apparent when comparing the values in Table 1 and Table 2.

For evaporating sea water, when the chemical activity of H_2O falls below 0.93 due to net evaporation of water into air having a relative humidity less than 93 percent, calcium sulfate precipitates (Kinsman 1976, p. 273). In this same water, when the chemical activity of H_2O falls below 0.77 due to net evaporation of water into air having a relative humidity less than 77 percent, halite precipitates (Kinsman 1976, p. 274-5). Thus, as water evaporates, the chemical activity of water in the brine decreases, forcing less hygroscopic, less soluble salts to precipitate before more hygroscopic, more soluble salts. Based on the values in Table 1 and Table 2, it follows that the sequence of precipitation in a calcium-poor (carbonate-rich) brine is likely sodium sulfate followed by halite.

The most reliable method for determining the sequence of precipitation reactions, however, is to track the aqueous activities of the dissolved components during evaporation and precipitation. When the ion activity product of a salt exceeds the solubility equilibrium constant of the precipitation reaction, the salt will begin to precipitate, assuming the rate of the reaction is sufficiently rapid (Stumm and Morgan 1996, pp. 351-9). Precipitation will stop as soon as the ion activity product falls to the point where it is equal the solubility equilibrium constant of the reaction.

Evaporative precipitation generally results in the precipitation of dissolved solids from solution. One exception is carbonate because it equilibrates with carbon dioxide and can degas. Degassing of carbon dioxide in alkaline brines results in the reaction:

$$2HCO_3^- = CO_3^{2-} + CO_2 + H_2O \qquad \text{(Eq. 3)}$$

which causes the pH to rise (Drever 1988, p. 244). This pH rise is enhanced by the decrease in carbon dioxide solubility as salinity increases (Eugster and Jones 1979, pp. 614). However, despite carbon dioxide degassing, continued evaporation results in the precipitation of sodium carbonate salts, such as trona (Jones et al. 1977, p. 64; Eugster and Hardie 1978, p. 246).

For silica, wetting and drying cycles tend to cause much of the silica precipitation in alkaline brines. At Lake Magadi in Kenya, complete evaporation causes the formation of silica crusts that do not easily dissolve during the following wetting cycle due to slow kinetics. As a result, only the most soluble salts, e.g., Na, K, Cl, and SO_4 dissolve into the recharged interstitial waters (Eugster and Hardie 1978, pp. 245-6).

6.1.3 Potential Brines and Salt Precipitates at Yucca Mountain

A number of simulations and experimental studies have been performed in the past few years to directly assess evaporative precipitation effects within and near the potential repository in Yucca Mountain. According to these studies, water entering the drift will have variable composition as a function of time as a result of the boiling/condensation and reaction of both heated and condensed waters with minerals and gases in the fractures of the host rocks (Arthur and Murphy 1989; Glassley 1994; Murphy 1993; Wilder 1996; Lichtner and Seth 1996; Glassley 1997; Hardin 1998, Section 6.2.2). These reacted, or thermally perturbed, fluid compositions may flow down fracture pathways and enter potential emplacement drifts where they could undergo reaction with introduced materials or be boiled again depositing mineral precipitates containing salts (Glassley 1994; Murphy and Pabalan 1994; Wilder 1996; Lichtner and Seth 1996). The

total amounts of salts deposited within the drifts will depend on the composition of ambient water within the unsaturated zone.

As temperature increases, a number of changes may affect the geochemical behavior of the near-field environment. Mineral stabilities and phase equilibria are temperature dependent, and the rates at which reactions occur will generally increase at higher temperatures. Both continuous reactions such as the gradual dehydration or shift in cation composition of a solid phase, and discontinuous reactions such as the disappearance of a phase outside of its stability range, will occur as temperature increases (Glassley 1994; Murphy 1993; Hardin 1998, Sections 5 and 6). The higher temperatures in the near-field may result in regions where attainment of thermochemical equilibrium can be assumed (Glassley 1994).

The increased temperatures are predicted to vaporize much of the water in the near-field as an above-boiling zone forms within the drift and in the very near-field (Glassley 1994). This transition would increase the capacity of the system to transport moisture as volatiles and would result in precipitation of dissolved solids from boiling fluids in the near-field. Condensation of water in cooler regions above the potential repository horizon may dissolve new material, which could be transported through fractures back down into the boiling zone with subsequent boiling and phase precipitation.

Because boiling of fluids will occur, mineral precipitates including salts will form in the region of boiling. Water undergoing boiling/evaporation or reacting with precipitated salts will become concentrated in a number of dissolved constituents either in close proximity to, or within, potential emplacement drifts (Hardin 1998, Section 6.2.2). Such fluids represent a second end-member for reaction with the EBS. Currently these fluid compositions are primarily constrained by the results of geochemical mass-transfer calculations for simplified systems designed to simulate the evaporation/boiling that would occur within a thermally perturbed repository environment. Results from two such calculations (Murphy and Pabalan 1994; Wilder, 1996; Hardin 1998, Section 6.2.2) are discussed here.

In one calculation (Wilder 1996; Hardin 1998 Section 6.2.2), J-13 water evaporates/boils along a temperature rise from ambient to 95°C at equilibrium with atmospheric gases. These calculations represent 95 percent evaporation. The second set of calculations (Murphy and Pabalan 1994) starts with model water evolved at 75°C (heated J-13 water that has reacted with tuff) and heats it instantaneously to 100°C in equilibrium with atmospheric oxygen and the calculated CO_2 fugacity. (This latter parameter value is higher than atmospheric values and was derived from a coupled reactive transport calculation in which both gas and fluid flow were calculated.) The compositions resulting from this second set are given up to about 99.6 percent evaporation. Even though the results of these two calculations are not directly comparable (because they represent different compositional systems and different controls on the gas phase), they appear to be roughly consistent. Relative to ambient compositions these fluids have, in general, high ionic strength (greater than 1 molal stoichiometric ionic strength for the 99.6 percent evaporated case), are enriched in alkalis, chloride, sulfate, and other ligands (F^-, and HCO_3^-), and have higher pH (~9.5).

Because mineral precipitation occurs throughout these calculations (calcite, silica polymorphs, etc.), these compositions do not represent simply concentrated ambient values, but are selectively

concentrated. In both sets of calculations, the dissolved Ca content is low (<50 mg/kg) because calcite precipitation depletes the fluid of Ca. However, other elements that are conservative within the aqueous phase are orders of magnitude higher than at ambient conditions. For example, at the 99 and 99.6 percent evaporation points, chloride concentrations are about 100-times and about 250-times higher, respectively, than the average value for J-13 water (Murphy and Pabalan 1994).

Modeling results of water evaporation indicate that resultant composition may be profoundly affected by the gas phase assumed to be in equilibrium with the evaporating water and whether the system behaves as open to the atmosphere or in a closed manner (Wilder 1996; Hardin 1998, Section 6.2.2). In equilibrium with the atmosphere gas, initial J-13 well water evolves to higher pH (>9.5) and lower Eh (~+500 mV) at high degrees of evaporation, compared to the case where the system is isolated from the atmosphere for which the final values are pH < 6.8 and Eh > +650 mV. The model results are very sensitive to the constraints on CO_2 fugacity (Murphy and Pabalan 1994), with different solid phases precipitating for lower CO_2 fugacities. When refluxed water is nearly completely evaporated, more calcite precipitates in an open system compared to a closed system (Glassley 1993; Murphy and Pabalan 1994). These results emphasize the need to have a model that incorporates consistently the evolution of near-field gas composition, and the need to have such constraints defined for each scenario.

In another modeling study, Lichtner and Seth (1996) used a multiphase, multicomponent, nonisothermal reactive transport code to simulate the evolution, vaporization, and condensation of groundwater through the vertical centerline of the repository during the boiling period. This type of code does not fix local gas fugacities within the grid block, but evaluates them based on multiphase reactions. Their results predict that in the vicinity of the potential repository, the pH rises to about 10 and chloride concentration increases to approximately 100 mg/L in the vicinity of the drift. Lichtner and Seth (1996) indicate that a 10-fold increase in J-13 fluid concentrations (for conservative elements) could be a reasonable water composition entering the drift through fractures during the boiling period. Quartz and calcite were predicted to dissolve where water condenses and precipitate where water evaporates (Lichtner and Seth 1996).

6.1.4 Precipitates/Salts Model Developed for the TSPA-VA

The conceptual model developed in Section 6.2 evolved from the salts/precipitates model developed for the TSPA-VA (CRWMS M&O 1998b). The purpose of the TSPA-VA model was to derive a set of bounding analyses for the timing, accumulation, and total amount of salts that accumulate and dissolve in the drift and the effects of these salts and evaporative processes on the chemical composition of the water. The model considered the elements Al, C, Ca, Cl, F, Fe, H, K, Mg, N, Na, S, and Si.

6.1.4.1 Salt Precipitation Results

The EQ3/6 results of the TSPA-VA model suggested that the most soluble components, Na, Si, S, Cl, K, N, and F, increase in concentration in proportion to the amount of vaporization. Changes in carbonate concentrations were similar; however, because carbonate concentration was a function of pH and the partial pressure of carbon dioxide, deviations from direct

proportionality occurred. As the water became more saline and approached an ionic strength of 1 molal, the pH increased to values between 10.3 and 11.7 (CRWMS M&O 1998b).

Precipitation reactions caused concentrations of Ca, Al, Mg, and Fe to decrease or remain essentially unchanged as water vaporized. As a result, approximately 98 percent or more of these dissolved solids were precipitated as the seepage water became 98 percent vaporized. Ca concentrations were controlled primarily by calcite ($CaCO_3$) or wollastonite ($CaSiO_3$), depending on the pH and the partial pressure of carbon dioxide.

Na and K accounted for more than 99.9 percent of the positive charge. As a result, Na and K salts were responsible for the overwhelming majority of all salt precipitation in the late stage calculations. The elements Si, Cl, S, C, F, and N and their stable hydrolyzed species were the primary sources of negative charge in the seepage water.

For precipitation occurring at ionic strength greater than 1 molal, a simple spreadsheet calculation was used. Normative binary salts were chosen to precipitate based on handbook solubilities, relative ion activity products, and conservation of mass and charge. All Ca precipitated as calcite due to its low solubility and an excess of carbonate. Next, sodium sulfate precipitated. The high concentration of sodium relative to sulfate caused the complete depletion of sulfate while depleting the sodium concentration by approximately 20 percent.

The spreadsheet calculation was not capable of predicting the changes in pH. Because silica salt solubility is a function of pH at high pH, it was difficult to determine which salt would be the last to precipitate. After collaboration with researchers at LLNL, who were performing J-13 evaporation experiments, it was determined that nitrate would precipitate last along with potassium due to its high solubility. Because there was slightly more nitrate than potassium in the reflux water, some nitrate was precipitated as sodium nitrate. Consistent with mass balance and charge balance constraints, the rest of the components, Na, Cl, C, F, and Si, precipitated as NaCl, Na_2CO_3, $NaHCO_3$, NaF, $Na_2Si_2O_5$, and Na_2SiO_3. The total accumulation of these normative salts on the waste package was directly proportional to the seepage rate.

6.1.4.2 Salt Dissolution Results

At early times, the high temperature and low relative humidity in the drift allowed all normative salts in the TSPA-VA analysis to precipitate and all seepage water to vaporize. The dissolution of salt phases was essentially instantaneous once the relative humidity exceeded the maximum allowed for a stable solid phase. Such rapid dissolution is consistent with the observation that puddles of dissolved salt (primarily NaCl brine) occur overnight on salt flats when the relative humidity rises above the maximum equilibrium relative humidity for solid-phase NaCl but remains far below the dew point (Kinsman 1976). These same puddles then dry up during the day as soon as the relative humidity falls below the critical relative humidity.

The first critical value of relative humidity encountered as the potential drift cools was determined to correspond to the nitrate phases. At about 160 years, the relative humidity was predicted to rise above 50 percent and the temperature to fall to about 117 °C. This was taken to be the approximate relative humidity value that would cause $NaNO_3$ to dissolve. Also, the temperature at this time was below the boiling point of a concentrated solution of $NaNO_3$, which

is around 120 °C (Saxton et al. 1928, V. 3, p. 326). Thus, $NaNO_3$ condensed water from the in-drift gas phase and dissolved to a saturated solution at this point in time. KNO_3 was also allowed to dissolve at this relative humidity value.

The next threshold was encountered at approximately 80 percent relative humidity, which corresponded to approximately 800 years. NaCl, NaF, Na_2CO_3, $NaHCO_3$, $Na_2Si_2O_5$, and Na_2SiO_3 were assumed to dissolve at this point. Except for NaCl, there are few data available on the maximum relative humidity values for these solid phases.

The final threshold was crossed at 1,250 years when the relative humidity exceeded approximately 90 percent. Na_2SO_4 was no longer stable and was determined to completely dissolve, representing the last of the highly soluble salts precipitated throughout the boiling period. This left $CaCO_3$ as the only normative salt remaining and accumulating on a potential waste package beyond 1,250 years.

6.2 CONCEPTUAL MODEL

The conceptual model presented in this section describes the processes that control the aqueous compositional changes and precipitation and dissolution of salts and minerals within the drift resulting from H_2O vaporization and condensation. Because the conceptual model is designed to provide bounding and scoping calculations, it is only intended to approximate the effects of the complex processes involved.

The conceptual model is that boiling and evaporation of water within the drift will cause dissolved solids in the water to concentrate and precipitate. The degree of vaporization of H_2O and precipitation of salts and minerals may change with time as conditions change. The precipitates that form will depend on the temperature, gas fugacities, vaporization rate, seepage rate, and seepage composition.

High temperatures and low values of relative humidity are expected to create dry conditions within the drift during the early years. Although potential seepage water entering the drift during the dry period may not remain long enough to initiate considerable corrosion or other potentially deleterious effects, as it boils away it will deposit its dissolved, nonvolatile constituents as salts and minerals. These phases, which may range from relatively insoluble minerals like silicates and carbonates to salts with high solubilities, have the potential to affect water composition within the drift after temperatures fall to the point that stable brines develop.

Because salts are typically hygroscopic, their accumulation within the drift will reduce the duration of dry conditions. Relative humidity values above the critical value for a salt will cause that salt to condense water from water vapor and form a brine (Kinsman 1976). How large of an effect this process may have on in-drift water chemistry is one of the questions that this model attempts to assess.

As drift temperatures fall, relative humidity rises. Eventually, the average rate at which incoming water enters the drift will exceed the evaporation rate, and the result will be an evaporated water composition within the drift that is no longer controlled by the relative humidity and the solubilities of the soluble salts. As a result, the evaporated water composition

within the drift will become more dilute over time as the temperatures fall. The end point of the conceptual model is when temperature and relative humidity within the drift reach ambient conditions. When ambient conditions are achieved, the incoming seepage and water chemistry within the drift are no longer markedly altered by evaporative processes.

6.3 MODEL DESIGN

The Precipitates/Salts model was developed to simulate the conceptual model. The intended use of the model is to estimate, within an appropriate level of confidence, the pH, chloride concentration, and ionic strength of water on the drip shield or other location within the drift during the post-closure period, based on evaporative processes that are subject to a broad range of potential environmental conditions. An additional intended use is to estimate the environmental conditions required for complete vaporization of water. These specific outputs (pH, chloride concentration, ionic strength, and conditions required for complete vaporization) are important for total system performance calculations conducted outside of this AMR.

The appropriate level of confidence for the model is the ability to predict chloride concentrations and ionic strength within an order of magnitude (factor of 10) and pH within a pH unit for expected conditions within the drift. Although these are not highly stringent criteria, this level of confidence nevertheless greatly reduces the potential ranges of these variables, thereby considerably reducing uncertainty. At the same time, the fairly broad range of acceptable uncertainty is necessary because it allows for model validation for the intended use. Without a broad range of acceptable uncertainty, the currently available laboratory and handbook data might not have been able to support development of a quantitative model that could be convincingly validated for the intended use.

The Precipitates/Salts model consists of two sub-models which handle the two predominant regimes described in Section 6.2. The first regime occurs at low relative humidity where the solubilities of soluble salts control the water chemistry. In this regime, incoming seepage water either completely evaporates, thereby precipitating all dissolved solids in the seepage, or it evaporates to a stable brine. The model used to simulate this regime is referred to as the Low Relative Humidity (LRH) salts model. It is a simple bounding model that consists of a set of simplified algebraic calculations performed within a Mathcad file.

In the second regime, the relative humidity is higher. In this regime, the steady state water composition is controlled by the ratio of the rates of evaporation and seepage. This ratio is always less than one in this regime. If it were not, steady state conditions would either be dry (if the relative humidity were sufficiently low) or consist of a steady state brine, either of which are simulated using the LRH model for the first regime. The model used to simulate this second regime is referred to either as the EQ3/6 Pitzer model or the High Relative Humidity (HRH) salts model. This model is simulated using the geochemical code EQ3/6. Like the LRH model, it relies on simplifying assumptions that are justified for the intended use of the model. The HRH model is not intended to meet the strict criteria generally applied to the development of universal Pitzer databases. The simplifying assumptions (Section 5.3) are justified for the intended use by comparing model predictions of pH, chloride concentration and ionic strength to laboratory data (Section 6.5) and ensuring that these outputs are predicted within the fairly broad range permitted for uncertainty.

The two sub-models are designed to provide a piece-wise continuous Precipitates/Salts model for all time periods simulated.

6.3.1 Input Parameters and Boundary Conditions

6.3.1.1 Seepage Water Composition

The elements in the model include Na, K, Ca, Mg, Cl, F, C, S, N, Si, Fe(III), Al, H, and O. The incoming seepage water composition (C_i^s) over time will eventually be provided by the THC model. For this document, however, average J-13 well water is used. Its composition is presented in Table 7.

6.3.1.2 Time Period Modeled

The model is designed to apply to periods of time in which the inputs are either constant or abstracted for constant input conditions. For changing input conditions of an entire target modeling period, the period is divided into discrete blocks of time in which the input conditions are abstracted to constants.

6.3.1.3 Locations Modeled

The Precipitates/Salts model can be used to describe evaporative processes at any location where evaporative processes occur. The most likely locations are in the backfill, on the drip shield, and on the waste package surface.

6.3.1.4 Temperature and Gas Composition

The temperature and gas composition in the near-field geochemical environment of the repository will change over time. The important gas components for the Precipitates/Salts model are carbon dioxide and water. Fugacities of carbon dioxide within the drift over time will be provided by a separate performance assessment analysis. Relative humidity values for a given cell and time increment will come from TH modeling results when they are available.

In this AMR, relative humidity values (RH) from 0 to 100%, temperatures (T) of 25°C, 45°C, 75°C, and 95°C, and carbon dioxide gas fugacity values (f_{CO2}) of 10^{-1}, 10^{-3}, and 10^{-6} are modeled.

6.3.1.5 Relative Evaporation Rate

Relative evaporation rate (R^{es}) becomes important in the model after the relative humidity rises above 85%. This AMR presents calculations for the following relative evaporation rate values: 0, 0.1, 0.5, 0.9, 0.99, 0.999, and 1.

6.3.2 Model Output

Model output consists of calculations for pH, chloride molality, and ionic strength (in molality) for the input parameter values described in Section 6.3.1. A complete set of these outputs is summarized in this AMR by a set of lookup tables that can be used to interpolate model output for input conditions within the ranges modeled.

The ionic strength (I) parameter in the figures and lookup tables in this AMR is not the true ionic strength calculated by an equilibrium code, except when it is called the true ionic strength. Instead, it is an approximation based on the following equation:

$$I = C_{Na} + C_K + 4(C_{Ca} + C_{Mg}) \qquad \text{(Eq. 4)}$$

where C_i is the molality of component i. This approximation is identical to that used in the colloids model (CRWMS M&O 1998b), and is particularly appropriate for the Precipitates/Salts model lookup tables because the colloids model is the primary downstream user of the ionic strength calculations. In the case of the LRH salts model, the approximation is simply the sum of the Na and K molalities because Ca and Mg are not tracked by the model. As observed in the EQ3/6 HRH model, the contributions of Ca and Mg to the ionic strength are small. This is especially true when the ionic strength is high, as is the case in all of the LRH salts model calculations.

6.3.3 Model Limitations

The conceptual model is a simplification of evaporative salt processes and their effects on the chemistry and quantity of liquids and salts at a particular location. Prediction of the actual salts and brines that would form in the drift due to these processes cannot be determined with a high degree of confidence using available thermodynamic data. Therefore, this model is designed to approximate the overall effects of evaporative processes on salt and brine formation so that bounding calculations can be performed to assess the potential implications of these processes on total system performance.

6.3.4 Condensed Water Model

An additional model named the Condensed Water model was requested for inclusion in this AMR. This model is designed to predict the composition of condensed water that may form on dry inert surfaces, such as the underside of the drip shield. The conceptual model is that pure water vapor condenses on dry inert surfaces wherever the temperature and relative humidity permit. The model does not attempt to predict the timing, amount, or location of the condensed water. Rather, it simply predicts the equilibration of pure water with the local temperature and fugacity of carbon dioxide so that values for pH and ionic strength can be determined. Because these surfaces are assumed to be free of dust, salt, and other sources of dissolved solids (Assumption 5.6, above), concentrations of dissolved solids other than carbonate are zero. EQ3/6 is used to predict the equilibrium chemistry at carbon dioxide gas fugacity values (f_{CO2}) of 10^{-1}, 10^{-3}, 10^{-4}, 10^{-5}, 10^{-6}, 10^{-7}, and 10^{-9} and temperatures (T) of 25°C, 45°C, 75°C, and 95°C.

6.4 MODEL IMPLEMENTATION

The LRH and HRH models are linked together at a RH of 85 percent. At this RH, the equilibrium activity and mole fraction of water in solution should be approximately 0.85 (Kinsman 1976, p. 275). As presented later, the EQ3/6 Pitzer calculations of the HRH model indicates that evaporation of average J-13 well water to a water activity and mole fraction of about 0.85 occurs at an ionic strength of around 10 molal. At this point in the EQ3/6 calculations, Na, K, NO_3, Cl, CO_3, and SO_4 are highly concentrated in the evaporated solution,

but because the EQ3/6 Pitzer model may be close to or beyond its range of validity at this ionic strength, salt reactions at higher ionic strengths (lower relative humidity) are reserved for the simpler LRH salts model.

Sections 6.4.1 and 6.4.2 present the details of how the LRH and HRH salts models are implemented. The assumptions implicit in the implementation are addressed in Section 5.

6.4.1 Low Relative Humidity Model

In the LRH salts model, seepage water enters a specified location within the drift where it is subjected to evaporation processes. This location is called a "reactor" in this document.

At early times, the relative humidity (*RH*) is sufficiently low to vaporize all incoming water and maintain dry conditions within the reactor. As a result, only the dissolved solids in the incoming seepage accumulate during this time. The accumulation for component i is equivalent to the cumulative mass of component i ($M_i^{s,t}$) entering the reactor during time t. It is calculated using the equation:

$$M_i^{s,t} = C_i^s Q^s t \qquad \text{(Eq. 5)}$$

where C_i^s is the incoming seepage concentration (mass/volume) of component i and Q^s is the incoming seepage rate (Assumptions 5.5.1, 5.5.2, 5.5.7, and 5.5.8). This equation is derived by dimensional analysis.

As explained in Section 5.5, accumulated nitrate salts will dissolve in the model when the *RH* rises to approximately 50 percent (Assumption 5.5.3). At this *RH*, a nitrate brine is determined by the model to be stable and will not evaporate to dryness due to the hygroscopic nature of nitrate salts. The model calculates the mass of water in this brine using equation 2. For brine generated from evaporated average J-13 well water, the nitrate brine is mostly a KNO_3 brine. However, because the average J-13 well water contains a higher molality of NO_3 to K, the remainder of the nitrate brine is $NaNO_3$.

During the time *RH* rises from 50 to 85 percent, the model simulates brine generation. This time period is divided into equal time increments in which all brine generated during a time increment flows out of the reactor at the end of the time increment (However, as discussed later, the model allows for some mixing between time increments.). Brine is generated by gradually dissolving the Cl, CO_3, and SO_4 sodium and potassium salts that have accumulated (and potentially continue to accumulate) in the reactor. The model dissolves these salts according to the following equation:

$$f_{i,j} = 10^{\frac{4(t_j - t^{85\%})}{t^{85\%} - t^{50\%}}} \qquad \text{(for } i = \text{Cl, } CO_3\text{, or } SO_4\text{)} \qquad \text{(Eq. 6)}$$

where $f_{i,j}$ is the dissolved fraction of moles of Cl, CO_3, and SO_4 in the reactor at time increment j and t_j is the time (Assumption 5.5.4). The constants $t^{50\%}$ and $t^{85\%}$ are the times when *RH* reaches 50 and 85 percent. Thus, at time $t^{50\%}$ the fraction dissolved is 0.0001, while at time $t^{85\%}$ it is 1.0

and the salts are completely dissolved. The value of $f_{i,j}$ increases exponentially as t_j approaches $t^{85\%}$. This equation is an empirical equation that was derived in this AMR to approximate a smooth and reasonable transition from a concentrated nitrate brine to a dilute brine equilibrated with a relative humidity of approximately 85 percent. For NO_3 and K, the fraction dissolved is one as soon as *RH* reaches 50 percent.

The moles of each component *i* in the reactor at a given time increment *j* ($M^r_{i,j}$) is the sum of the moles in the reactor that are dissolved and undissolved. Because the model requires brine generated during a time increment to flow out of the reactor at the end of the time increment, $M^r_{i,j}$ is calculated by taking the moles in the reactor from the previous time increment ($M^r_{i,j-1}$), subtracting the dissolved fraction from the previous time increment, and adding moles from seepage during the current time increment (M^s_i), i.e.:

$$M^r_{i,j} = M^r_{i,j-1} - M^r_{i,j-1} f_{i,j} + M^s_i \qquad \text{(Eq. 7)}$$

where

$$M^s_i = C^s_i Q^s (t_j - t_{j-1}) \qquad \text{(Eq. 8)}$$

However, because equation 7 does not allow mixing between time increments, the nitrate brine generated in the first time increment would be completely removed by the second time increment. Therefore, mixing is incorporated into the LRH model by subdividing each time increment into half increments, such that the moles in the cell at each half time increment ($M^{rh}_{i,k}$) is calculated from the equation:

$$M^{rh}_{i,k} = M^{rh}_{i,k-1} - \frac{1}{2} M^{rh}_{i,k-1} f_{i,\frac{(k-1)}{2}} + \frac{1}{2} M^s_i \qquad \text{(Eq. 9)}$$

where k is the set of all integers from 1 to 2*j*. These calculations are then converted back to $M^r_{i,j}$ by the equation:

$$M^r_{i,j} = M^{rh}_{i,2j} \qquad \text{(Eq. 10)}$$

From these calculations, the moles of dissolved solids in the brine generated at each time increment ($M^d_{i,j}$) can be calculated from the equation:

$$M^d_{i,j} = M^r_{i,j} f_{i,j} \qquad \text{(Eq. 11)}$$

and the mass of water in the generated brine at each time increment (m^w_j) can be calculated from equation 2 (Assumption 5.5.5). These calculations allow determination of the mass fractions of each component *i* ($C_{i,j}$) [units: mass/mass] in the generated brine at each time increment using the equation (Assumption 5.5.6):

$$C_{i,j} = \frac{M_{i,j}^{d}}{m_j^{w}} \qquad \text{(Eq. 12)}$$

To this point, only equations 5 and 8 are used for Na calculations because these two equations involve incoming seepage only and are not affected by the processes that occur within the reactor. The moles, mole fractions, and mass fractions of Na in the reactor are calculated by charge balance after the values for the other components are determined (Assumptions 5.5.9 and 5.5.10). The general equation is:

$$B_{Na,j} = \sum_a B_{a,j} z_a - B_{K,j} z_K + E \sum_a 2B_{a,j} z_a (1+E) \qquad \text{(Eq. 13)}$$

where $B_{i,j}$ represents $M_{i,j}^{r}$, $M_{i,j}^{d}$, or $C_{i,j}$ depending on which Na calculation is being performed: Na moles in reactor, dissolved Na moles in reactor, or dissolved Na mass fraction. K, a, and z_i represent potassium, anions, and the valency of component i, respectively. The third term in equation 13 is included to maintain any original charge balance error (E) introduced by the incoming seepage. In this way, any potential errors in the charge balance calculations themselves will not affect the results of the model. E is calculated from the equation:

$$E = \frac{\sum C_c^s z_c - \sum C_a^s z_a}{\sum C_c^s z_c + \sum C_a^s z_a} \qquad \text{(Eq. 14)}$$

where C_c^s and C_a^s represent the concentrations of cations and anions in the incoming seepage (Freeze and Cherry 1979, p. 97). An example calculation using the LRH model is provided in Attachment I.

6.4.2 High Relative Humidity Model

Evaporative concentration of dissolved solids in dilute water is typically performed using a geochemical equilibrium code, such as EQ3/6. Pure water is removed from the original solution, and depending on mineral saturation indices and interaction with the gas phase, this causes the dissolved ions to concentrate in solution, precipitate, or degas. These reactions are routinely simulated to an ionic strength of about 1 molal using traditional ion activity correction equations such as the B-dot equation (Wolery 1992b, p. 38).

The HRH model is simulated using the ion-interaction Pitzer equations in EQ3/6 version 7.2b. The ion-interaction model was adopted to increase the model's upper ionic strength limit to approximately 10 molal. The EQ3/6 software package, however, includes Pitzer databases that can only be used for a subset of the elements and conditions required for the HRH model. Ion-interactions involving CO_3, Si, Al, and Fe(III) at high ionic strength and high temperature cannot be simulated using the Pitzer databases in the EQ3/6 software package. Thus, a Pitzer database called PT4 was developed from the PIT database of EQ3/6 for the HRH model. The development of PT4 and the associated assumptions are discussed in Section 5.

The EQ3/6 HRH model is used in two modes, a simple evaporation mode and a mode that simulates both flow-through and evaporation simultaneously. The first mode is used to predict the simple evolution of a given solution as water evaporates. The second mode is used to predict the evaporative evolution of a constant incoming seepage. These modes are described in the subsections that follow.

6.4.2.1 Simple Evaporation

The simple evaporation mode is used in this analysis to predict the evolution of a given water composition at a given temperature and carbon dioxide fugacity as it concentrates by evaporation to a water activity of approximately 0.85. Such calculations are especially useful in model validation when analytical results of laboratory evaporation studies are compared with HRH model predictions.

Evaporation may be accomplished by the titration feature in EQ3/6 in two ways in this analysis. The traditional way is to declare an evaporation reactant (e.g., "H2O") and assign it an "aqueous" reactant type and a rate constant (rk1) of -1.0. Then reaction progress is allowed to go from 0 to about 55.5, which is the approximate number of moles of water in a kilogram of water. The actual maximum reaction progress must be finely and iteratively adjusted to achieve the final target ionic strength. The other method is to declare the evaporation reactant is a "special" reactant and include the molalities of H and O (approximately 111.0 molal and 55.5 molal, respectively). For "special" reactants, the rate constant (rk1) is set at -1.0 and the reaction progress is varied from 0 to nearly 1.0.

6.4.2.2 Evaporation with Solid-Centered Flow-Through

The EQ3/6 HRH model simulates evaporation within the drift using the solid-centered flow-through mode. In this mode, seepage into the reactor is at a constant rate. In the current version of the HRH model, the solid-centered flow-through addendum for EQ3/6 version 7.2b is used [CSCI: URCL-MA-110662 V7.2b, MI: 30084-M04-001 (Addendum Only), CRWMS M&O 1998a]. This addendum has the limitation that the flux of equilibrated solution out of the cell is equal to the flux of incoming water. Thus, any evaporation of water within the cell will result in a net outward flux of mass within the cell.

For the EQ3/6 HRH model, it would be more realistic for the flux of equilibrated solution out of the cell to be the difference of the fluxes of incoming seepage and evaporation. This would be a more realistic representation of conditions within the drift because (assuming constant climate conditions) as evaporation rates decrease with time, water volumes within the drift will increase and eventually level off due to the emergence of a steady flow-through regime. In this way, the volume of solution within the cell would not decrease and the dissolved solids would not flush from the cell as quickly. Version 8 of EQ3/6, which at the time of this writing is not qualified for use on the Yucca Mountain Project, allows simulation of this more realistic approach.

The current version of EQ3/6 (7.2b) with the solid-centered flow-through addendum is still useful, however, because it can approximate the evaporative evolution of incoming seepage. Although the total volume and mass within the cell decreases with time, the expected steady state concentrations are generally achieved by the model given a sufficient number of pore volumes of

incoming seepage. Thus, if the model is used to evaluate the chemical evolution of evaporated incoming seepage in a flow-through cell during a time period that has a sufficiently high number of pore volume flushes (e.g., more than 100), then the model will correctly approach the expected steady state concentrations.

The steady state concentrations are primarily controlled by the seepage composition and the relative evaporation rate (R^{es}) defined in equation 1 (Section 4). For example, a R^{es} value of 0.9 (i.e., an effective evaporation rate equal to 90 percent of the incoming seepage rate) implies that the steady state concentration of a highly soluble dissolved component in the cell (e.g., Cl) will be 10 times the concentration in the incoming seepage. The derived general equation (confirmed by model results) is:

$$\frac{C_i^{rs}}{C_i^{s}} = \frac{1}{1 - R^{es}} \qquad \text{(Eq. 15)}$$

where C_i^{rs} is the steady state molal concentration of soluble component i in the reactor (or cell) and C_i^{s} is the molal concentration of the component in the incoming seepage. This equation must be used with caution, however, because less soluble components may reach solubility limits. These limits may also be affected by the evolution of the pH and fixed partial pressure of CO_2 (g).

The solid-centered flow-through option of the EQ3/6 version 7.2b addendum is implemented by defining two reactants and reactant types, a displacer and a special reactant. The incoming seepage is the displacer and water evaporation is the special reactant (not the customary "aqueous" reactant type). By setting the displacer reactant rate constant (rk1) equal to 1.0 for all simulations, the reaction progress is equivalent to the number of liters (or pore volumes) entering the cell. The reactant rate constant (rk1) for the evaporation reactant is then set equal to negative R^{es}, thus setting the relative evaporation rate.

6.4.3 Condensed Water Model

The Condensed Water model (see Section 6.3.4) uses EQ3/6 to predict the pH and ionic strength of the condensate under a full range of potential temperatures and carbon dioxide fugacities. The COM database from the EQ3/6 software package is used for this analysis (DTN: MO9911SPATHD62.002). The results are plotted and tabulated in a set of lookup tables so that downstream users can easily incorporate the predicted compositions into their analyses.

6.5 MODEL VALIDATION

This section presents the validation performed for the HRH and LRH models, which together compose the Precipitates/Salts model. Model validation is a process for determining and documenting the adequacy of the scientific bases for a model and to demonstrate the model is appropriate and adequate for its intended use. The intended use for the Precipitates/Salts model is described in Section 1.

6.5.1 HRH Model Validation

For the HRH model, model predictions are compared against four sets of experimental data. The first three sets of data consist of LLNL results from the evaporation of synthesized average J-13 water or Topopah Spring Tuff pore water. These three comparisons are presented in Sections 6.5.1.1 through 6.5.1.3. The fourth data set, presented in Section 6.5.1.4, consists of the handbook solubilities of ten simple salts whose solubilities exceed one molal. No other data have been located that are appropriate for validation purposes for this model.

The validation criteria for the HRH model are:

1. The model predicts the results of laboratory evaporation experiments within an order of magnitude (factor of 10) for chloride concentrations and ionic strength and within a pH unit for pH predictions.

2. The model predicts handbook solubilities within an order of magnitude (factor of 10) for chloride concentrations and ionic strength.

This level of confidence is justified because it greatly reduces the potential ranges of these variables, thereby considerably reducing uncertainty. The LLNL experimental data are currently in the process of being qualified. Although some of the LLNL experimental data may be determined not to meet the strict standards required for instrument calibration and documentation (e.g., pH data), these data are nevertheless believed to be of high quality and sufficiently accurate for model validation purposes. As for the handbook solubility data, they are accepted data and are therefore qualified, but they do not include pH data.

As shown in detail in the following subsections, the model validation criteria are met in every case. The LLNL pH data were predicted within a pH unit or better, the chloride concentrations were predicted within 20 percent, and the ionic strength, as approximated using equation 4, was predicted within a factor of 2. In addition, handbook solubilities for the ten simple salts having solubilities greater than 1 molal were easily predicted within an order of magnitude and almost always within a factor of two, implying criteria for chloride and ionic strength predictions are met for these data as well. These results demonstrate that the HRH model is likely valid for its intended use.

6.5.1.1 Evaporation of Average J-13 Well Water at 85°C

Rosenberg et al. (1999a) evaporated synthesized J-13 water at 85°C in a pyrex beaker, as described in Section 4.1.2. The results (presented in Table 3 and Table 4) were modeled by the HRH model using the PT4 database. Figure 2 shows close agreement between the laboratory measured pH and modeled pH. The modeled pH is assumed to be controlled by the fugacity of carbon dioxide which is fixed at $10^{-3.4}$ to approximate the laboratory condition of a beaker open to the atmosphere. Water in evap4 was concentrated to 157 times the original solution. According to the EQ6 calculations, its ionic strength approximation (equation 4) was around 0.34 molal compared to the 0.25 molal ionic strength approximation calculated from the data.

As shown in Figure 3, Figure 4, and Figure 5 at a concentration factor of 157, the modeled results approximate the Na, F, HCO_3, Cl, K, NO_3 and SO_4 concentrations when compared to the laboratory data. However, as shown in Figure 5 and Figure 6 at a concentration factor of 157, the modeled results underestimate the aqueous Si and Ca concentrations by an order of magnitude when compared to the laboratory data. Also, in Figure 6 the modeled results underestimate the aqueous Mg concentration by two orders of magnitude when compared to the laboratory data. The differences in the Si, Ca, and Mg concentrations do not invalidate the model, however, because the intended use of the model is to predict pH, Cl concentration, and ionic strength within acceptable limits, which the model does well.

The discrepancies in the Si, Ca, and Mg concentrations and pH may be due to errors or uncertainty in the PT4 thermodynamic database or to kinetic limitations of precipitation reactions. The relatively short laboratory experiments may not have permitted equilibrium precipitation of chalcedony, calcite and sepiolite. Precipitation of calcite when the pH is below 10 results in the release of a proton from the bicarbonate ion. Thus, slow precipitation of calcite can also explain why the model predicts lower pH than observed. These minerals precipitate in the model at a concentration factor of 157 as shown in Figure 7. Later, at a concentration factor of 1000, the model results also predict fluorite precipitation. Mineral identification by XRD was not presented for this laboratory experiment.

Another possible explanation for the discrepancies is the assumed carbon dioxide fugacity. In a solution that is boiling or evaporating from a beaker, it is possible that the atmospheric partial pressure of carbon dioxide is below atmospheric values because of an increased partial pressure of water vapor and a net flux of vapor flowing out of the beaker. If this is the case, the actual carbon dioxide fugacity would be lower. A lower assumed carbon dioxide fugacity would increase pH predictions.

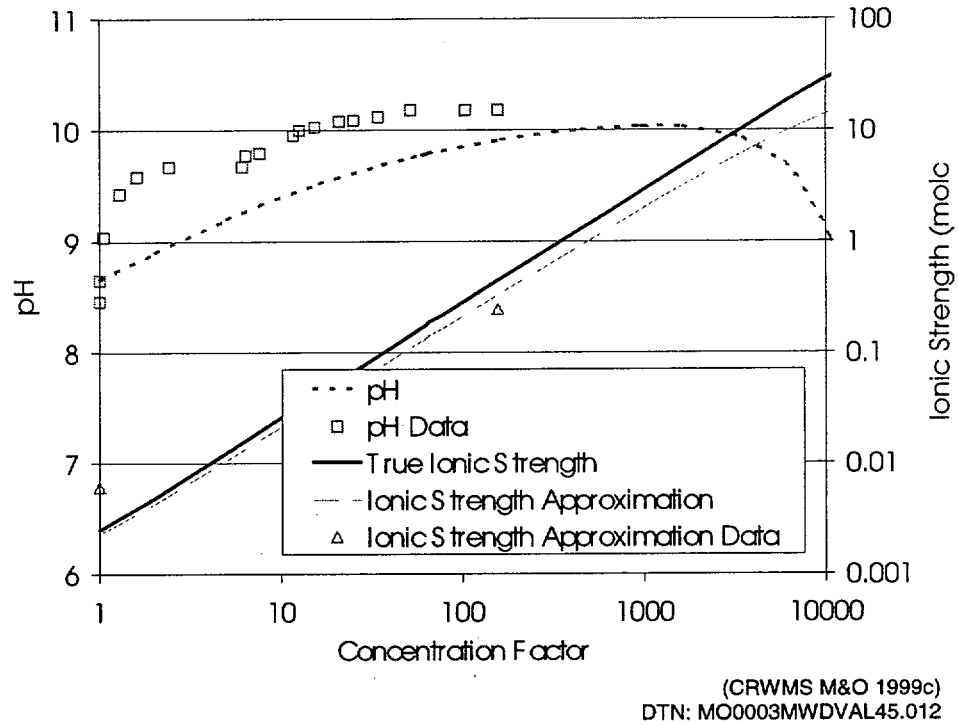

Figure 2. pH and Ionic Strength Predictions vs. J-13 Evaporation Data from Rosenberg et al. (1999a, evap4)

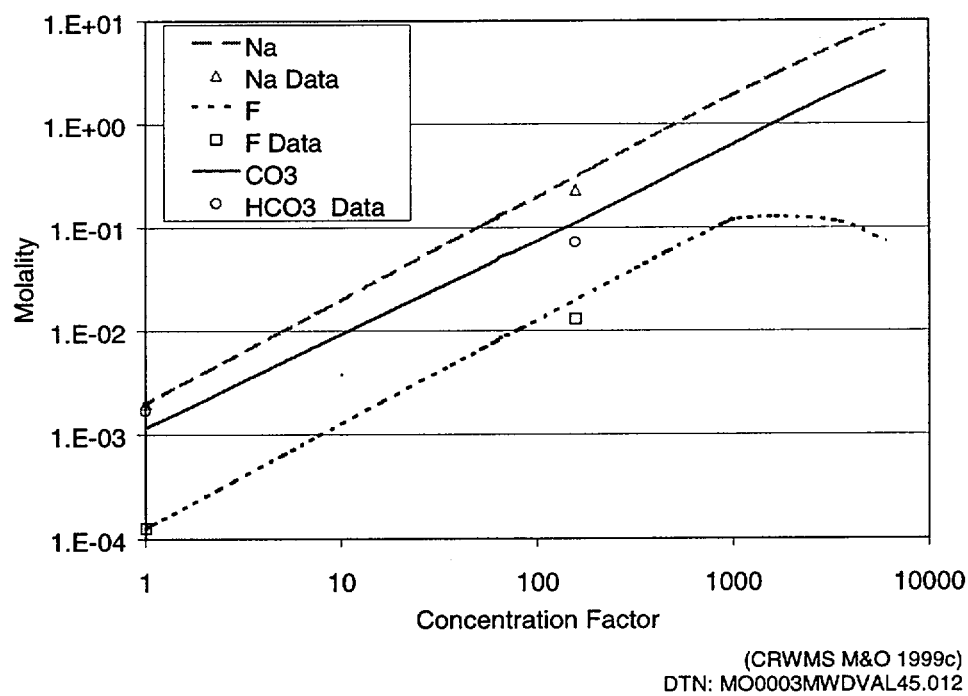

Figure 3. Na, CO_3, and F Predictions vs. J-13 Evaporation Data from Rosenberg et al. (1999a, evap4)

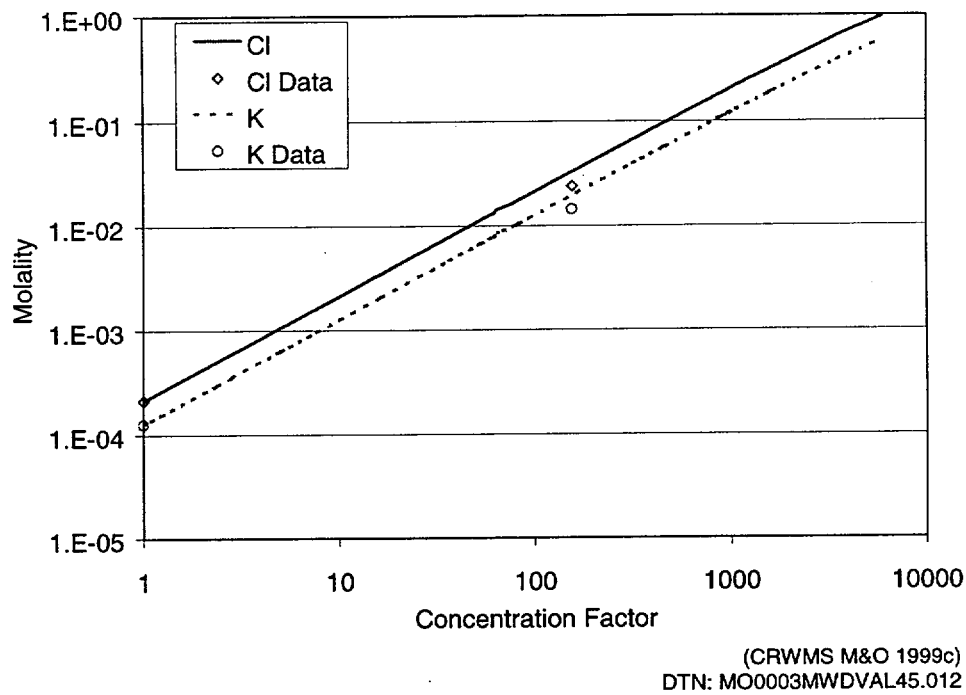

Figure 4. Cl and K Predictions vs. J-13 Evaporation Data from Rosenberg et al. (1999a, evap4)

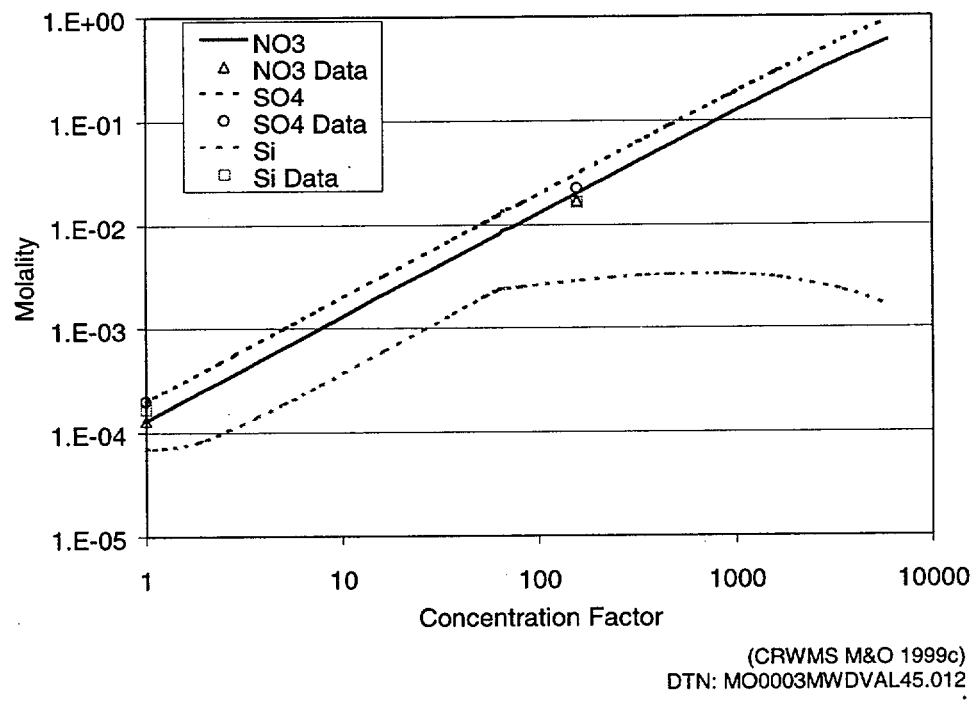

Figure 5. NO_3, SO_4, and Si Predictions vs. J-13 Evaporation Data from Rosenberg et al. (1999a, evap4)

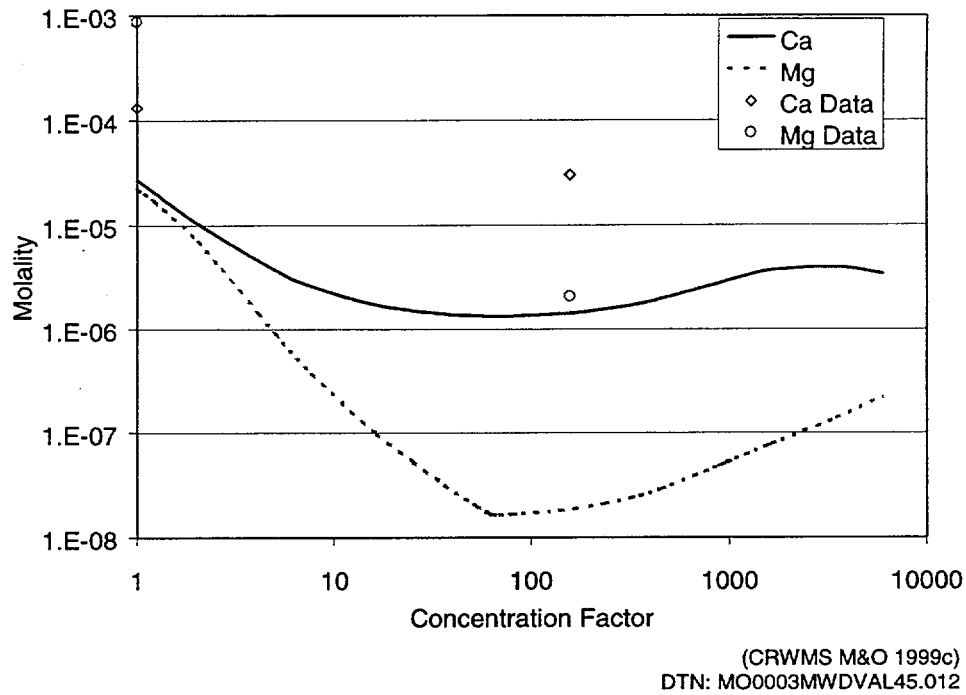

Figure 6. Ca and Mg Predictions vs. J-13 Evaporation Data from Rosenberg et al. (1999a, evap4)

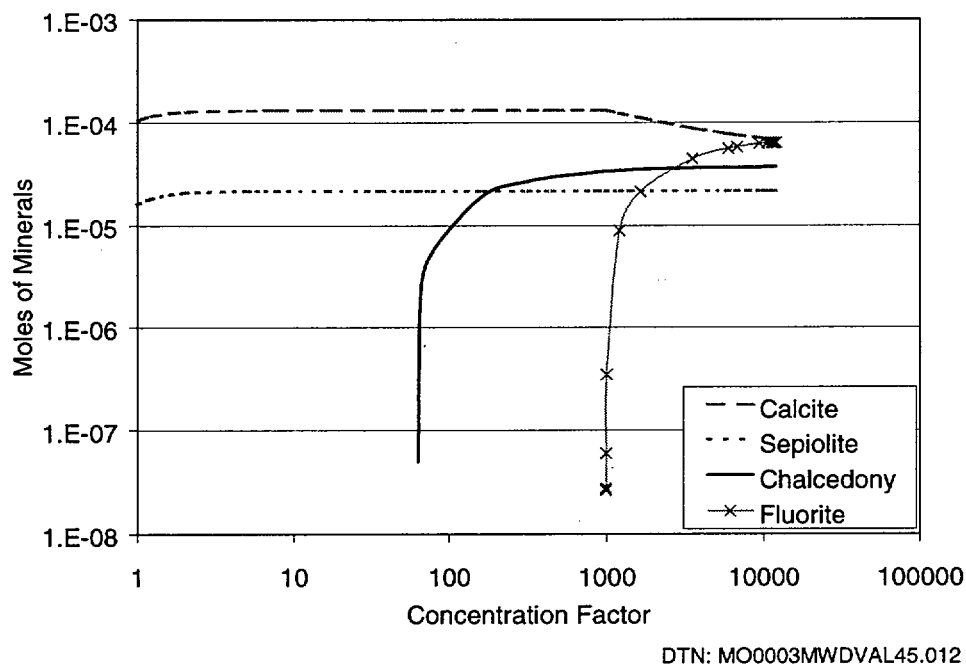

Figure 7. Mineral Precipitation Predictions for J-13 Evaporation Experiment of Rosenberg et al. (1999a, evap4)

6.5.1.2 Evaporation of 100x Average J-13 Well Water at 90°C and 85 Percent Relative Humidity

As described in Section 4.1.2, a synthesized concentrated J-13 solution was evaporated in an open beaker and the results reported in CRWMS M&O (2000, Sections 4.1.20 and 6.5.3, Batch 1). The original synthesized solution contained major ions that were approximately 100 times (100x) the average J-13 well water composition. After contact with crushed tuff at 90°C, the solution was dripped into a teflon beaker open to the atmosphere where the solution evaporated to a volume of approximately five percent the original volume, based on the concentration factors reported. The actual volume or mass decrease in the solution was not reported.

The laboratory results (presented in Table 5) were simulated by the HRH model at 90°C using the PT4 database. Figure 8 shows the predicted change in pH and ionic strength as a function of the concentration factor. No pH measurements were reported. The fugacity of carbon dioxide (CO_2) was fixed at $10^{-3.4}$ and the temperature set at 85°C. The ionic strength approximation (equation 4) for the final experimental solution was around 3.7 molal, which is the approximate ionic strength approximation calculated by the model.

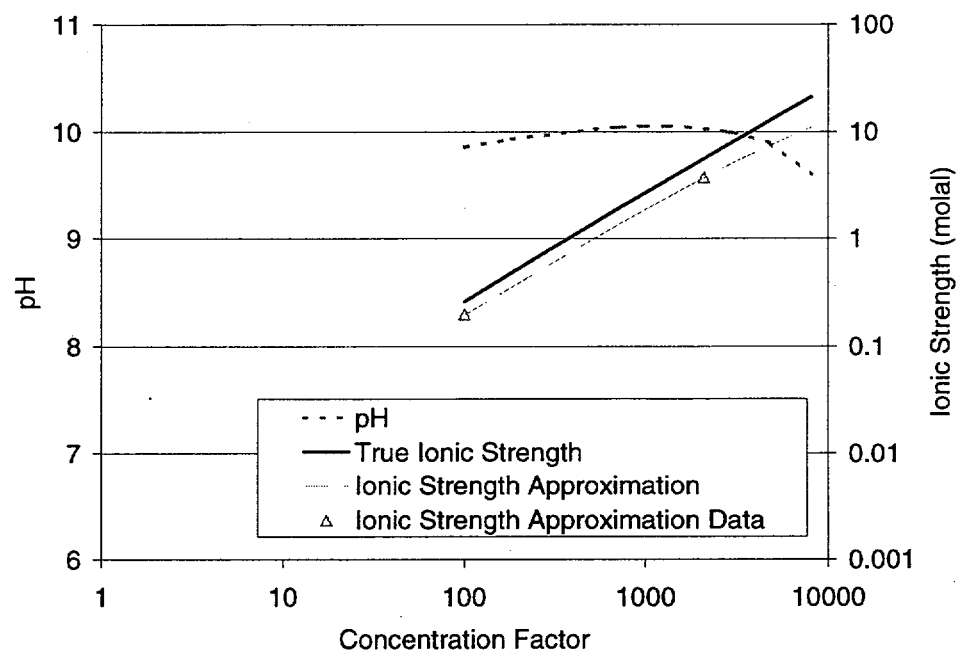

DTN: LL000202905924.117
DTN: MO0003MWDVAL45.012

Figure 8. pH and Ionic Strength Predictions for 100x J-13 Evaporation Experiment by CRWMS M&O (2000, Batch 1)

Figure 9, Figure 10, and Figure 11 show that the modeled results closely approximate the Na, F, Cl, K, NO_3, HCO_3, and SO_4 concentrations when compared to the laboratory data (Batch 1). To compare the results to the data, the reported nitrate concentration factor of 20.7 is used to represent the concentration factor of the solution. As shown in the figures, the agreement

between the Na, F, Cl, K, and SO_4 data and predictions indicate that the concentration factor of the solution is well-represented by the nitrate concentration factor.

In Figure 12, the modeled concentrations underestimate Ca and Mg by about 2 orders of magnitude or more when compared to the laboratory data (Batch 1). At a factor of around 2000, the model's underestimation of Ca and Mg species occurs due to the precipitation of minerals such as calcite, brucite, sellaite, fluorite, and villiaumite, as shown in Figure 13. One explanation for a larger amount of predicted precipitation may be that mineral precipitation is kinetically limited in the experiment, whereas there is no such limitation in the model. Laboratory analysis of the precipitates was not performed. Other possible explanations are errors or uncertainties in the PT4 database and/or the assumed carbon dioxide fugacity.

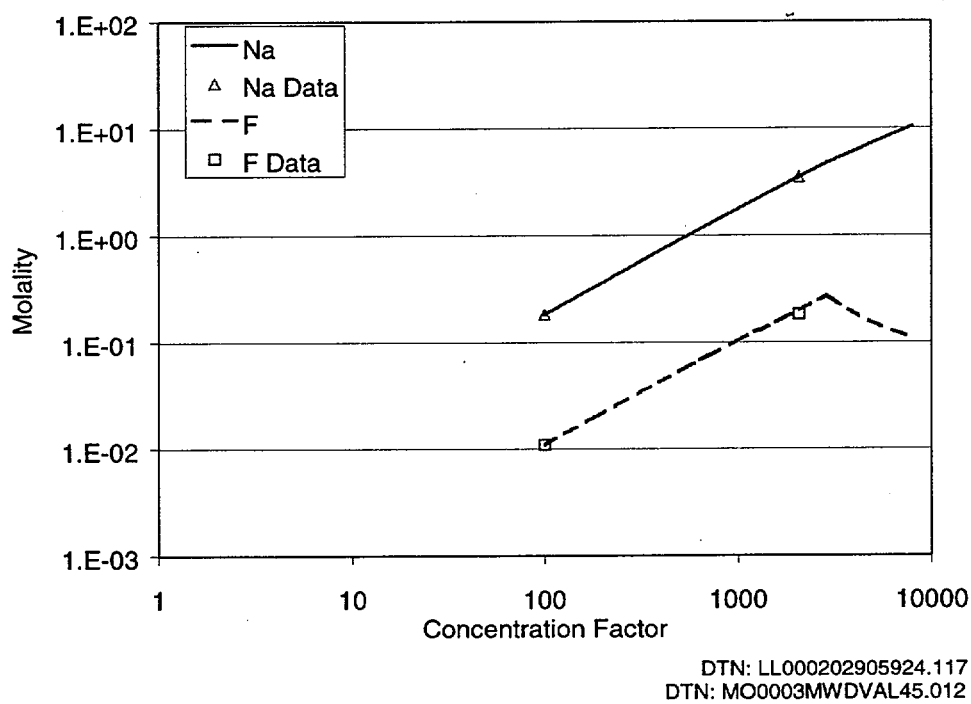

Figure 9. Na and F Predictions vs. 100x J-13 Evaporation Data from CRWMS M&O (2000, Batch 1)

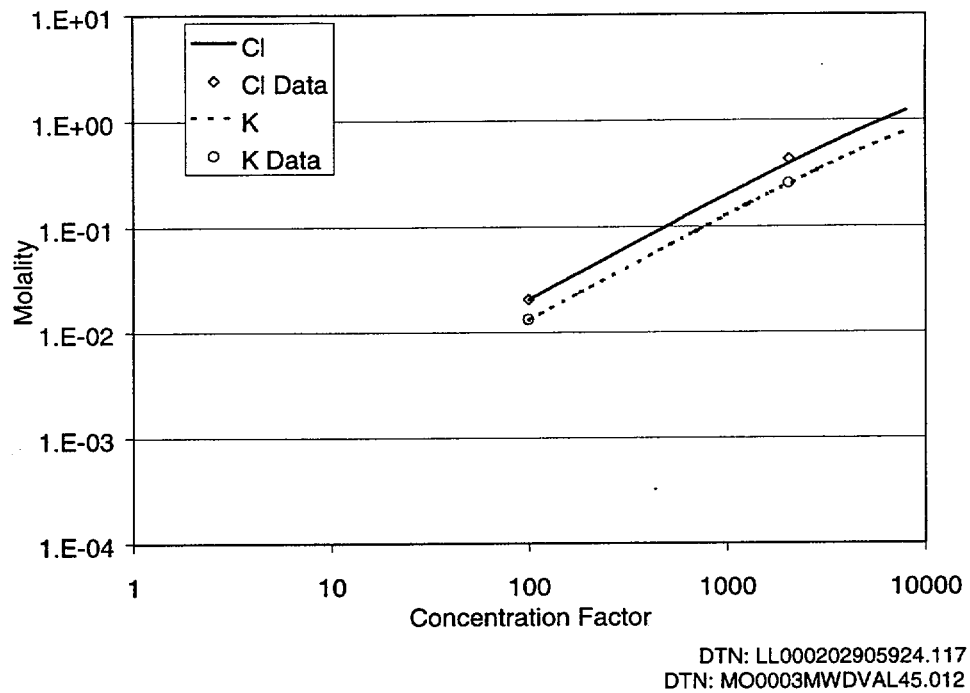

Figure 10. Cl and K Predictions vs. 100x J-13 Evaporation Data from CRWMS M&O (2000, Batch 1)

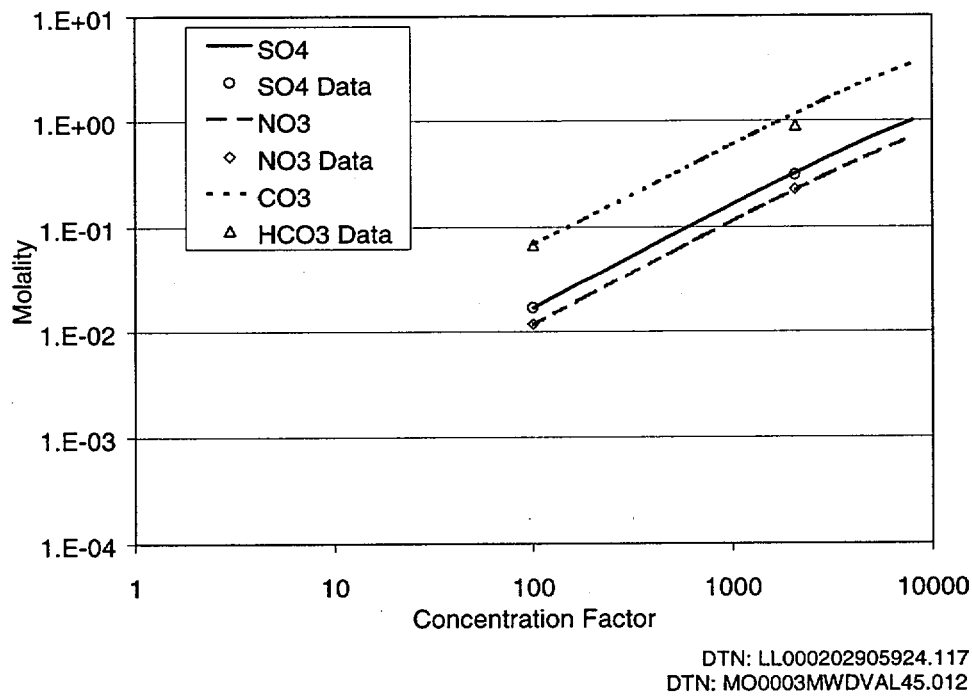

Figure 11. NO_3, SO_4, and CO_3 Predictions vs. 100x J-13 Evaporation Data from CRWMS M&O (2000, Batch 1)

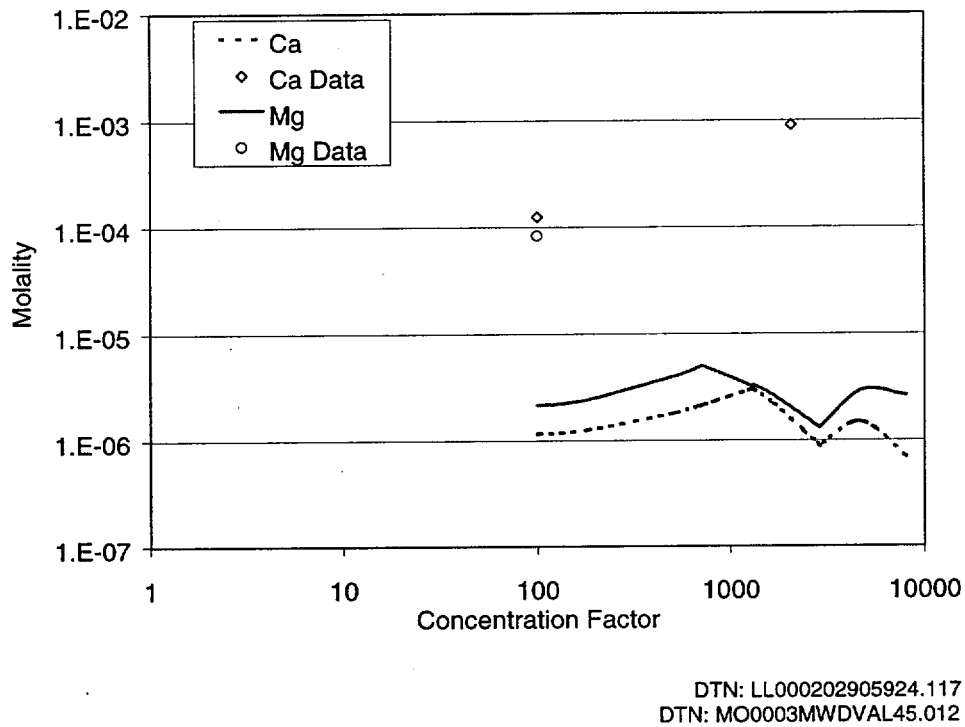

Figure 12. Ca and Mg Predictions vs. 100x J-13 Evaporation Data from CRWMS M&O (2000, Batch 1)

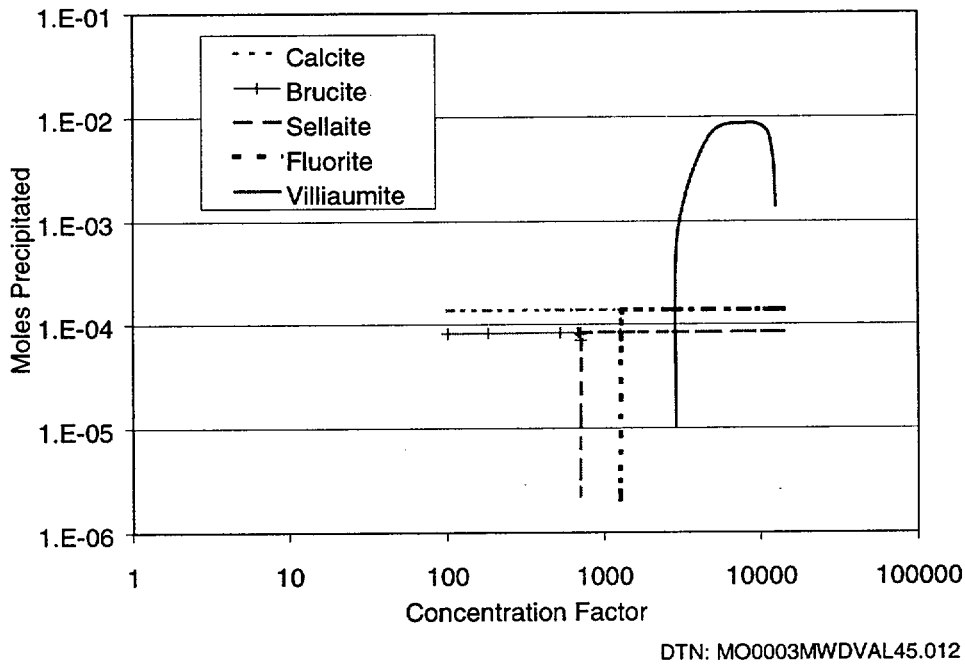

Figure 13. Mineral Precipitation Predictions for 100x J-13 Evaporation Experiment of CRWMS M&O (2000, Batch 1)

6.5.1.3 Evaporation of Topopah Spring Tuff Pore Water at 75°C

Rosenberg et al. (1999b) evaporated synthesized Topopah Spring water at 75°C in a pyrex beaker as described in Section 4.1.2. The results (presented in Table 6) were modeled by the HRH model using the PT4 database. Figure 14 shows close agreement between the laboratory measured pH and modeled pH, which both fell from about 7.7 to about 6.3. The modeled pH is controlled by the fugacity of carbon dioxide which is fixed at $10^{-3.4}$ to approximate the laboratory condition of a beaker open to the atmosphere. The water was concentrated to 1243 times the original solution. According to the EQ6 calculations, its ionic strength approximation (equation 4) was approximately 5 molal compared to the 2.8 molal ionic strength approximation calculated from the data.

Figure 15 and Figure 16 show that the modeled results closely approximate the measured Na, Mg, Ca, Cl, and K concentrations. At a concentration factor of 1243, modeled results underestimate the measured Si and SO_4 concentrations by 1 to 1.5 orders of magnitude as shown in Figure 17. NO_3, HCO_3, and F laboratory data are not reported in Rosenberg et al. (1999b).

Figure 18 shows predicted mineral precipitation. Precipitation of chalcedony and anhydrite are responsible for limiting the predicted Si and SO_4 concentrations in the concentrated solution. The higher concentrations measured in the experiment could possibly be the result of slow precipitation and, thus, nonequilibrium conditions. Gypsum, which is similar to anhydrite, was identified by XRD in the laboratory experiment at the 1243 concentration factor. Upon complete evaporation, tachyhydrite, which also was predicted to precipitate (Figure 18), was identified by XRD. Other minerals predicted to precipitate (calcite, carnallite, fluorite, sellaite and halite) were not observed in the laboratory experiment. Their absence may be the result of kinetic factors inhibiting their precipitation or of minuscule quantities making identification difficult. This assumes that the model predictions are accurate, which may not be the case due to possible errors and uncertainty in the PT4 database. Nevertheless, the HRH model results for pH, chloride concentration, and ionic strength strongly agree with the laboratory results, thus satisfying model validation criteria.

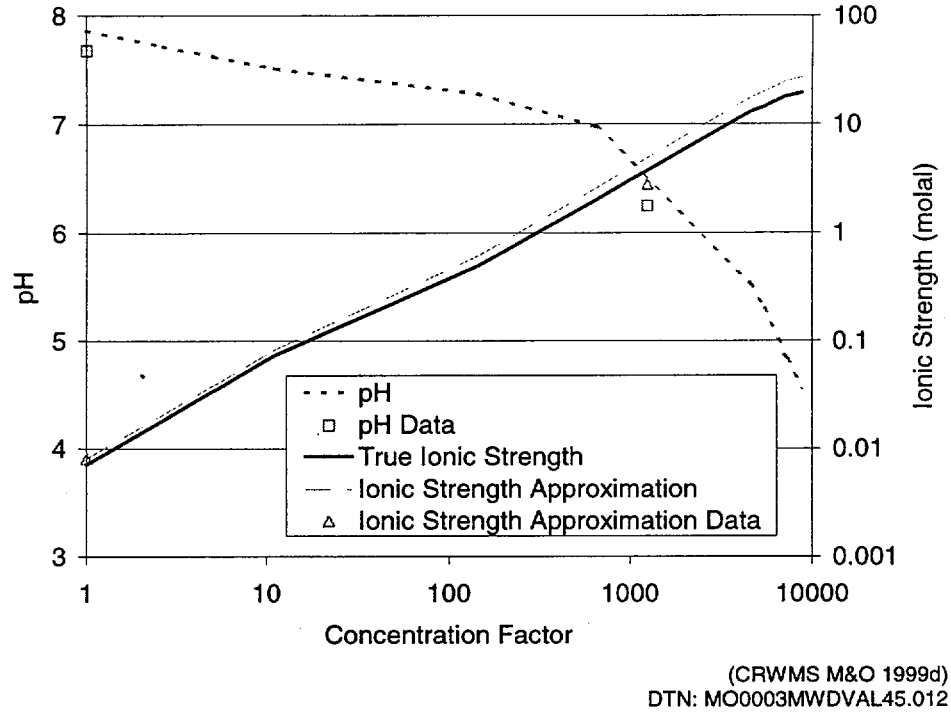

Figure 14. pH and Ionic Strength Predictions vs. Topopah Spring Tuff Pore Water Evaporation Data from Rosenberg et al. (1999b, evap3)

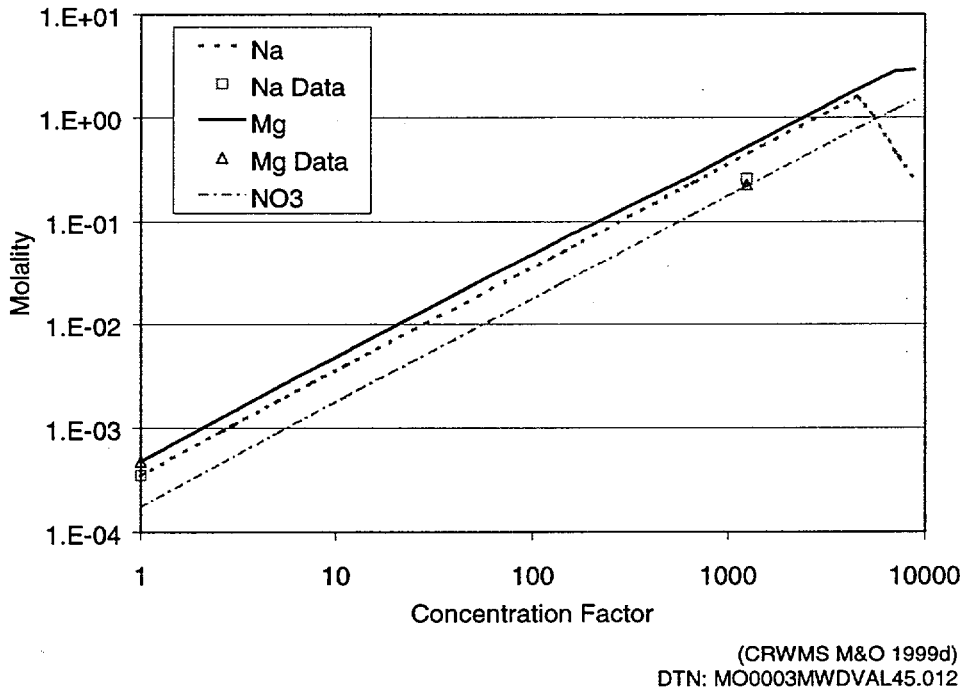

Figure 15. Na, Mg, and NO_3 Predictions vs. Topopah Spring Tuff Pore Water Evaporation Data from Rosenberg et al. (1999b, evap3)

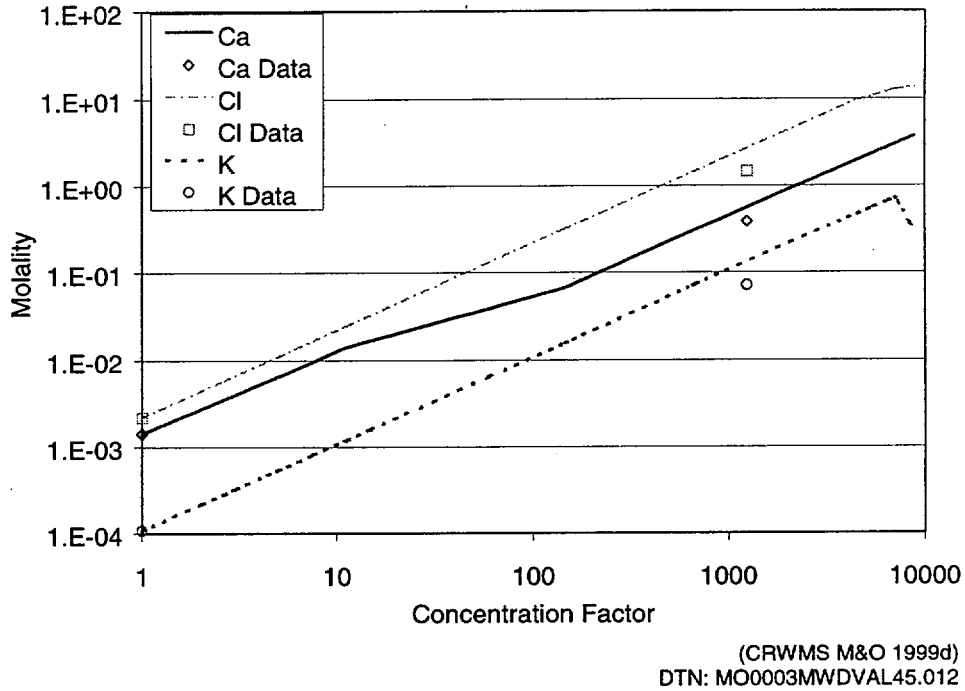

Figure 16. Cl, Ca, and K Predictions vs. Topopah Spring Tuff Pore Water Evaporation Data from Rosenberg et al. (1999b, evap3)

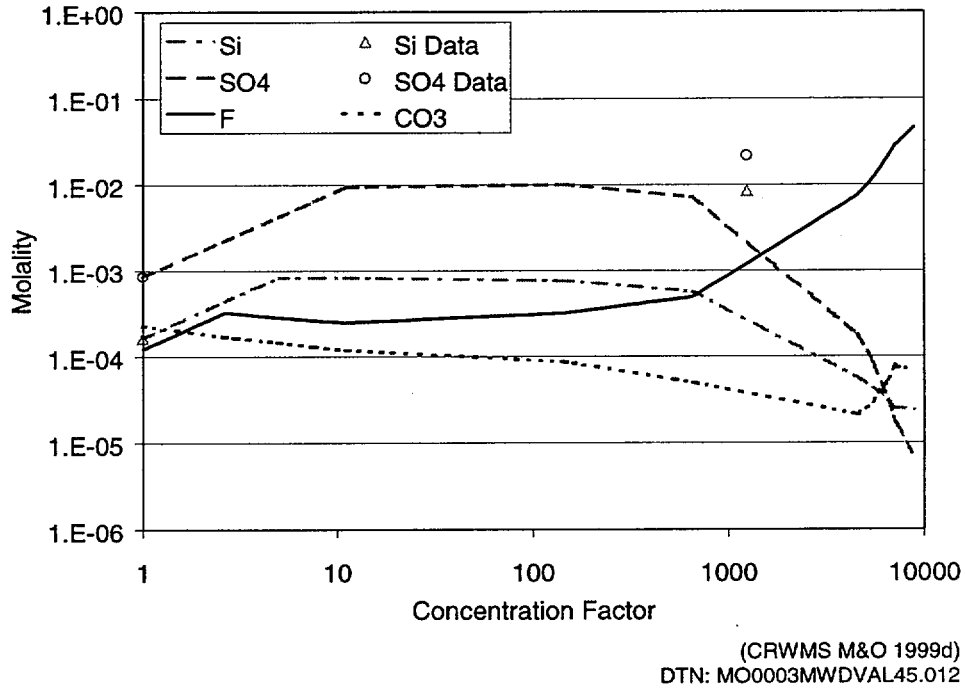

Figure 17. SO_4, CO_3, Si, and F Predictions vs. Topopah Spring Tuff Pore Water Evaporation Data from Rosenberg et al. (1999b, evap3)

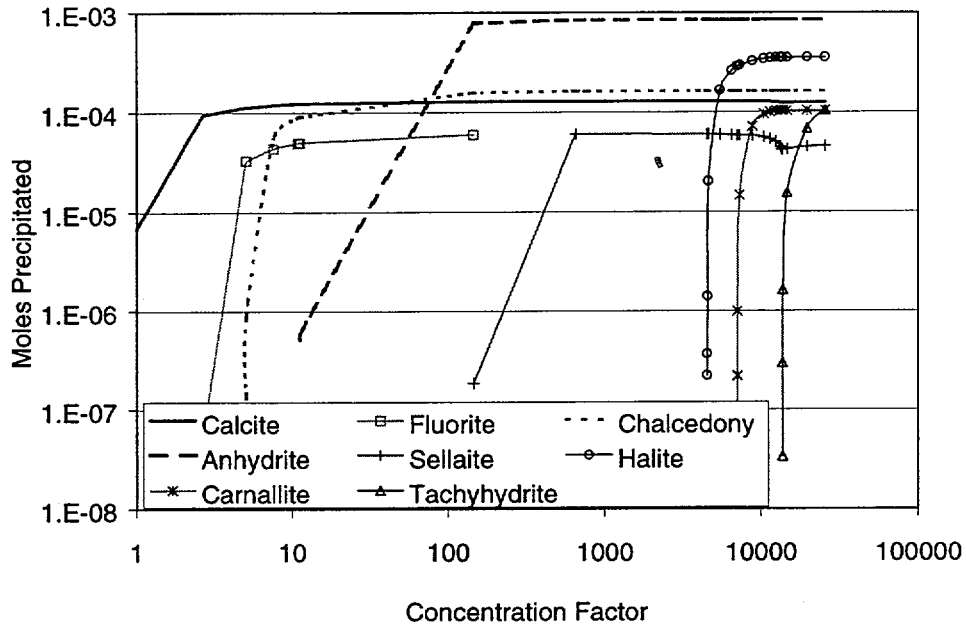

DTN: MO0003MWDVAL45.012

Figure 18. Mineral Precipitation Predictions for Topopah Spring Tuff Pore Water Evaporation Experiment of Rosenberg et al. (1999b, evap3)

6.5.1.4 Evaporation of Pure Salt Solutions

For additional model validation, the HRH model was used to predict the solubility of ten sodium and potassium salts that are potentially important in evaporated J-13 well water. The solubilities calculated are compared to handbook values. Salts that are predicted by the model to have solubilities exceeding 10 molal are shown as "> 10" molal. The results are presented in Table 17.

The comparison shows that for nearly every salt in the table (excluding the salts whose solubilities are out of the range of the model, "> 10" molal), the HRH model predicts a solubility within a factor of two of handbook values. In fact, many of the predictions are within 20 percent. The only large differences observed are for sodium and potassium nitrate salts. Their solubilities are underpredicted by the model by a factor of about 6, likely due to error in the thermodynamic constants for these nitrate salts. The consequence is that the model may predict precipitation of these nitrate salts when it should not. However, no nitrate precipitation is predicted in any of the EQ3/6 modeling results generated for the lookup tables in Section 6.6.3. The combination of a number of dissolved solids in solution prevents model-predicted saturation of nitrate salts before the true ionic strength reaches 10 molal, which is the approximate upper limit of the HRH model.

Table 17. Comparison of Handbook Aqueous Solubilities of Sodium and Potassium Salts at 100°C With Values Calculated Using the EQ3/6 HRH Model.

Salt	Handbook Aqueous Solubility at 100°C (molal) [a]	Pure Phase Solubility at100°C Calculated by EQ3/6 HRH Model (molal) [b]
NaCl	6.70	7.21
KCl	7.60	6.12
$Na_2CO_3 \cdot H_2O$	4.2	3.99
K_2CO_3	11.3	> 10 [c]
NaF	1.21	1.01
KF	26	> 10 [c]
Na_2SO_4	3.01	1.55
K_2SO_4	1.38	0.83
$NaNO_3$	21.2	3.60
KNO_3	24.4	3.60

[a] See Table 1 for references.

[b] DTN: MO0003MWDVAL45.012

[c] exceeds range of model

6.5.2 LRH Model Validation

The LRH salts model is a semi-empirical model that was developed to estimate pH, chloride concentrations, and ionic strength in highly concentrated solutions beyond the range of the HRH model. The validation criteria for the LRH model are:

1. The pH, chloride concentration, and ionic strength agree (within 20 percent) with the results of the HRH model where the two models are joined (i.e., at a water activity of about 0.85, which corresponds to an ionic strength of about 10 molal).

2. For relative humidity values below 85 percent, the predicted chloride concentrations and ionic strength are conservative or within an order of magnitude and the pH is conservative or within a pH unit.

This level of confidence is justified because it greatly reduces the potential ranges of these variables, thereby considerably reducing uncertainty.

Unfortunately, no relevant data for these types of possible brines have been found to compare to the model results. Validation of the LRH model is therefore based largely on review of calibration parameters for reasonableness and comparison of analysis results with the results from alternative conceptual models, including supporting information to establish basis for confidence (per AP-3.10Q Rev. 2 ICN 0, Sections 5.3.c.3 and 5.3.c.4).

The first criterium is met by using the HRH model results to bound the LRH model. The major ion ratios in the incoming seepage are adjusted to achieve the ratios in the evaporatively concentrated final solution predicted by the HRH model. Thus, the chloride concentrations and

ionic strength approximations (sodium plus potassium) predicted by the LRH model at 85 percent relative humidity (approximately 10 molal ionic strength) are within 20 percent of the targeted HRH values. As for pH, it is fixed for the entire LRH model range at the value provided by the HRH model.

The second criterium is met by examining calibration parameters, apparent trends based on the HRH model, and supporting information on salt solubilities. For chloride and ionic strength, the LRH model is calibrated on each end of its applicable range. On one end, it is calibrated by the results of the HRH model (previous paragraph), and on the other end it is calibrated to the approximate solubilities of sodium and potassium nitrate salts (Table 1). This range covers a water activity of about 0.85 to 0.5, corresponding to an equilibrium relative humidity of about 85 to 50 percent. The model, which has a reasonable theoretical basis and relies on reasonable assumptions and simplifications (Section 6.4.1), provides a smooth and reasonable transition for chloride and ionic strength over this range. Because of the boundary conditions on each end of this range and the incorporated (effective) solubility limits of the non-nitrate salts, the results are expected to be within the order-of-magnitude criteria.

Fixing pH for the entire LRH model range at the values provided by the HRH model at the LRH/HRH boundary is expected to satisfy the criterium that pH is either predicted within a pH unit or is conservative. Figure 19 suggests pH may peak before the HRH/LRH boundary (about 10 molal ionic strength). This figure also shows that for the HRH model range (ionic strength less than about 10 molal), pH increases by about one and a half pH units while the concentration factor increases by about three and a half orders of magnitude. The LRH model range covers about one half an order of magnitude, a much smaller concentration factor range (log scale). Thus, fixing pH at the value provided by the HRH model at the LRH/HRH boundary is believed to be justified based on the specified criteria.

In summary, the LRH model is likely valid for its intended use per AP-3.10Q Rev. 2 ICN 0, Sections 5.3.c.3 and 5.3.c.4. Model validation criteria are achieved for the following reasons:

1. The boundary conditions on each end of the applicable range are reasonable and justified within specified criteria.

2. Over the applicable range of the model, the results exhibit reasonable trends supported by accepted solubility data, a scientific basis for estimating effective solubilities of non-nitrate salts, and conservation of mass and charge. These results are also justified within specified criteria.

6.6 MODEL RESULTS

The Precipitates/Salts model results are divided into two major subsections corresponding to the submodel used. Section 6.6.1 presents the results of the EQ3/6 High Relative Humidity (HRH) salts model and Section 6.6.2 presents the results of the Low Relative Humidity (LRH) salts model.

6.6.1 High Relative Humidity Model Results

The EQ3/6 HRH model was used to predict the evolution of water subjected to simple evaporation and to simple evaporation combined with titration of incoming seepage. The first subsection (6.6.1.1) presents the results of simulating the evaporation of average J-13 well water. Section 6.6.1.2 presents the results when a constant incoming seepage is allowed.

6.6.1.1 Evaporation of Average J-13 Well Water

Evaporation of average J-13 water, as given in Table 7, was simulated using the EQ3/6 Pitzer model using the PT4 database. The temperature was increased to 95°C and the carbon dioxide fugacity was fixed at 1E-3. Figure 19 shows the modeled pH values approach 10, then fall to about 9 as the concentration factor approaches 10,000. Concentration factors are calculated by dividing the number of moles of H_2O in one liter of pure water (55.5 moles) by the number of moles of H_2O remaining in solution. The calculated true ionic strength rises sharply to over 25 molal, which is likely far beyond the range where the model is valid. Although the Precipitates/Salts model uses EQ3/6 to produce deliverable outputs up to a maximum calculated true ionic strength of approximately 10 molal, results beyond this range are presented in this section to show what the model does at these extreme values.

As shown in Figure 20 and Figure 21 the elements C, Cl, K, Na, N, and S appear to simply concentrate as the concentration factor increases because they do not precipitate at all or precipitate only in small quantities. Figure 21 shows F concentrating until fluorite precipitates, as seen in Figure 24. Figure 21, Figure 22, and Figure 23 show elements Si, Al, Ca, Mg and Fe precipitating in considerable quantities relative to their concentrations.

Figure 24 predicts calcite and chalcedony as having the most moles precipitated. Sepiolite and fluorite (at later time) are the next most abundant. The model predicts precipitation of several smectite type clays (montmorillonite-Ca, nontronite-Na, nontronite-Ca) and a zeolite (clinoptilolite-hy-Na) at several orders of magnitude less than chalcedony and calcite.

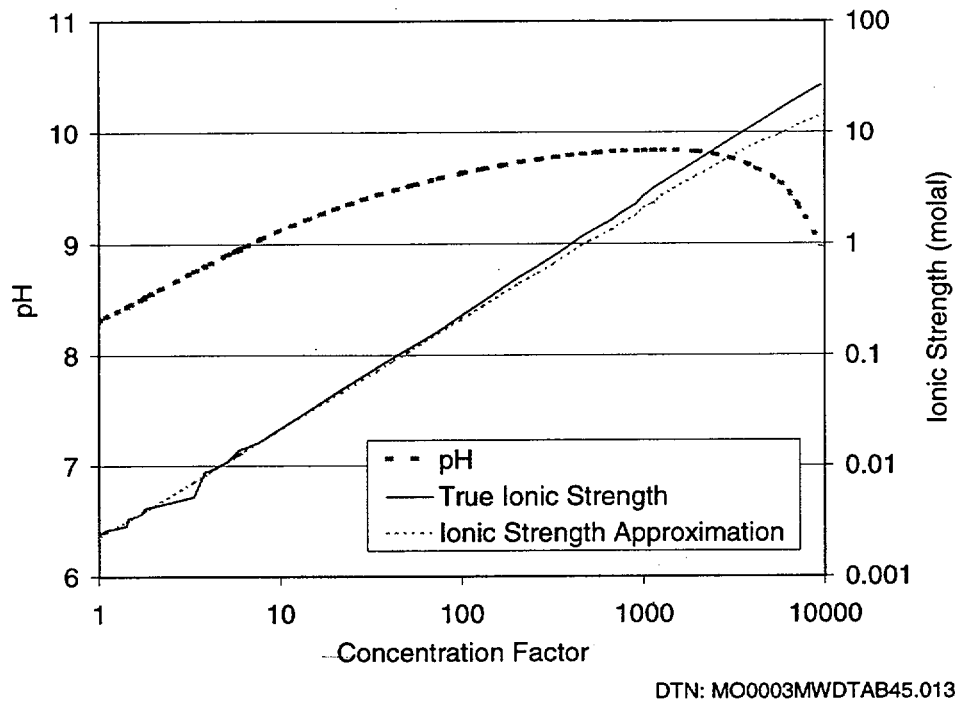

Figure 19. pH and Ionic Strength Predictions from Simple Evaporation of Average J-13 Well Water at 95ºC and f_{CO2} of 10^{-3}

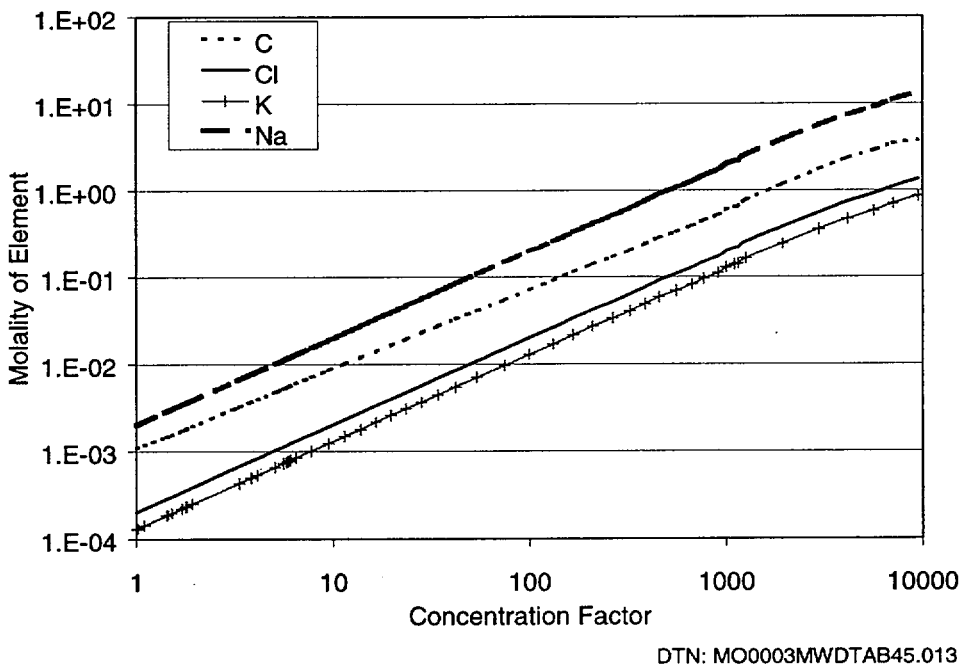

Figure 20. Cl, CO_3, K, and Na Predictions from Simple Evaporation of Average J-13 Well Water at 95ºC and f_{CO2} of 10^{-3}

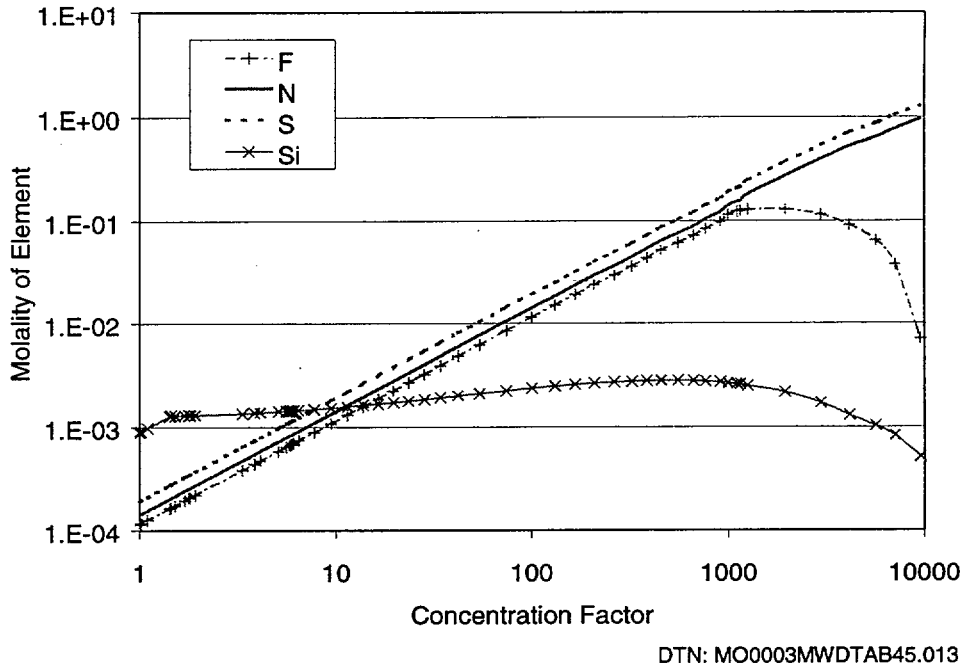

Figure 21. NO_3, SO_4, Si, and F Predictions from Simple Evaporation of Average J-13 Well Water at 95ºC and f_{CO2} of 10^{-3}

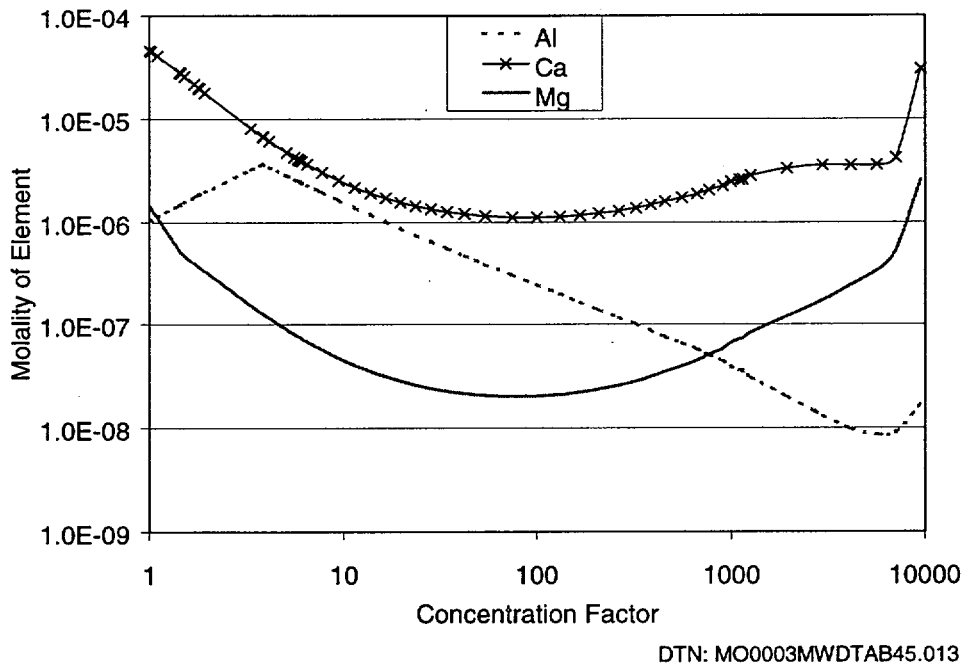

Figure 22. Ca, Mg, and Al Predictions from Simple Evaporation of Average J-13 Well Water at 95ºC and f_{CO2} of 10^{-3}

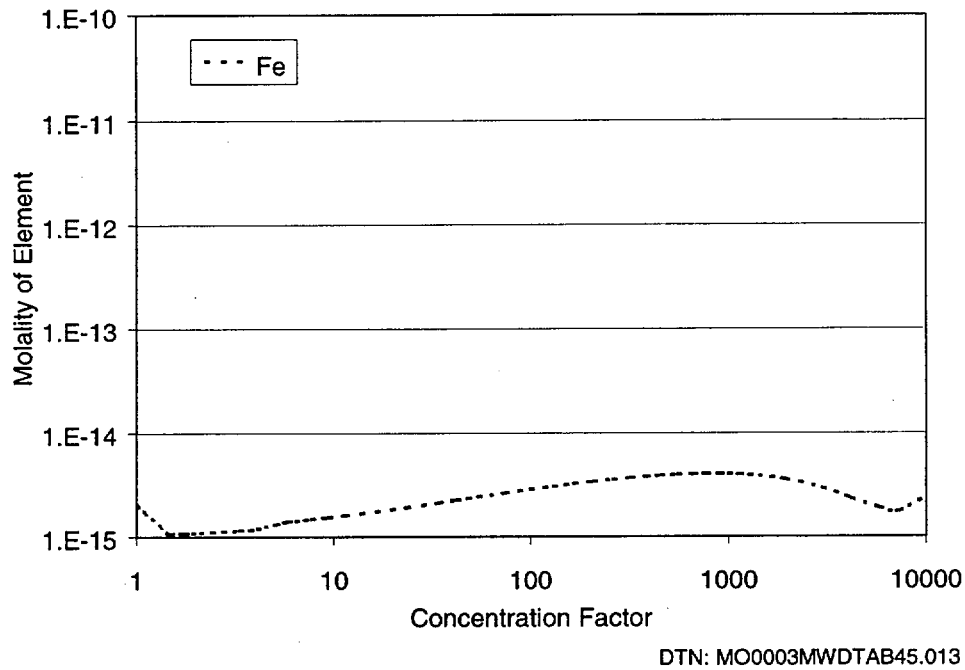

Figure 23. Fe Predictions from Simple Evaporation of Average J-13 Well Water at 95ºC and f_{CO2} of 10^{-3}

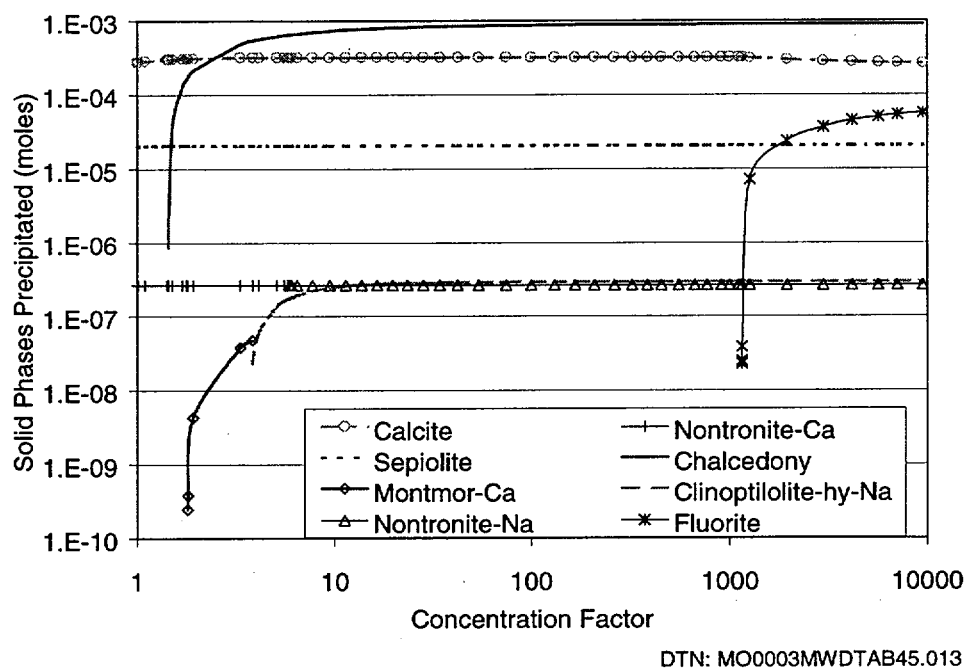

Figure 24. Mineral Precipitation Predictions from Simple Evaporation of Average J-13 Well Water at 95ºC and f_{CO2} of 10^{-3}

6.6.1.2 Results of Evaporation with a Constant Incoming Seepage

The Precipitates/Salts model asserts that when the evaporation flux exceeds or equals the flux of incoming seepage, the water within the control volume will become increasingly concentrated such that the only possible steady state conditions are complete vaporization (i.e., dry conditions with salt deposits) or a brine system that is controlled by the relative humidity. These cases generally involve highly concentrated systems that the EQ3/6 HRH model cannot simulate. However, when the flux of incoming seepage is less than the evaporation flux, a steady state condition that can be predicted by the EQ3/6 HRH model will develop after a sufficient number of pore volumes.

The evolution of water upon the drip shield or other location within the drift as temperature falls and relative humidity rises over time can be generalized as an evolution from a brine to increasingly dilute water that becomes more and more like the incoming water over time. However, for an abstracted period when the incoming seepage composition and flux are constant and the temperature and evaporation flux are constant, the system will reach a steady state as described in Section 6.4.2.2.

Figure 25 shows the Cl results for a simulation where the relative evaporation rate (R^{es}) is 0.99, the starting solution is average J-13 well water evaporated to 10 molal true ionic strength (water activity of approximately 0.85), and the incoming seepage is average J-13 well water. The Cl concentration is plotted as a function of pore volume. The number of pore volumes is determined in this report as the cumulative number of liters of incoming seepage for a given cell having a capacity of one liter.

The figure shows that the model converges to a steady state solution after about 10 pore volumes. This appears to be true for any starting solution, i.e., the steady state solution appears to be independent of the initial starting solution within the cell, as suggested by equation 15. The relative evaporation rate and incoming seepage composition are the important input parameters. The independence of the initial starting solution is important because it negates the need for building additional response surfaces for different starting compositions.

The steady state response surfaces represent the parameter values that are predicted after a sufficient number of pore volumes have flushed through the cell to achieve steady state conditions. Figure 26, Figure 27, and Figure 28, display the EQ3/6 HRH model results for average J-13 well water seepage equilibrated with carbon dioxide fugacities of 10^{-1}, 10^{-3}, and 10^{-6}, respectively. These plots show that pH is more sensitive to the carbon dioxide fugacity than to the relative evaporation rate.

Figure 29 shows the results for Cl for all temperatures and carbon dioxide fugacities modeled. The results indicate that the Cl concentration for an incoming seepage of average J-13 well water is not sensitive to temperature or carbon dioxide fugacity. Instead, it shows that equation 15 can be used to predict the Cl concentration for incoming seepage similar to J-13 well water.

The results for ionic strength are presented in Figure 30, Figure 31, and Figure 32 for carbon dioxide fugacities of 10^{-1}, 10^{-3}, and 10^{-6}, respectively. Although they indicate that the ionic strength is slightly affected by carbon dioxide fugacity and temperature, they show that the ionic

strength can be plausibly accurately approximated using equation 15 for J-13 incoming seepage. The deviations using equation 15 are due to precipitation of salts and minerals.

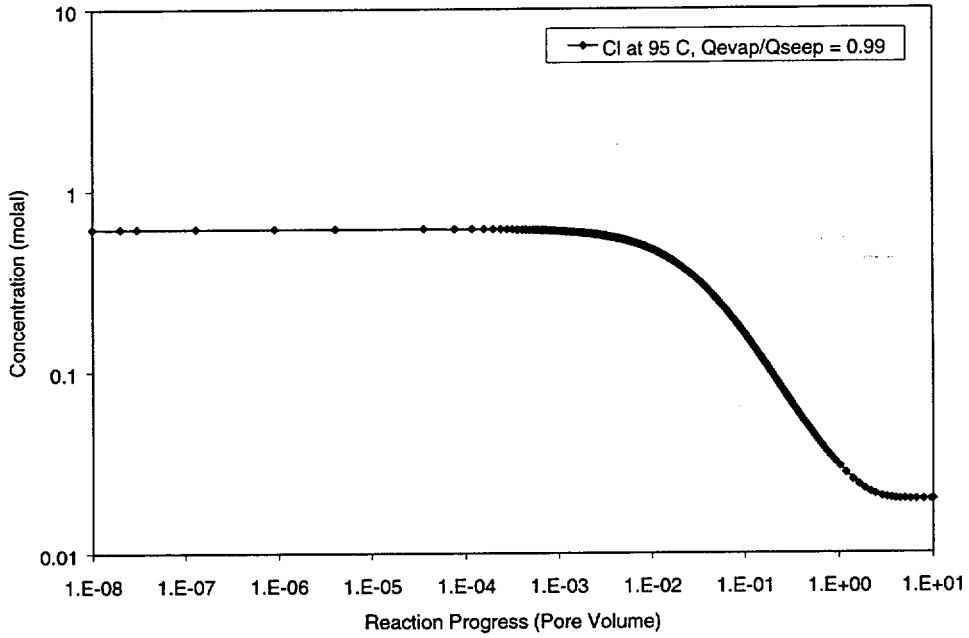

DTN: MO0003MWDTAB45.013

Figure 25. Cl Concentration Predictions vs. Pore Volume for R^{es} = 0.99, T = 95ºC, f_{CO2} = 10^{-3}, C^s = 0.0002 molal, and Initial C = 0.6 molal

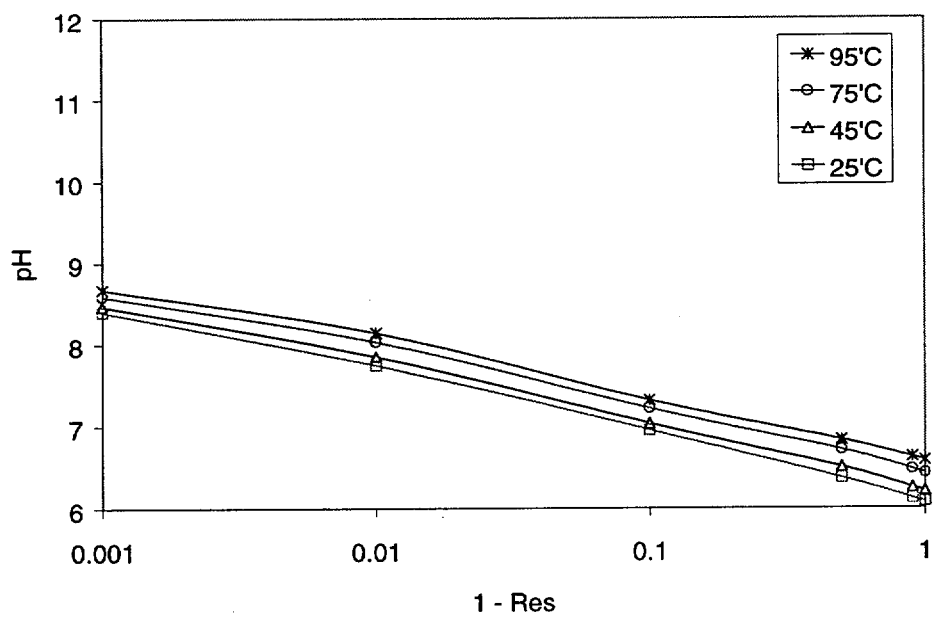

DTN: MO9912SPAISP45.004

Figure 26. J-13 Steady State pH vs. (1-R^{es}) and Temperature (f_{CO2} = 10^{-1})

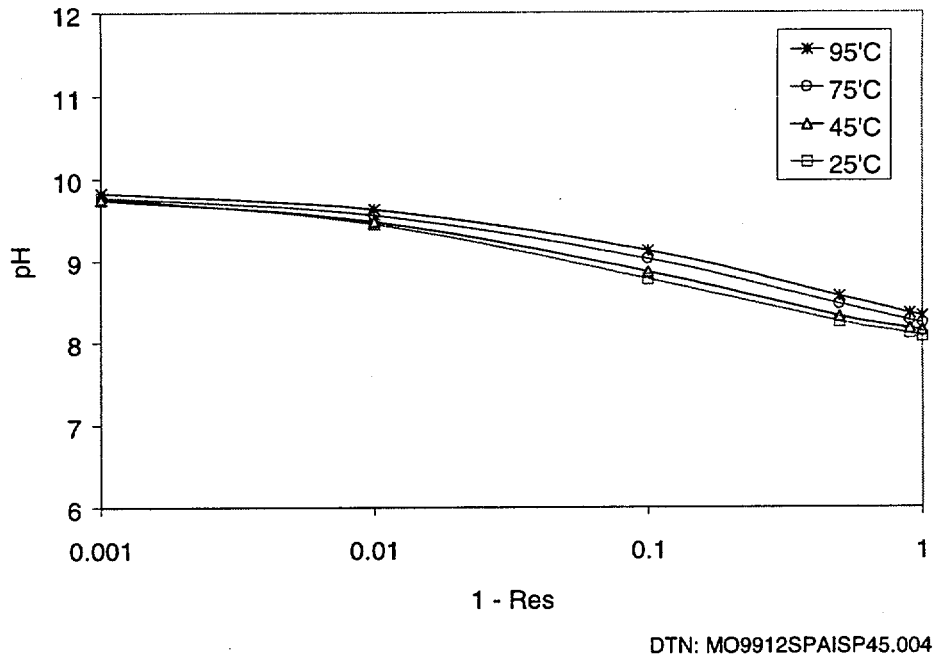

Figure 27. J-13 Steady State pH vs. (1-R^{es}) and Temperature ($f_{CO2} = 10^{-3}$)

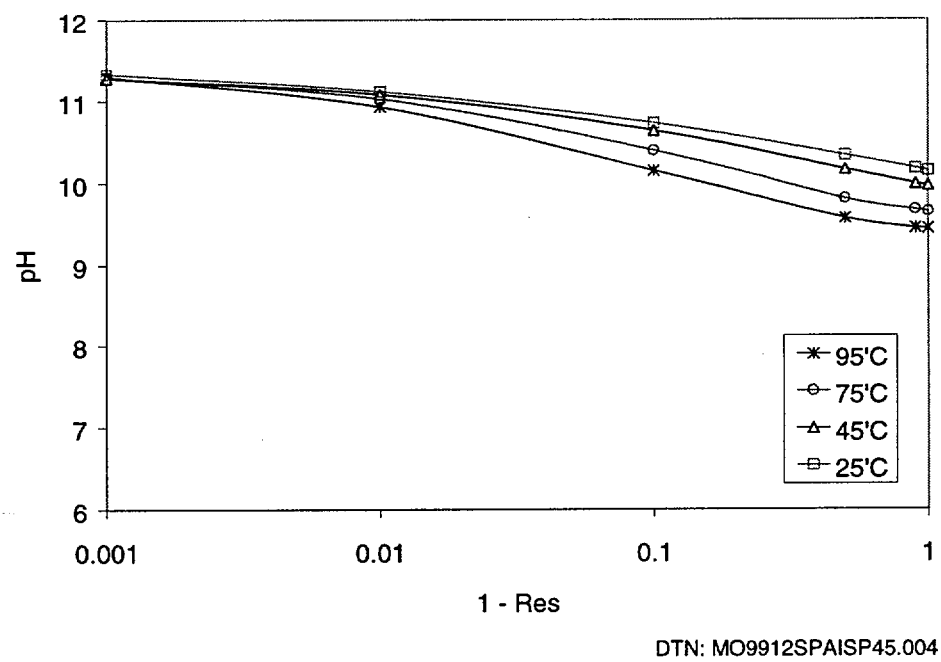

Figure 28. J-13 Steady State pH vs. (1-R^{es}) and Temperature ($f_{CO2} = 10^{-6}$)

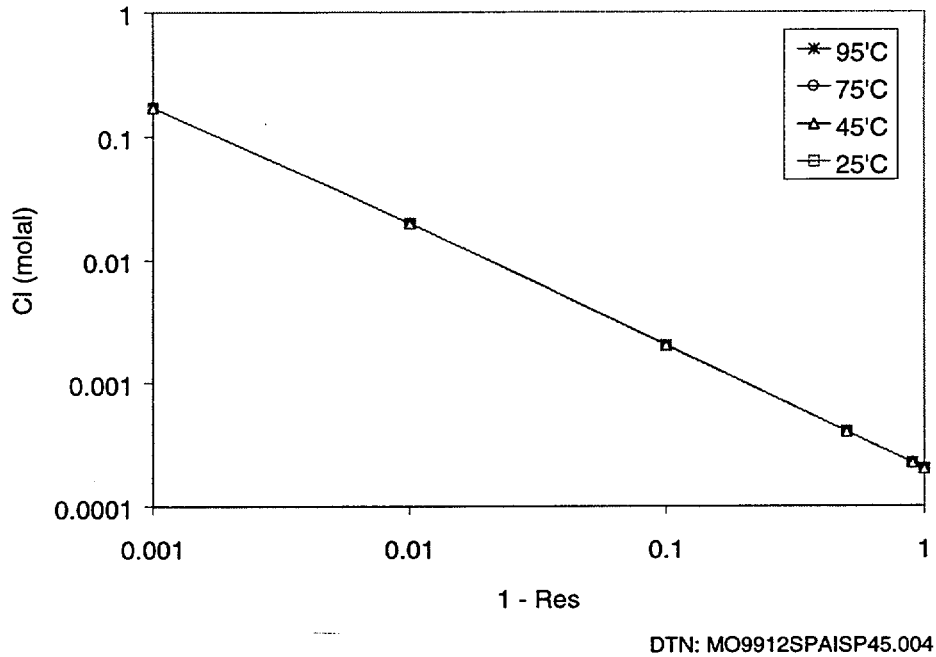

Figure 29. J-13 Steady State Cl vs. (1-R^{es}) and Temperature (identical for $f_{CO2} = 10^{-1}$, 10^{-3}, and 10^{-6})

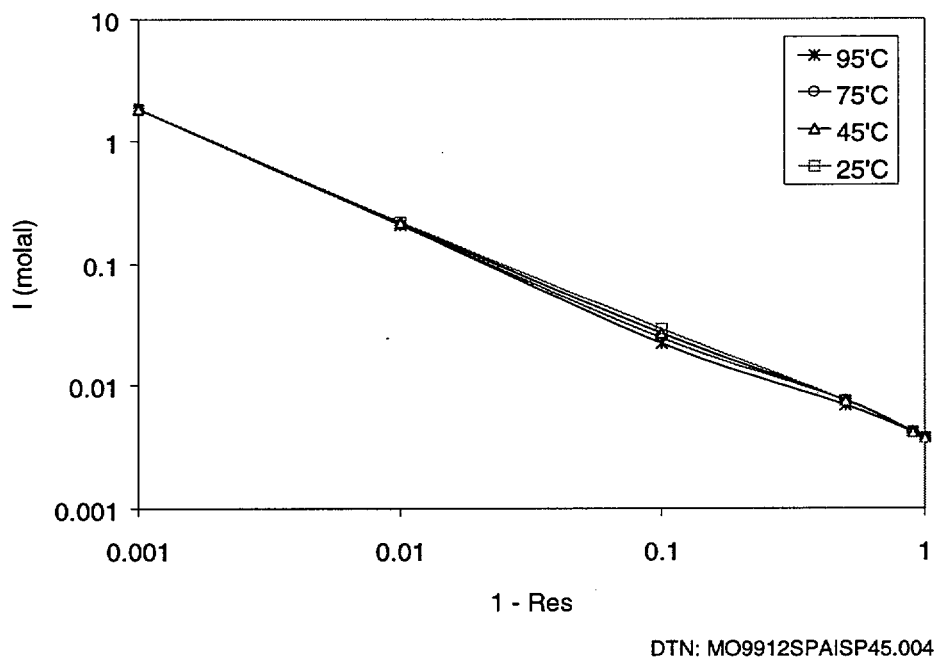

Figure 30. J-13 Steady State Ionic Strength vs. (1-R^{es}) and Temperature ($f_{CO2} = 10^{-1}$)

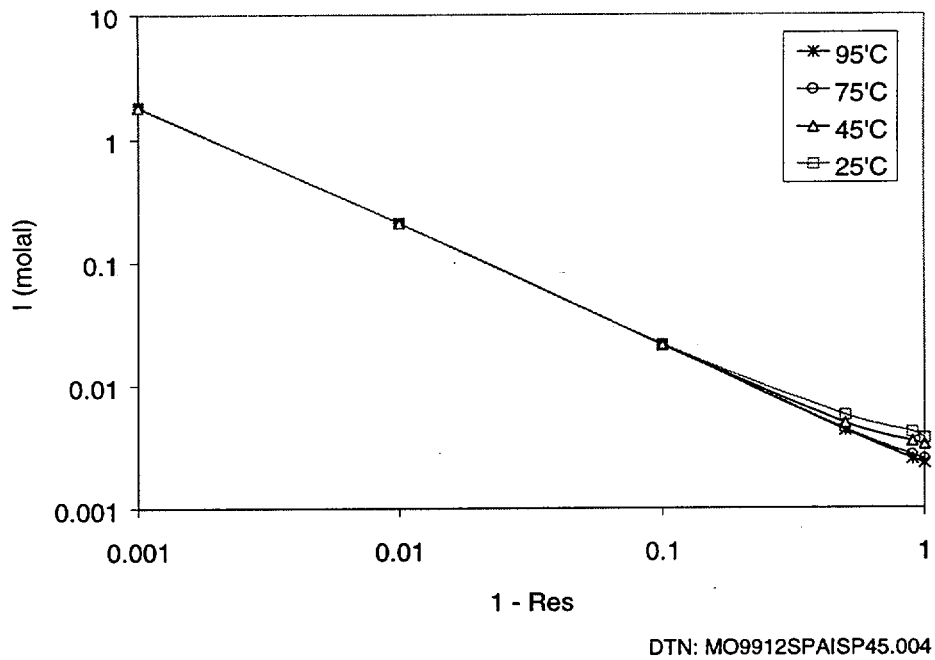

Figure 31. J-13 Steady State Ionic Strength vs. (1-R^{es}) and Temperature ($f_{CO2} = 10^{-3}$)

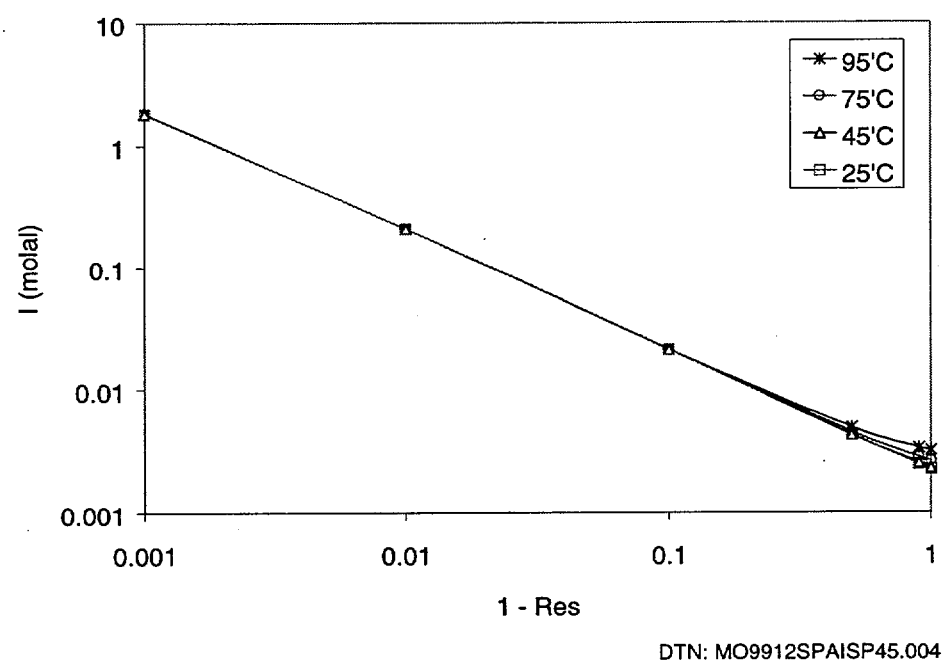

Figure 32. J-13 Steady State Ionic Strength vs. (1-R^{es}) and Temperature ($f_{CO2} = 10^{-6}$)

6.6.2 Low Relative Humidity Model Results

The results that are displayed in Figure 33 through Figure 38 are for an incoming seepage flux of one liter per year of average J-13 well water and a fixed carbon dioxide fugacity of 10^{-3}. Figure 33 is a plot of the cumulative mass of each component entering the reactor over time. The fraction of each component in the reactor that is dissolved as a function of time is presented in Figure 34. These values except for Na were predetermined by the LRH salts model. Na values were calculated by the model by charge balance.

Figure 35 includes some of the output sought from the Precipitates/Salts model. It displays a plot of aqueous component concentrations as a function of time. Mass balance calculations (i.e., the moles of dissolved plus solid-phase components in the reactor, the moles of dissolved components in the reactor, and the cumulative masses of water and dissolved solids generated in the brine) are plotted as a function of time in Figure 36, Figure 37, and Figure 38.

The results are fairly insensitive to the fugacity of carbon dioxide. Nevertheless, the effects of varying the fugacity of carbon dioxide are incorporated into the lookup tables described in the following section. The temperature was fixed a 95°C for all runs of the LRH salts model because lower temperatures correlate with relative humidity values that are incongruously high for the LRH salts model.

The equations in Section 6.4.1 (i.e., equations 5 through 14) and repeated runs of the LRH model show that the lookup table values are insensitive to the incoming seepage flux and the cumulative masses and volumes of salts and brine. In other words, altering the seepage flux will not alter the results displayed in Figure 35. The complete Mathcad calculation is presented in Attachment I.

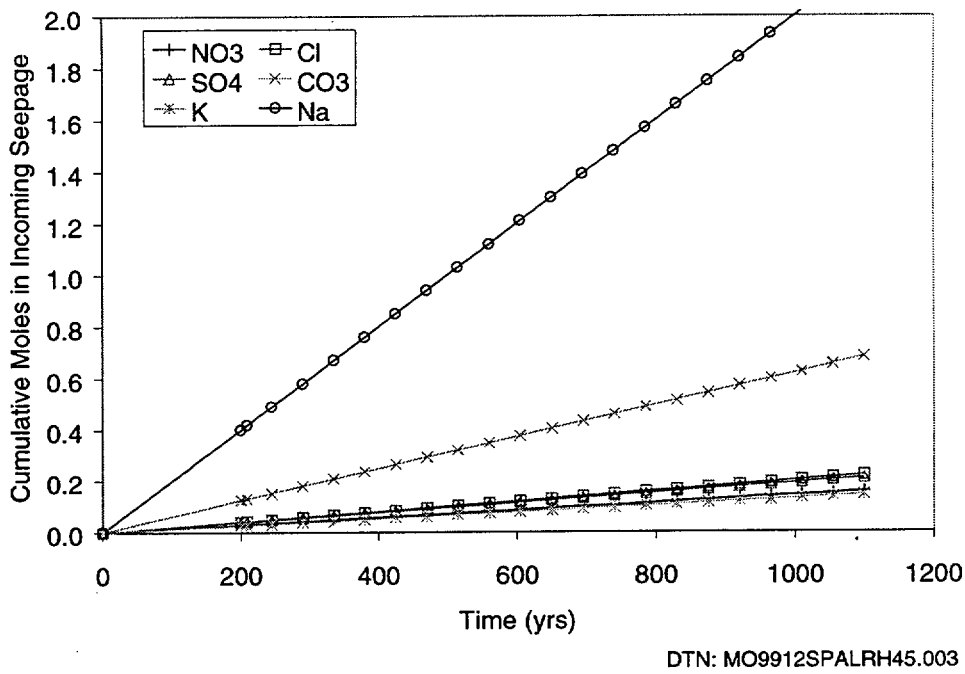

Figure 33. Cumulative Moles of Incoming Seepage Dissolved Solids vs. Time (J-13, Q^s = 1 L/yr, f_{CO2} = 10^{-3})

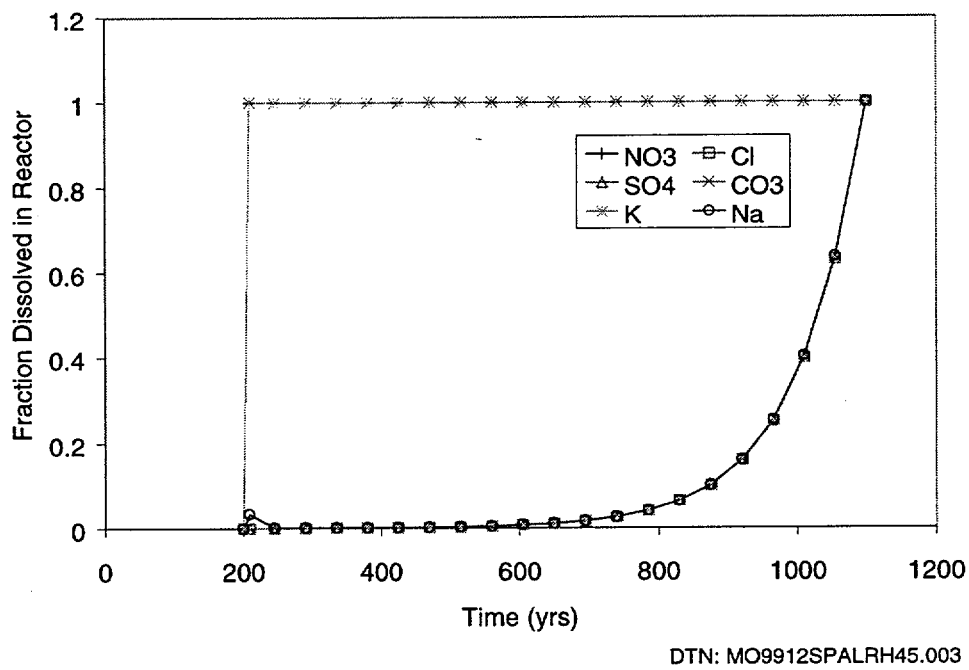

Figure 34. Fraction of Moles Dissolved Within Reactor vs. Time (J-13, Q^s = 1 L/yr, f_{CO2} = 10^{-3})

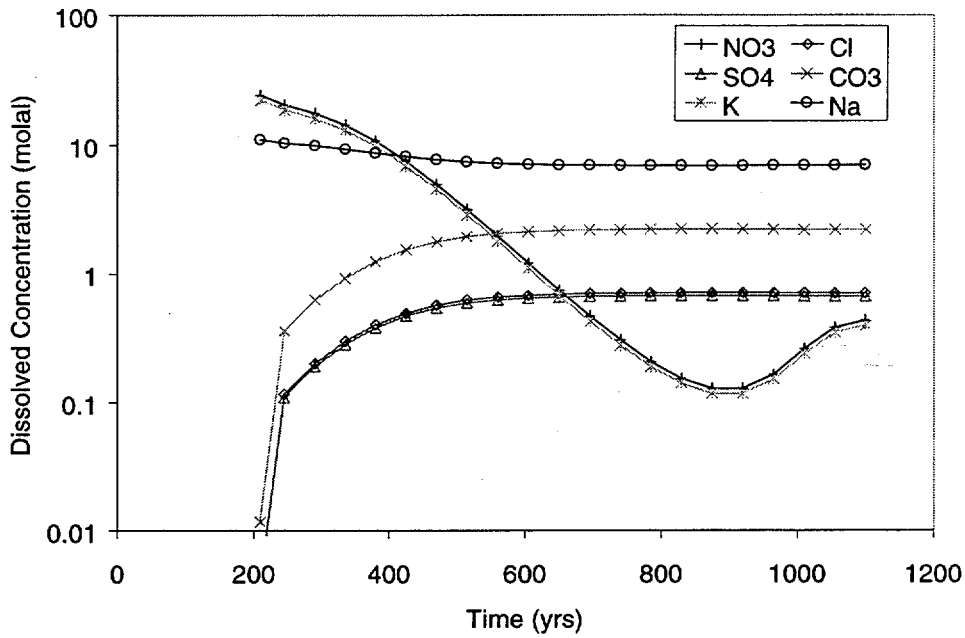

Figure 35. Dissolved Concentration vs. Time (J-13, Q^s = 1 L/yr, $f_{CO2} = 10^{-3}$)

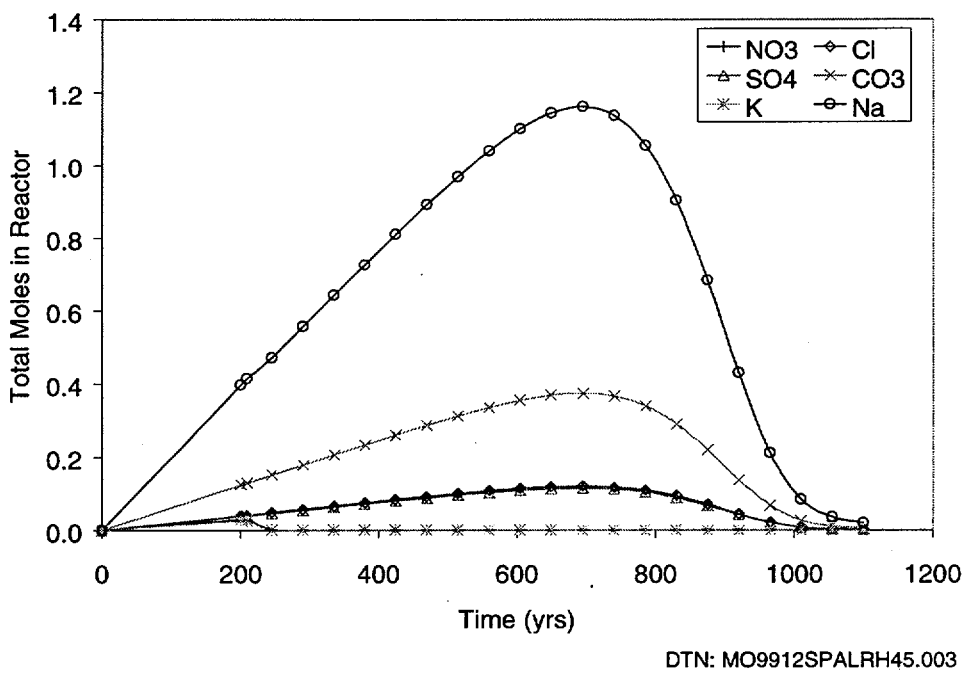

Figure 36. Total Moles in Reactor vs. Time (J-13, Q^s = 1 L/yr, $f_{CO2} = 10^{-3}$)

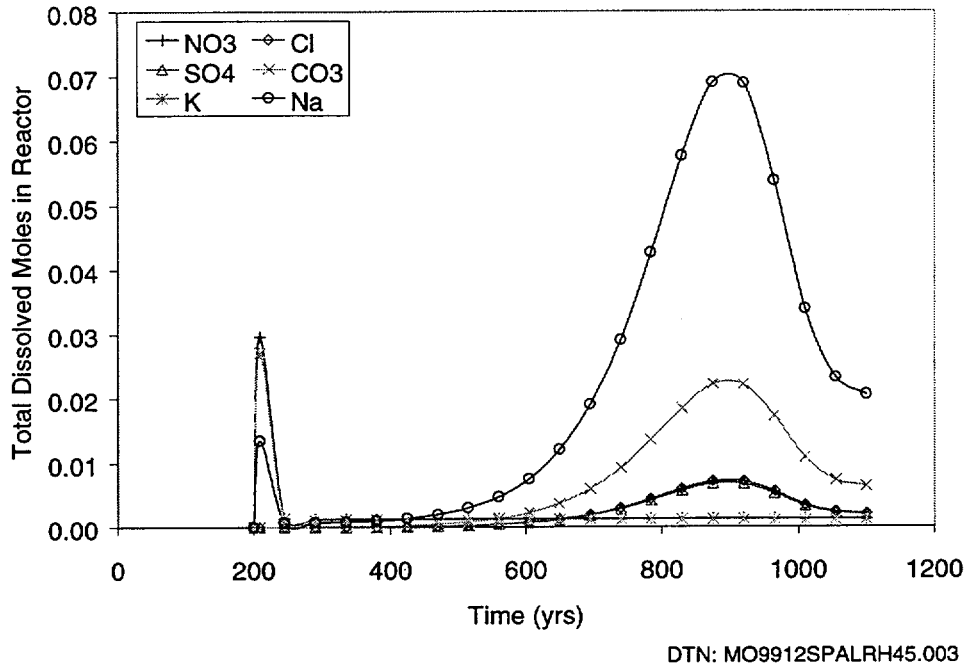

Figure 37. Total Dissolved Moles in Reactor vs. Time (J-13, Q^s = 1 L/yr, $f_{CO2} = 10^{-3}$)

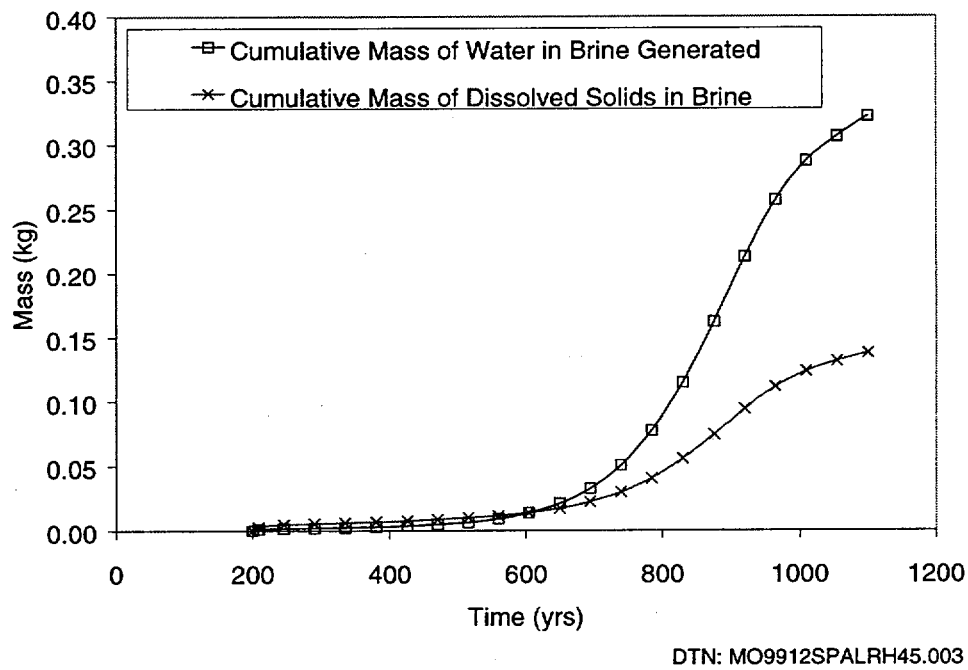

Figure 38. Cumulative Mass of Water and Dissolved Ions in Generated Brine vs. Time (J-13, Q^s = 1 L/yr, $f_{CO2} = 10^{-3}$)

6.6.3 Precipitates/Salts Model Lookup Tables

The outputs required from the Precipitates/Salts model are the values for pH, Cl concentration, and ionic strength for a given set of inputs intended to encompass the likely scenarios that could occur. These outputs are summarized in a set of lookup tables presented Table 18 through Table 20. For the Precipitates/Salts model, the important independent variables are the incoming seepage composition (C_i^s), relative humidity (RH), temperature (T), relative evaporation rate (R^{es}), and the fugacity of carbon dioxide (f_{CO2}). These lookup tables include outputs from the LRH salts model (RH < or = 85 percent) and the EQ3/6 HRH salts model (RH > 85 percent).

The LRH salts model incorporates a functional relationship between RH and time. This relationship is apparent in equation 6. For the lookup tables, time is avoided as an independent input variable by imposing a linear relationship between RH and time (Assumption 5.2.4.2). By definition, the parameters $t^{50\%}$ and $t^{85\%}$ in equation 6 are the times when RH equals 50 and 85 percent, respectively. Increasing RH linearly with time from 50 to 85 percent provides the abstraction used to generate the lookup values for RH less than or equal to 85 percent.

The ionic strength values presented in the lookup tables are an approximation of the true ionic strength, as described in Section 6.3.2 (equation 4). An additional approximation is required for lookup table pH values when the RH is less than or equal to 85 percent. Because pH cannot be calculated using the LRH salts model, it is approximated by using the EQ3/6 HRH model to perform a simple evaporation of the incoming seepage water to a true ionic strength of 10 molal (i.e., to a water activity of approximately 0.85). These values for pH are included in the lookup tables for cases in which RH is less than or equal to 85 percent.

Finally, for the case in which the relative evaporation rate (R^{es}) is one or greater, the ionic strength and Cl concentrations are set at the values obtained by the LRH salts model at 85 percent relative humidity for the given carbon dioxide fugacities and temperatures. This is done to approximate a reasonable transition between the LRH and HRH model results.

The values in the lookup tables may be used to define response surfaces so that interpolations or extrapolations may be obtained for input values not provided in the tables. Because a number of input and output variables have ranges over several orders of magnitude, it is strongly recommended that interpolations or extrapolations be based on relationships between the following modified variables: RH, T, ($\log f_{CO2}$), ($\log (1 - R^{es})$), pH, ($\log C_{Cl}$), and ($\log I$).

Table 18. Lookup Table for Average J-13 Well Water Seepage at $f_{CO2} = 10^{-1}$

Input Parameters			Precipitates/Salts Model Output		
RH (%)	*T* (°C)	R^{es}	pH	Cl (molal)	*I* (molal)
< 50.3	na[a]	na	dry	dry	dry
50.3	na	na	8.65	3.77E-03	3.65E+01
51.0	na	na	8.65	4.52E-02	3.49E+01
53.1	na	na	8.65	1.87E-01	2.95E+01
55.2	na	na	8.65	3.06E-01	2.49E+01
60.5	na	na	8.65	6.03E-01	1.35E+01
65.7	na	na	8.65	7.26E-01	8.77E+00
71.0	na	na	8.65	7.56E-01	7.62E+00
76.2	na	na	8.65	7.62E-01	7.39E+00
81.5	na	na	8.65	7.58E-01	7.56E+00
85.0	na	na	8.65	7.52E-01	7.79E+00
> 85	95	0	6.58	2.01E-04	3.74E-03
> 85	95	0.1	6.62	2.23E-04	4.15E-03
> 85	95	0.5	6.83	4.02E-04	6.85E-03
> 85	95	0.9	7.31	2.01E-03	2.21E-02
> 85	95	0.99	8.14	1.98E-02	2.09E-01
> 85	95	0.999	8.67	1.73E-01	1.82E+00
> 85	95	> or = 1	8.65	7.52E-01	7.79E+00
> 85	75	0	6.42	2.01E-04	3.74E-03
> 85	75	0.1	6.47	2.23E-04	4.15E-03
> 85	75	0.5	6.71	4.02E-04	7.51E-03
> 85	75	0.9	7.21	2.01E-03	2.44E-02
> 85	75	0.99	8.03	1.98E-02	2.09E-01
> 85	75	0.999	8.59	1.73E-01	1.82E+00
> 85	75	> or = 1	8.65	7.52E-01	7.79E+00
> 85	45	0	6.21	2.01E-04	3.74E-03
> 85	45	0.1	6.25	2.23E-04	4.15E-03
> 85	45	0.5	6.50	4.02E-04	7.47E-03
> 85	45	0.9	7.03	2.01E-03	2.66E-02
> 85	45	0.99	7.85	1.98E-02	2.16E-01
> 85	45	0.999	8.47	1.73E-01	1.82E+00
> 85	45	> or = 1	8.65	7.52E-01	7.79E+00
> 85	25	0	6.08	2.01E-04	3.74E-03
> 85	25	0.1	6.12	2.23E-04	4.16E-03
> 85	25	0.5	6.37	4.02E-04	7.47E-03
> 85	25	0.9	6.95	2.01E-03	2.91E-02
> 85	25	0.99	7.74	1.98E-02	2.21E-01
> 85	25	0.999	8.40	1.73E-01	1.84E+00
> 85	25	> or = 1	8.65	7.52E-01	7.79E+00

DTN: MO9912SPAISP45.004

[a] not applicable

Table 19. Lookup Table for Average J-13 Well Water Seepage at $f_{CO2} = 10^{-3}$

Input Parameters			Precipitates/Salts Model Output		
RH (%)	*T* (°C)	R^{es}	pH	Cl (molal)	*I* (molal)
< 50.3	na[a]	na	dry	dry	dry
50.3	na	na	9.75	3.76E-03	3.34E+01
51.0	na	na	9.75	4.50E-02	3.18E+01
53.1	na	na	9.75	1.83E-01	2.67E+01
55.2	na	na	9.75	2.97E-01	2.24E+01
60.5	na	na	9.75	5.69E-01	1.22E+01
65.7	na	na	9.75	6.78E-01	8.15E+00
71.0	na	na	9.75	7.04E-01	7.18E+00
76.2	na	na	9.75	7.09E-01	6.99E+00
81.5	na	na	9.75	7.05E-01	7.13E+00
85.0	na	na	9.75	7.00E-01	7.32E+00
> 85	95	0	8.31	2.01E-04	2.30E-03
> 85	95	0.1	8.35	2.23E-04	2.51E-03
> 85	95	0.5	8.56	4.02E-04	4.30E-03
> 85	95	0.9	9.12	2.01E-03	2.12E-02
> 85	95	0.99	9.63	1.98E-02	2.09E-01
> 85	95	0.999	9.83	1.72E-01	1.82E+00
> 85	95	> or = 1	9.75	7.00E-01	7.32E+00
> 85	75	0	8.23	2.01E-04	2.50E-03
> 85	75	0.1	8.26	2.23E-04	2.68E-03
> 85	75	0.5	8.46	4.02E-04	4.38E-03
> 85	75	0.9	9.02	2.01E-03	2.12E-02
> 85	75	0.99	9.56	1.98E-02	2.09E-01
> 85	75	0.999	9.78	1.72E-01	1.82E+00
> 85	75	> or = 1	9.75	7.00E-01	7.32E+00
> 85	45	0	8.14	2.01E-04	3.30E-03
> 85	45	0.1	8.17	2.23E-04	3.49E-03
> 85	45	0.5	8.31	4.02E-04	4.91E-03
> 85	45	0.9	8.86	2.01E-03	2.13E-02
> 85	45	0.99	9.48	1.97E-02	2.09E-01
> 85	45	0.999	9.75	1.73E-01	1.82E+00
> 85	45	> or = 1	9.75	7.00E-01	7.32E+00
> 85	25	0	8.07	2.01E-04	3.73E-03
> 85	25	0.1	8.11	2.23E-04	4.16E-03
> 85	25	0.5	8.25	4.02E-04	5.71E-03
> 85	25	0.9	8.77	2.01E-03	2.17E-02
> 85	25	0.99	9.45	1.98E-02	2.09E-01
> 85	25	0.999	9.78	1.73E-01	1.82E+00
> 85	25	> or = 1	9.75	7.00E-01	7.32E+00

DTN: MO9912SPAISP45.004

[a] not applicable

Table 20. Lookup Table for Average J-13 Well Water Seepage at $f_{CO2} = 10^{-6}$

Input Parameters			Precipitates/Salts Model Output		
RH (%)	*T* (°C)	R^{es}	pH	Cl (molal)	*I* (molal)
< 50.3	na[a]	na	dry	dry	dry
50.3	na	na	11.26	3.76E-03	2.76E+01
51.0	na	na	11.26	4.51E-02	2.65E+01
53.1	na	na	11.26	1.85E-01	2.26E+01
55.2	na	na	11.26	3.02E-01	1.94E+01
60.5	na	na	11.26	5.88E-01	1.16E+01
65.7	na	na	11.26	7.05E-01	8.34E+00
71.0	na	na	11.26	7.33E-01	7.57E+00
76.2	na	na	11.26	7.38E-01	7.42E+00
81.5	na	na	11.26	7.34E-01	7.53E+00
85.0	na	na	11.26	7.29E-01	7.68E+00
> 85	95	0	9.44	2.01E-04	3.17E-03
> 85	95	0.1	9.45	2.23E-04	3.34E-03
> 85	95	0.5	9.57	4.02E-04	4.88E-03
> 85	95	0.9	10.15	2.01E-03	2.12E-02
> 85	95	0.99	10.93	1.98E-02	2.09E-01
> 85	95	0.999	11.3	1.73E-01	1.82E+00
> 85	95	> or = 1	11.26	7.29E-01	7.68E+00
> 85	75	0	9.65	2.01E-04	2.63E-03
> 85	75	0.1	9.67	2.23E-04	2.82E-03
> 85	75	0.5	9.81	4.02E-04	4.51E-03
> 85	75	0.9	10.4	2.01E-03	2.12E-02
> 85	75	0.99	11.03	1.98E-02	2.09E-01
> 85	75	0.999	11.29	1.73E-01	1.82E+00
> 85	75	> or = 1	11.26	7.29E-01	7.68E+00
> 85	45	0	9.97	2.01E-04	2.30E-03
> 85	45	0.1	9.99	2.23E-04	2.53E-03
> 85	45	0.5	10.17	4.02E-04	4.25E-03
> 85	45	0.9	10.64	2.01E-03	2.12E-02
> 85	45	0.99	11.08	1.98E-02	2.09E-01
> 85	45	0.999	11.28	1.72E-01	1.82E+00
> 85	45	> or = 1	11.26	7.29E-01	7.68E+00
> 85	25	0	10.15	2.01E-04	2.24E-03
> 85	25	0.1	10.18	2.23E-04	2.46E-03
> 85	25	0.5	10.34	4.02E-04	4.29E-03
> 85	25	0.9	10.73	2.01E-03	2.12E-02
> 85	25	0.99	11.12	1.98E-02	2.09E-01
> 85	25	0.999	11.33	1.72E-01	1.82E+00
> 85	25	> or = 1	11.26	7.29E-01	7.68E+00

DTN: MO9912SPAISP45.004

[a] not applicable

6.6.4 Condensed Water Composition and Lookup Tables

The results of the Condensed Water model show that the pH and ionic strength of the condensed water is sensitive to temperature and the fugacity of carbon dioxide. The EQ3/6 input and output files for this model have a DTN of MO9912MWDEQ345.002. The summary results have a DTN of MO9912SPAISP45.005.

Figure 39 shows that the pH decreases considerably as the carbon dioxide fugacity increases above 10^{-5}. In this range, a higher temperature results in a higher equilibrium pH. At low carbon dioxide fugacities, the pH is insensitive to the carbon dioxide fugacity and temperature.

The ionic strength shown in Figure 40 and presented in the lookup table (Table 21) is the true ionic strength calculated by EQ3/6 and not the ionic strength approximation (equation 4) used in the seepage evaporation calculations. The true ionic strength is used here because the Condensed Water model does not include Na, K, Ca, or Mg in solution (Assumption 5.6). Figure 40 shows that the true ionic strength is fairly low for all of the conditions modeled. The trends indicate that temperature is more important to ionic strength predictions when the carbon dioxide fugacity is low. When the fugacity of carbon dioxide is high, the carbon dioxide fugacity becomes more important than temperature to ionic strength predictions.

The values in the lookup table may be used to define response surfaces so that interpolations or extrapolations may be obtained for input values not provided in the tables. Because a number of input and output variables have ranges over several orders of magnitude, it is recommended that interpolations or extrapolations be based on relationships between the following modified variables: T, ($\log f_{CO2}$), pH, and ($\log I$).

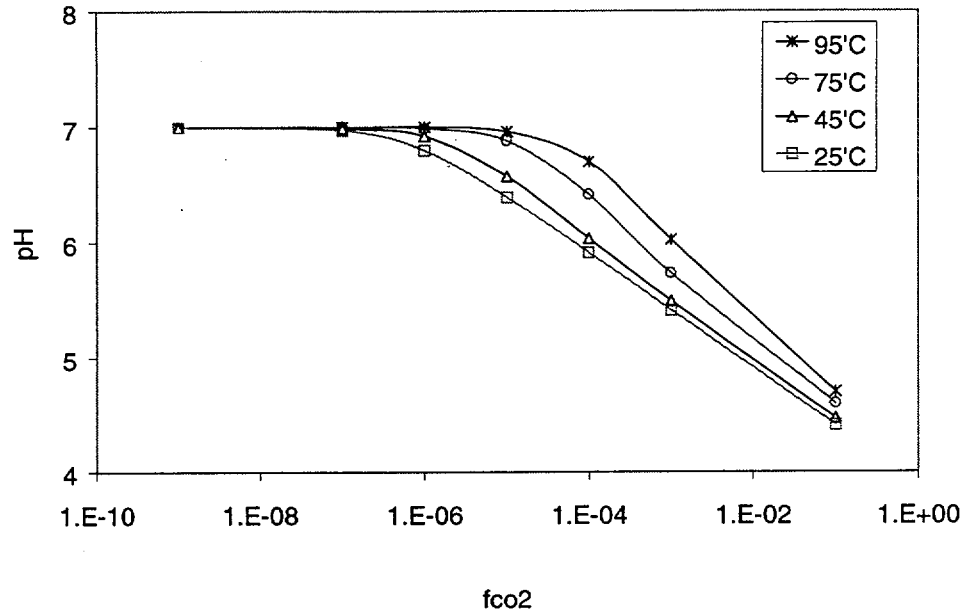

DTN: MO9912SPAISP45.005

Figure 39. Predicted pH of Condensed Water for a Range of Temperatures (*T*) and Fugacities of Carbon Dioxide (f_{CO2}).

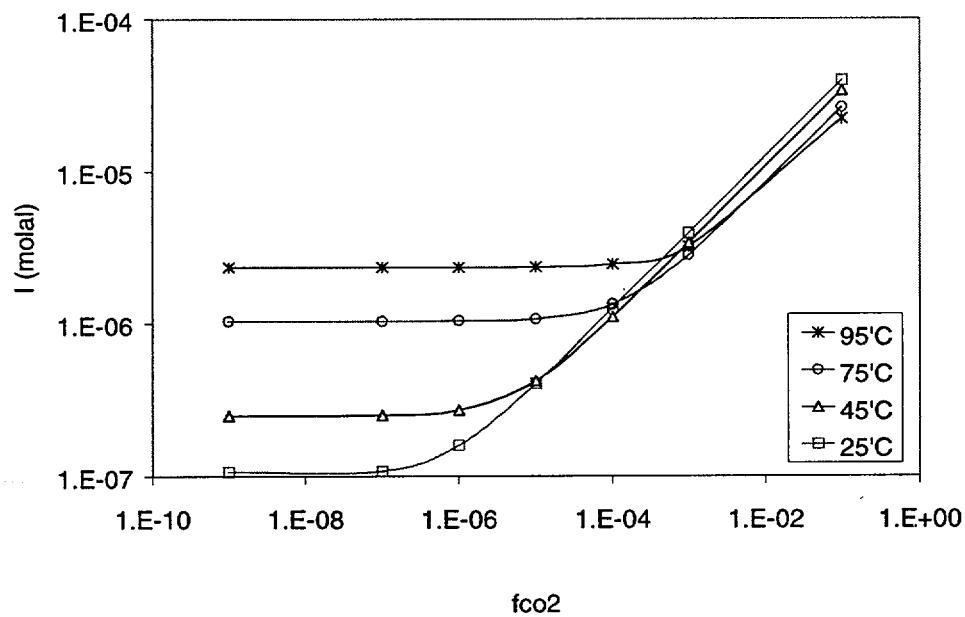

DTN: MO9912SPAISP45.005

Figure 40. Predicted Ionic Strength of Condensed Water for a Range of Temperatures (*T*) and Fugacities of Carbon Dioxide (f_{CO2}).

Table 21. Lookup Table for Condensed Water Model.

Input Parameters		Condensed Water Model Output		
T (°C)	f_{CO2}	pH	Cl (molal)	I (molal)
95	1.E-01	4.70	0.0	2.22E-05
95	1.E-03	6.02	0.0	3.21E-06
95	1.E-04	6.70	0.0	2.45E-06
95	1.E-05	6.96	0.0	2.36E-06
95	1.E-06	7.00	0.0	2.35E-06
95	1.E-07	7.00	0.0	2.35E-06
95	1.E-09	7.00	0.0	2.35E-06
75	1.E-01	4.60	0.0	2.63E-05
75	1.E-03	5.73	0.0	2.82E-06
75	1.E-04	6.41	0.0	1.33E-06
75	1.E-05	6.88	0.0	1.07E-06
75	1.E-06	6.99	0.0	1.04E-06
75	1.E-07	7.00	0.0	1.03E-06
75	1.E-09	7.00	0.0	1.03E-06
45	1.E-01	4.47	0.0	3.39E-05
45	1.E-03	5.49	0.0	3.39E-06
45	1.E-04	6.03	0.0	1.10E-06
45	1.E-05	6.57	0.0	4.20E-07
45	1.E-06	6.92	0.0	2.72E-07
45	1.E-07	6.99	0.0	2.52E-07
45	1.E-09	7.00	0.0	2.50E-07
25	1.E-01	4.41	0.0	3.95E-05
25	1.E-03	5.41	0.0	3.93E-06
25	1.E-04	5.91	0.0	1.25E-06
25	1.E-05	6.39	0.0	4.05E-07
25	1.E-06	6.80	0.0	1.60E-07
25	1.E-07	6.97	0.0	1.08E-07
25	1.E-09	7.00	0.0	1.07E-07

DTN: MO9912SPAISP45.005

7. CONCLUSIONS

The In-Drift Precipitates/Salts analysis was developed to evaluate the effects of water vaporization (evaporation) on water composition at a given location in the EBS (e.g., the drip shield surface). Vaporization has a profound effect upon water composition and, according to the current EBS design, it will likely result in the formation of brines and salts.

The important variables for the Precipitates/Salts model are:

- Relative humidity
- Temperature

- Fugacity of carbon dioxide
- Evaporation flux
- Incoming seepage flux
- Incoming seepage chemical composition

The outputs of the Precipitates/Salts model that are important to TSPA are:

- pH
- Chloride concentration
- Ionic strength
- Approximate maximum relative humidity for dry conditions to exist

These effects are important in estimating colloid mobility and corrosion rates for the drip shield and waste package. In addition, these effects may be important in predicting spent fuel dissolution rates and radionuclide transport.

Although the list of output variables is short, the entire major ion chemistry of seepage water must be modeled to determine these outputs. Interactions between ions in solution, gas-phase carbon dioxide, and mineral precipitates are critical or are potentially critical to the Precipitates/Salts analysis. The following subsections summarize the conceptual model, results, abstraction, uncertainty, limitations, and importance of this analysis to TSPA.

7.1 MODEL AND RESULTS

The In-Drift Precipitates/Salts analysis was performed using the EQ3/6 code where possible. To extend the range of the EQ3/6 high relative humidity (HRH) model from a calculated true ionic strength of around 1 molal to approximately 10 molal, a Pitzer database was developed and used (Section 5.3). The Pitzer database increases the concentration range of the EQ3/6 HRH model by about one order of magnitude. However, the model is still limited to high relative humidity because under equilibrium conditions the mole fraction of water in solution is directly controlled by the relative humidity (Kinsman 1976). An ionic strength of 10 molal implies a mole fraction of water around 0.85 for evaporated J-13 well water. Thus, the EQ3/6 Pitzer (HRH) model is only used for relative humidity values greater than 85 percent. An additional model, called the LRH (low relative humidity) salts model was developed to approximate the water chemistry for relative humidity values less than 85 percent.

The LRH model is a simple bounding model. When the drift temperature is high and the relative humidity is below 50 percent, the model is designed to vaporize all water and precipitate and accumulate incoming dissolved solids. As the drift cools, the relative humidity rises. When it rises above 50 percent, all accumulated nitrate salts deliquesce and incoming nitrates concentrate to solubility limits and no longer precipitate (Section 6.4.1). This occurs because nitrate is highly soluble, and nitrate salts, which are hygroscopic, are assumed to be unstable above a relative humidity of 50 percent (Assumption 5.5.3). Thus, at 50 percent relative humidity and higher, the modeled location is wet. This reasonably conservative assumption reduces the duration of the estimated dry period, which is important for aqueous corrosion and transport models.

The LRH salts model is designed to make a smooth transition to the predictions of the EQ3/6 HRH model as the relative humidity rises from 50 to 85 percent. The transition is highly simplified (Assumption 5.5.4), but it maintains mass and charge balance in the solid and liquid phases and restricts aqueous concentrations of the important soluble components to approximate effective solubilities at all times. The conceptual model is further simplified by two requirements: 1) the volume of brine generated during a time increment flows out of the control volume at the end of the time increment (i.e., no "ponding" or "bathtub" effects), and 2) the dissolved fractions of chloride, sulfate, and carbonate salts increase with increasing relative humidity such that complete dissolution of these accumulated salts does not occur until the relative humidity reaches 85 percent. While the LRH model likely oversimplifies a system that is much more complicated, it provides a starting point that at a minimum allows an approximation of an important transition from dry conditions to the concentrated solutions predicted by the EQ3/6 HRH model.

The LRH model results that are important for TSPA are a decrease in ionic strength and an increase in chloride concentration as the relative humidity rises from 50 to 85 percent. The decrease in ionic strength is a direct result of an increase in the mole fraction of water, which generally must increase with increasing relative humidity.

The reason for the increase in chloride concentration as relative humidity increases from 50 to 85 percent is not as obvious. Under equilibrium conditions, the chloride, sulfate, and carbonate salts will dissolve into a nitrate brine only to the point that the ion activity product equals the solubility product (Section 6.1.2). Because the sodium and potassium concentrations are very high in the initial concentrated nitrate brines (e.g., when relative humidity is between 50 and 60 percent), the activities of the chloride, sulfate, and carbonate ions must be low to achieve ion activity products that equal their respective salt solubility products. As relative humidity increases with time, the sodium and potassium concentrations fall, allowing the chloride, sulfate, and carbonate concentrations to increase to maintain equilibrium with the remaining precipitated salts. By approximation, the LRH salts model accounts for these effects. It also approximates and accounts for the additive effects on solubilities for a mixture of salts.

The LRH model results indicate that chloride concentrations increase from less than 0.004 to above 0.5 molal as the relative humidity increases from 50 to above 60 percent. From 60 to 85 percent relative humidity, the chloride concentration increases by less than 40 percent. Thus, the increase in chloride concentration quickly approaches the high ionic strength end point of the EQ3/6 HRH model (see Figure 35 and Figure 20). These approximations are presented as reasonable upper bounds on the chloride concentrations expected when the relative humidity is 85 percent and below for the modeled gas and incoming seepage compositions.

Above 85 percent relative humidity, the EQ3/6 Pitzer model, or HRH (high relative humidity) model, is used to predict pH, chloride concentration, and ionic strength. The solid-centered flow-through mode is used to predict the steady state conditions that develop as a constant flux of seepage of a constant composition enters the specified location (or cell) given a constant relative evaporation flux.

The relative evaporation flux (i.e., the evaporation flux divided by the incoming seepage flux) is allowed to range from zero to one. Because the HRH model is used only when relative humidity

is 85 percent or higher, soluble salts (e.g., chloride, sulfate, and nitrate salts) are determined to be dissolved under these conditions. A relative humidity of 85 percent or higher requires the mole fraction of water in solution to be approximately 0.85 or higher. The HRH model results indicate that these soluble salts are dissolved when the mole fraction of water is approximately 0.85 or higher.

At a relative evaporation flux of one, a stable brine of these salts develop whose composition is approximated by the 0.85 water activity solution determined from simple evaporation of the incoming water. Steady state relative evaporation fluxes greater than one are not possible because the mole fraction of water would have to decrease, which is not possible when the relative humidity is maintained at 85 percent or higher. For relative evaporation fluxes less than one, the solid-centered flow-through mode shows that the calculated steady state composition for a given scenario is primarily a function of the incoming seepage composition and the relative evaporation rate. As might be expected, the initial solution composition in the cell does not affect the steady state solution. In summary, the calculations show that as the relative evaporation flux decreases, as would be expected over time in the potential repository, the steady state water composition within the cell will trend toward the composition of the incoming seepage water.

In a separate analysis, the composition of condensed water on dry inert surfaces was predicted as a function of the temperature and the fugacity of carbon dioxide. The potential effects of interaction with dust was not considered (Assumption 5.6). The results indicate that pH decreases with increasing carbon dioxide fugacity but slightly increases with increasing temperature. The ionic strength of the condensed water, while shown to be sensitive to temperature and carbon dioxide fugacity, is predicted to be low for all conditions simulated.

7.2 ABSTRACTION

The results of the Precipitates/Salts analysis are intended as input for models that couple evaporative/salts effects with other processes. In these abstractions, the modeling period of the potential repository is divided into a set of time periods in which the inputs are abstracted to representative constant values. The inputs important to the Precipitates/Salts model include temperature, relative humidity, seepage flux, seepage flux composition, and the evaporation flux. Thus, for each combination of values for these inputs, a unique solution from the Precipitates/Salts model is needed.

The combinations of potential values of these inputs are unlimited. Therefore, the results from a subset of these combinations were obtained to define the response surface for interpolating results for all potential input values and combinations of input values. The input variables were limited to a small number of values which included their approximate minimum and maximum potential values. Temperature was varied between the values 25°C, 45°C, 75°C, and 95°C. The fugacity of carbon dioxide was varied between the values 10^{-1}, 10^{-3}, and 10^{-6}. The relative humidity was varied among a number of values between and including < 50 percent and > 85 percent, and the relative evaporation flux was varied between the values 0, 0.1, 0.5, 0.9, 0.99, 0.999, and 1.

The resulting response surfaces are defined by the set of pH, chloride concentration, and ionic strength results for the combinations of input values simulated. These outputs are summarized in a set of lookup tables presented in Table 18, Table 19, and Table 20. For the given input variable values of a given abstracted time increment, the steady state pH, chloride concentration, and ionic strength can be obtained or interpolated from these tables.

Several trends and relationships are observed in the lookup tables for the average J-13 well water. First, as relative humidity increases to 85 percent, ionic strength decreases and chloride concentration increases. Second, an increase in the fugacity of carbon dioxide causes pH to decrease. Third, a decrease in the relative evaporation rate causes the steady-state pH, chloride concentration, and ionic strength to decrease toward incoming values. Finally, temperature effects, except for those implicit in the relative evaporation rate, are small, especially for predictions of chloride concentration and ionic strength.

7.3 VALIDATION, UNCERTAINTY, AND LIMITATIONS

Given accurate inputs, the Precipitates/Salts model is expected to provide results that are within an order of magnitude for chloride concentrations and ionic strength and within a pH unit for pH predictions. This degree of accuracy is expected to be acceptable because it greatly reduces the potential ranges of these variables, thereby considerably reducing uncertainty.

To demonstrate the accuracy of the EQ3/6 Pitzer (HRH) model as part of the model validation process, results were compared to handbook solubility values and experimental data from three laboratory evaporation experiments conducted at LLNL (Section 6.5). Handbook solubilities were predicted within an order of magnitude and almost always within a factor of two (Table 17). Of the laboratory experiments, two used synthetic average J-13 well water and one used synthetic Topopah Spring tuff pore water. In each case, the pH was predicted within a pH unit (Figure 2 and Figure 14), and the chloride concentration was predicted within 20 percent (Figure 4, Figure 10, and Figure 16). The ionic strength prediction, as approximated using equation 4, was not as accurate as the chloride prediction, but it was still within a factor of 2 (Figure 2, Figure 8, and Figure 14).

There were no data available to evaluate the accuracy of the low relative humidity (LRH) salts model. However, the model produced reasonable trends and results in chloride and ionic strength outputs while negotiating the transition from dry conditions to the range where the HRH model could take over.

Although simplifying assumptions were required to reduce the complexity of the Precipitates/Salts analysis and to avoid sophisticated approaches where data were lacking, these assumptions tended to err on the side of conservatism. In particular, they tended to result in a shorter dry period, by not allowing dry conditions above a relative humidity of 50 percent, and higher chloride concentrations at lower relative humidities. Judging by the accuracy of the model predictions compared to experimental data (Section 6.5), the greatest uncertainties of the Precipitates/Salts analysis for TSPA are likely the TH and THC predictions and other predicted inputs that feed the analysis.

A final method used to evaluate and account for uncertainty in the Precipitates/Salts analysis is the generation of a set of lookup tables intended to cover the range of possible combinations of input values. These lookup tables can be used in several ways. Initially, they can be used to evaluate the sensitivity of input variables on outputs. For example, the sensitivity of pH to the relative evaporation flux can be evaluated by comparing the pH output for a range of values for the relative evaporation flux. In the Precipitates/Salts analysis, input variables that are not included in the tables are not sensitive inputs (except perhaps for the composition of the incoming seepage water, which was held constant in this analysis). Similarly, an estimate of the approximate maximum range of possible values of a given output variable for a range of input conditions can be assessed from the lookup tables (For graphically displayed relationships, see Figure 26 through Figure 32.). However, the primary objective of the lookup tables is to summarize the effects of evaporation processes for a wide range of possible conditions so that downstream users (e.g., corrosion modelers or developers of an in-drift geochemical model abstraction) can easily incorporate evaporation effects and uncertainty into coupled analyses.

7.4 TBVs

The development of the EQ3/6 Pitzer (HRH) model required the development and use of one input whose status remains TBV (TBV-3916), the thermodynamic database values from EQ3/6. Although these are currently TBV, they are used by the model to predict, within acceptable limits, handbook solubilities of soluble salts in the 1 to 10 molal range and the results from laboratory evaporation experiments. While the data from some of the experiments would also be TBV if they were used to produce direct model output, the associated uncertainty in the data is expected to be small. Once these experimental data are qualified as part of a technical assessment, it is expected that the model can be qualified. The model validation in Section 6.5 provides a strong argument to justify model qualification for the intended use. The intended use of the model is to predict pH and the molalities of chloride and ionic strength within acceptable limits of uncertainty.

The low relative humidity (LRH) model uses no data that are TBV. The approximate relative humidity over time is a reasonable assumption that is used to generate an example simulation of the model (Section 5.2.4). The model abstraction does not require a history of relative humidity, only the relative humidity itself. Thus, the results can be applied to any location with any history of relative humidity. Also, the seepage rate affects the total amounts of salts and brine generated but it does not affect the aqueous composition, which is the model output. Furthermore, evaporation rate does not affect the output because the relative humidity and hygroscopic behavior of salts control the aqueous chemistry. Finally the composition of the incoming seepage, which was assumed in this analysis to be average J-13 well water equilibrated with the fugacity of carbon dioxide, is qualified level 2 data.

For the condensed water vapor model, the only TBV input used is the COM database (TBV-3916). Because only a few reactions involving carbonate are used from this database and these reactions are widely accepted, it is expected that the relevant TBV data will be qualified for the intended use.

This document and its conclusions may be affected by technical product input information that requires confirmation. Any changes to the document or its conclusions that may occur as a result

of completing the confirmation activities will be reflected in subsequent revisions. The status of the input information quality may be confirmed by review of the Document Input Reference System database.

7.5 FEPs

Table 22 lists the FEPs in Table 8 and the conclusions based on the Precipitates/Salts analysis.

Table 22. FEPs and the AMR Conclusions

YMP FEP Number	NEA Category	FEP Name	AMR Conclusions
2.1.04.02.00	2.1.04au	Physical and chemical properties of backfill	Based on the results of this AMR, the aqueous chemistry within the backfill may be primarily controlled by evaporative processes and not by interactions with backfill. Affects of backfill on aqueous chemistry are addressed in the Seepage/Backfill Interactions AMR.
2.1.04.03.00	2.1.04r	Erosion or dissolution of backfill	This FEP is not addressed by this AMR and therefore is not affected.
2.1.04.05.00	2.1.04b	Backfill evolution	This FEP is not addressed by this AMR. Backfill evolution is addressed in the Seepage/Backfill Interactions AMR.
2.2.08.04.00	2.2.08c	Redissolution of precipitates directs more corrosive fluids to containers	Although this AMR does not consider pulses, redirection of flow, or corrosion itself, the generation of corrosive fluids by evaporative processes is considered and predicted. All of the fluids predicted by this AMR may be directed to corrosion models by downstream users.

ACC: MOL.19991214.0518, MOL.19991214.0519

8. REFERENCES

8.1 DOCUMENTS

Arthur, R.C. and Murphy, W.M. 1989. "An Analysis of Gas-Water-Rock Interactions During Boiling in Partially Saturated Tuff." *Science Geology Bulletin, 42,* (4), 313-327. Strasbourg, France: Sciences Geologiques Bulletin Publisher Strasbourg, Universite Louis Pasteur de Strasbourg. TIC: 235013.

Clegg, S.L. and Whitfield, M. 1991. "Activity Coefficients In Natural Waters." Chapter 6 of *Activity Coefficients In Electrolyte Solutions.* Pitzer, K.S., ed. Boca Raton, Florida: CRC Press. TIC: 246849.

CRWMS M&O (Civilian Radioactive Waste Management Services Management and Operations) 1998a. *Software Qualification Report (SQR) Addendum to Existing LLNL Document UCRL-MA-110662 PT IV: Implementation of a Solid-Centered Flow-Through Mode for EQ6 Version 7.2B.* CSCI: UCRL-MA-110662 V 7.2b. SCR: LSCR198. Las Vegas, Nevada: CRWMS M&O. ACC: MOL.19990920.0169.

CRWMS M&O 1998b. "Near-Field Geochemical Environment." Chapter 4 of *Total System Performance Assessment-Viability Assessment (TSPA-VA) Analyses Technical Basis Document.* B00000000-01717-4301-00004 REV 01. Las Vegas, Nevada: CRWMS M&O. ACC: MOL.19981008.0004.

CRWMS M&O 1998c. "Thermal Hydrology." Chapter 3 of *Total System Performance Assessment-Viability Assessment (TSPA-VA) Analyses Technical Basis Document.* B00000000-01717-4301-00003 REV 01. Las Vegas, Nevada: CRWMS M&O. ACC: MOL.19981008.0003.

CRWMS M&O 1999a. *Provide Sub-Models for the Physical and Chemical Environmental Abstraction Model for TSPA-LA.* TDP-WIS-MD-000006 REV 00. Las Vegas, Nevada: CRWMS M&O. ACC: MOL.19990902.0450.

CRWMS M&O 1999b. *YMP FEP Database Rev. 00C.* Las Vegas, Nevada: CRWMS M&O. ACC: MOL.19991214.0518; MOL.19991214.0519.

CRWMS M&O 1999c. Request for Data from LLNL Report UCRL-ID-134852 "Evaporation of J13 Water: Laboratory Experiments and Geochemical Modeling". Input Transmittal PA-EBS-99405.T. Las Vegas, Nevada: CRWMS M&O. ACC: MOL.19991217.0104.

CRWMS M&O 1999d. Data Transmittal for UCRL-ID-135765, "Evaporation of Topopah Spring Tuff Pore Water". Input Transmittal PA-EBS-99404.T. Las Vegas, Nevada: CRWMS M&O. ACC: MOL.19991217.0103.

CRWMS M&O 2000. Environment on the Surfaces of the Drip Shield and Waste Package Outer Barrier. ANL-EBS-MD-000001 REV 00. Las Vegas, Nevada: CRWMS M&O. ACC: MOL.20000328.0590.

Dean, J.A., ed. 1992. *Lange's Handbook of Chemistry.* 14th Edition. New York, New York: McGraw-Hill. TIC: 240690.

DOE (U.S. Department of Energy) 2000. *Quality Assurance Requirements and Description.* DOE/RW-0333P, Rev. 9. Washington, D.C.: U.S. Department of Energy, Office of Civilian Radioactive Waste Management. ACC: MOL.19991028.0012.

Drever, J.I. 1988. *The Geochemistry of Natural Waters.* 2nd Edition. Englewood Cliffs, New Jersey: Prentice-Hall. TIC: 242836.

Dyer, J.R. 1999. "Revised Interim Guidance Pending Issuance of New U.S. Nuclear Regulatory Commission (NRC) Regulations (Revision 01, July 22, 1999), for Yucca Mountain, Nevada." Letter from Dr. J.R. Dyer (DOE/YMSCO) to Dr. D.R. Wilkins (CRWMS M&O), September 3, 1999, OL&RC:SB-1714, with enclosure, "Interim Guidance Pending Issuance of New NRC Regulations for Yucca Mountain (Revision 01)." ACC: MOL.19990910.0079.

Eugster, H.P. and Hardie, L.A. 1978. "Saline Lakes." Chapter 8 of *Lakes, Chemistry, Geology, Physics.* Lerman, A., ed. New York, New York: Springer-Verlag. TIC: 240782.

Eugster, H.P. and Jones, B.F. 1979. "Behavior of Major Solutes During Closed-Basin Brine Evolution." *American Journal of Science, 279,* 609-631. New Haven, Connecticut: Yale University, Kline Geology Laboratory. TIC: 234258.

Fishman, N.S.; Turner, C.E.; and Brownfield, I.K. 1995. *Authigenic Albite in a Jurassic Alkaline, Saline Lake Deposit, Colorado Plateau - Evidence for Early Diagenetic Origin.* Bulletin 1808-P. Denver, Colorado: U.S. Geological Survey. TIC: 247006.

Freeze, R.A. and Cherry, J.A. 1979. *Groundwater.* Englewood Cliffs, New Jersey: Prentice-Hall. TIC: 217571.

Garrels, R.M. and Mackenzie, F.T. 1967. "Origin of the Chemical Compositions of Some Springs and Lakes?." *Equilibrium Concepts in Natural Water Systems.* American Chemical Society Advances in Chemistry Series 67. Pages 222-242. Washington, D.C.: American Chemical Society. TIC: 246519.

Glassley, W. 1997. *Chemical Composition of Water Before Contact with Repository Materials.* Milestone SPLA1M4. Livermore, California: Lawrence Livermore National Laboratory. ACC: MOL.19971210.0031.

Glassley, W.E. 1993. "Coupled Hydro-Geochemical Processes and Their Significance for Yucca Mountain Site Characterization." Proceedings of the Topical Meeting on Site Characterization and Model Validation, Focus '93, September 26-29, 1993, Las Vegas, Nevada. Pages 122-126. La Grange Park, Illinois: American Nuclear Society. TIC: 102245.

Glassley, W.E. 1994. Report on Near-Field Geochemistry: Water Composition Changes Due to Evaporation. Milestone M0L26. Draft. Livermore, California: Lawrence Livermore National Laboratory. ACC: MOL.19950406.0153.

Hardin, E.L. 1998. *Near-Field/Altered-Zone Models Report.* UCRL-ID-129179. Livermore, California: Lawrence Livermore National Laboratory. ACC: MOL.19980630.0560.

Harrar, J.E.; Carley, J.F.; Isherwood, W.F.; and Raber, E. 1990. *Report of the Committee to Review the Use of J-13 Well Water in Nevada Nuclear Waste Storage Investigations.* UCID-21867. Livermore, California: Lawrence Livermore National Laboratory. ACC: NNA.19910131.0274.

Harvie, C. E.; Moller, N.; and J. H. Weare 1984. "The Prediction of Mineral Solubilities in Natural Waters: The Na–K–Mg–Ca–H–Cl–SO4–OH–HCO3–CO3–CO2–H2O System to High Ionic Strengths at 25°C." *Geochimica et Cosmochimica Acta, 48,* (4), 723-751. London, England: Pergamon Press. TIC: 239849.

Jones, B.F.; Eugster, H.P.; and Rettig, S.L. 1977. "Hydrochemistry of the Lake Magadi Basin, Kenya." *Geochimica et Cosmochimica Acta, 41,* 53-72. New York, New York: Pergamon Press. TIC: 246224.

Jones, B.F.; Rettig, S.L.; and Eugster, H.P. 1967. "Silica in Alkaline Brines." *Science, 158,* 1310-1314. Washington, D.C.: American Association for the Advancement of Science. TIC: 235387.

Kinsman, D.J.J. 1976. "Evaporites: Relative Humidity Control of Primary Mineral Facies." *Journal of Sedimentary Petrology, 46,* 273-279. Tulsa, Oklahoma: Society of Economic Paleontologists and Mineralogists. TIC: 238672.

Klein, C. and Hurlbut, C.S. 1999. *Manual of Mineralogy.* 21st Edition. New York, New York: John Wiley & Sons. TIC: 246258.

Koorevaar, P.; Menelik, G.; and Dirksen, C. 1983. *Elements of Soil Physics.* Developments in Soil Science 13. New York, New York: Elsevier Science B.V. TIC: 246286.

Lichtner, P.C. and Seth, M. 1996. "Multiphase-Multicomponent Nonisothermal Reactive Transport in Partially Saturated Porous Media." *Proceedings of the 1996 International Conference on Deep Geological Disposal of Radioactive Waste, September 16-19, 1996, Winnipeg, Manitoba, Canada.* Toronto, Ontario, Canada: Canadian Nuclear Society. TIC: 233923.

Mahan, B.H. 1975. *University Chemistry.* 3rd Edition. Reading, Massachusetts: Addison-Wesley Publishing Company. TIC: 240721.

Murphy, W.M. 1993. "Geochemical Models for Gas-Water-Rock Interactions in a Proposed Nuclear Waste Repository at Yucca Mountain." *Proceedings of the Topical Meeting on Site*

Characterization and Model Validation, Focus '93, September 26-29, 1993, Las Vegas, Nevada. La Grange Park, Illinois: American Nuclear Society. TIC: 102245.

Murphy, W.M. and Pabalan, R.T. 1994. *Geochemical Investigations Related to the Yucca Mountain Environment and Potential Nuclear Waste Repository.* NUREG/CR-6288. San Antonio, Texas: Southwest Research Institute. TIC: 227032.

Pitzer, K.S. and Kim, J.J. 1974. "Thermodynamics of Electrolytes. IV. Activity and Osmotic Coefficients for Mixed Electrolytes." *Journal of the American Chemical Society, 96,* (18), 5701-5707. Washington, D.C.: American Chemical Society. TIC: 246223.

Reardon, E.J. 1990. "An Ion Interaction Model for the Determination of Chemical Equilibria in Cement Water Systems." *Cement and Concrete Research, 20,* 175-192. Elmsford, New York: Pergamon Press. TIC: 239801.

Rosenberg, N.D.; Knauss, K.G.; and Dibley, M.F. 1999a. *Evaporation of J13 Water: Laboratory Experiments and Geochemical Modeling.* UCRL-ID-134852. Livermore, California: Lawrence Livermore National Laboratory. TIC: 246322.

Rosenberg, N.D.; Knauss, K.G.; and Dibley, M.F. 1999b. *Evaporation of Topopah Spring Tuff Pore Water.* UCRL-ID-135765. Livermore, California: Lawrence Livermore National Laboratory. TIC: 246231.

Saxton, B.; Austin, J.B.; Dietrich, H.G.; Fenwick, F.; Fleischer, A.; Frear, G.L.; Roberts, E.J.; Smith, R.P.; Solomon, M.; and Spurlin, H.M. 1928. "Boiling-Point Elevations, Non-Volatile Solutes." *International Critical Tables of Numerical Data, Physics, Chemistry and Technology, III,* 324-350. New York, New York: McGraw-Hill. TIC: 243268.

Sonnenfeld, P. 1984. "Evaporitic Minerals." Chapter 16 of *Brines and Evaporites.* Pages 449-472. Orlando, Florida: Academic Press. TIC: 246640.

Stumm, W. and Morgan, J.J. 1996. *Aquatic Chemistry: Chemical Equilibria and Rates in Natural Waters.* 3rd Edition. New York, New York: John Wiley & Sons. TIC: 246296.

Walton, J.C. 1994. "Influence of Evaporation on Waste Package Environment and Radionuclide Release from a Tuff Repository." *Water Resources Research, 30,* (12), 3479-3487. Washington, D.C.: American Geophysical Union. TIC: 246921.

Weast, R.C. and Astle, M.J., eds. 1981. CRC Handbook of Chemistry and Physics: A Ready Reference Book of Chemical and Physical Data. 62nd Edition. Boca Raton, Florida: CRC Press. TIC: 240722.

Wilder, D.G., ed. 1996. Near-Field and Altered-Zone Environment Report. UCRL-LR-124998. Volume II. Livermore, California: Lawrence Livermore National Laboratory. ACC: MOL.19961212.0121; MOL.19961212.0122.

Wolery, T.J. 1992a. *EQ3/6, A Software Package for Geochemical Modeling of Aqueous Systems. Package Overview and Installation Guide (Version 7.0).* UCRL-MA-110662 PT I. Livermore, California: Lawrence Livermore National Laboratory. TIC: 205087.

Wolery, T.J. 1992b. EQ3NR, A Computer Program for Geochemical Aqueous Speciation-Solubility Calculations. Theoretical Manual, User's Guide, and Related Documentation (Version 7.0). UCRL-MA-110662 PT III. Livermore, California: Lawrence Livermore National Laboratory. TIC: 205154.

Wolery, T.J. and Daveler, S.A. 1992. Theoretical Manual, User's Guide, and Related Documentation, Version 7.0. Volume IV of EQ6, A Computer Program for Reaction Path Modeling of Aqueous Geochemical Systems. UCRL-MA-110662. Draft 1.1. Livermore, California: Lawrence Livermore National Laboratory. TIC: 238011.

8.2 DATA, LISTED BY TRACKING NUMBER

8.2.1 INPUT DATA

LL000202905924.117. Environment on the Surfaces of the Drip Shield and Waste Package Outer Barrier. Submittal date: 2/15/2000.

LL980711104242.054. Report of the Committee to Review the Use of J-13 Well Water in Nevada Nuclear Waste Storage Investigations. Submittal date: 08/05/1998.

MO9911SPATHD62.002. EQ3/6 V7.2B Thermodynamic Databases. Submittal date: 11/22/1999.

MO9912SPAGIBFE.000. Standard Gibbs Free Energies of Formation for Five Minerals and Their Components. Submittal date: 12/06/1999.

SN0001T0872799.006. In-Drift Thermodynamic Environment and Percolation Flux. Submittal date: 01/27/2000.

SNT05071897001.010. Developed Thermal Hydrologic Results from the Base Case and the Sensitivity Studies Using the Thermal Hydrologic Multi-Scale Modeling and Abstraction Method. Submittal date: 07/27/1998.

8.2.2 DEVELOPED DATA

MO0003MWDMIN45.011. EQ3/6 Input/Output Files for In-Drift Precipitates Salts: Mineral Suppressions Reduced. Submittal date: 03/08/2000.

MO0003MWDTAB45.013. EQ3/6 Input/Output Files for In-Drift Precipitates Salts Lookup Tables. Submittal date: 03/13/2000.

MO0003MWDVAL45.012. EQ3/6 Input/Output Files for In-Drift Precipitates Salts Model Validation. Submittal date: 03/13/2000.

MO9912MWDEQ345.002. EQ3/6 Input/Output Files for Condensate Underneath the Drip Shield. Submittal date: 12/07/1999.

MO9912SPAISP45.004. Look-Up Tables for pH, Cl, and Ionic Strength Predicted by Precipitates/Salts Model. Submittal date: 12/08/1999.

MO9912SPAISP45.005. Lookup Tables for Condensate Composition Under Drip Shield. Submittal date: 12/08/99.

MO9912SPALRH45.003. Low Relative Humidity Salts Model Mathcad7 Files. Submittal date: 12/07/1999.

MO9912SPAPT4PD.001. PT4 Pitzer Database for EQ3/6. Submittal date: 12/06/1999.

8.3 CODES, STANDARDS, REGULATIONS, PROCEDURES, AND SOFTWARE

64 FR 8640. Disposal of High-Level Radioactive Wastes in a Proposed Geologic Repository at Yucca Mountain, Nevada. Proposed rule 10 CFR 63. Readily Available.

AP-2.13Q, Rev. 0, ICN 0. *Technical Product Development Planning*. Washington, D.C.: U.S. Department of Energy, Office of Civilian Radioactive Waste Management. ACC: MOL.19990701.0617.

AP-3.10Q, Rev. 2, ICN 0. *Analyses and Models*. Washington, D.C.: U.S. Department of Energy, Office of Civilian Radioactive Waste Management. ACC: MOL.20000217.0246.

AP-SI.1Q, Rev. 2, ICN 4. *Software Management*. Washington, D.C.: U.S. Department of Energy, Office of Civilian Radioactive Waste Management. ACC: MOL.20000223.0508.

ASTM C 1174-97. 1997. *Standard Practice for Prediction of the Long-Term Behavior of Materials, Including Waste Forms, Used in Engineered Barrier Systems (EBS) for Geological Disposal of High-Level Radioactive Waste.* West Conshohocken, Pennsylvania: American Society for Testing and Materials. TIC: 246015.

CRWMS M&O 1999e. *Software Code: EQ3/6, Version 7.2bLV*. V7.2bLV. 10075-7.2bLV-00.

NRC (U.S. Nuclear Regulatory Commission) 1999. *Issue Resolution Status Report Key Technical Issue: Evolution of the Near-Field Environment.* Rev. 2. Washington, D.C.: U.S. Nuclear Regulatory Commission. ACC: MOL.19990810.0640.

QAP-2-0, Rev. 5. *Conduct of Activities*. Las Vegas, Nevada: CRWMS M&O. ACC: MOL.19980826.0209.

ATTACHMENTS

Attachment	Title
I	Low Relative Humidity (LRH) Salts Model Calculations

Low Relative Humidity (LRH) Salts Model Calculations
(fco2 = 1e-1)

Conceptual Model. Water seeps into "reactor" (i.e, drip shield or backfill) at a constant rate during the boiling period. In the reactor, seepage water vaporizes and salts accumulate. Salts begin to dissolve when the relative humidity rises above 50%. This model (LRH) approximates the buildup and dissolution of soluble salts in the Na-K-N-S-Cl-C system. All fluid (brine) generated during each time interval flows out of reactor at the end of each time interval; however, mixing is allowed between half time intervals. The end point is designed to be equivalent to the evaporative evolution of seepage water to a stoichiometric ionic strength of 10 molal, as calculated using the EQ3/6 Pitzer model. The LRH salts model is a simplified approximation of salt accumulation and eventual dissolution caused by increasing relative humidity. It maintains mass and charge balance and estimates brine generation as a function of effective solubilities. Its purpose is to provide bounding and scoping calculations for an evaporite system that is has not been deeply studied.

Seepage - Constant rate and constant composition are assumed.

Seepage Name:

$s := \text{"avg. J-13"}$

CO_2 (g) Fugacity:

$CO_2 := 1 \cdot 10^{-1}$

	Seepage Comp. (molal) (Avg. J-13)	Valency	Seepage Rate
NO3	$Cs_1 := 0.000142 \cdot mol \cdot kg^{-1}$	$z_1 := 1$	$Qs := 1 \cdot \frac{kg}{yr}$
Cl	$Cs_2 := 0.00020 \cdot mol \cdot kg^{-1}$	$z_2 := 1$	
SO4	$Cs_3 := 0.00019 \cdot mol \cdot kg^{-1}$	$z_3 := 2$	
Soluble CO3	$Cs_4 := 0.00068 \cdot mol \cdot kg^{-1}$	$z_4 := 1$	
K	$Cs_6 := 0.00013 \cdot mol \cdot kg^{-1}$	$z_6 := 1$	
Na	$Cs_7 := 0.0020 \cdot mol \cdot kg^{-1}$	$z_7 := 1$	

Cs_4 is adjusted to achieve a Na:CO_3 ratio equivalent to the final I=10m solution calculated from the EQ3/6 Pitzer model. *Soluble* CO_3 represents the CO_3 fraction that precipitates with Na or K.

Charge Balance Error

$$E := \frac{\sum_{i=6}^{7} Cs_i \cdot z_i - \sum_{i=1}^{4} Cs_i \cdot z_i}{\sum_{i=1}^{7} Cs_i \cdot z_i}$$

$E = 0.206$

$E = 20.61 \cdot \%$

This charge balance error is maintained for the entire calculation.

Period 1 - Dry Conditions. Salts accumulate. No stable brine is generated. Period ends when relative humidity (RH) rises to level where nitrate salts are no longer stable.

Time Nitrate Salts Become Unstable: $t50 := 200 \cdot yr$ (time when RH exceeds ~50%)

$i := 1 .. 7$

	Total Accumulation in Period 1		Molecular Weight
NO3	$Mst_{i,0} := Cs_i \cdot Qs \cdot t50$	$Mst_{1,0} = 0.028 \cdot mol$	$W_1 := 62 \cdot gm \cdot mol^{-1}$
Cl		$Mst_{2,0} = 0.04 \cdot mol$	$W_2 := 35.5 \cdot gm \cdot mol^{-1}$
SO4		$Mst_{3,0} = 0.038 \cdot mol$	$W_3 := 96 \cdot gm \cdot mol^{-1}$
Soluble CO3		$Mst_{4,0} = 0.136 \cdot mol$	$W_4 := 60 \cdot gm \cdot mol^{-1}$
K		$Mst_{6,0} = 0.026 \cdot mol$	$W_6 := 39 \cdot gm \cdot mol^{-1}$
Na		$Mst_{7,0} = 0.4 \cdot mol$	$W_7 := 23 \cdot gm \cdot mol^{-1}$

Period 2 - Wet Conditions. Nitrate salts are unstable. Water vapor condenses to form nitrate brine. Soluble salts begin to dissolve as RH increases and completely dissolve by the end of the period.

Time Discretization in Period 2

End of Period 2 at 85% RH	$t85 := 1100 \cdot yr$	RH reaches 85% at about 980 years. At RH 85%, soluble salts are dissolved and I = ~10m because the activity of water at I=~10m is approximately 0.85.
Time Increments in Period 2	$j := 0 .. 100$	Specific Times of Increments $t_j := t50 + (t85 - t50) \cdot \frac{j}{100}$
Constant Time Increment	$delt := t_1 - t_0$	$delt = 9 \cdot yr$

Salt Solubilities

		Effective Solubility at 100'C (molal)	
NO3		$S_1 := 24.5 \cdot mol \cdot kg^{-1}$	(pure phase solubility at 100'C for KNO_3)
Other Salts	$k := 2 .. 4$	$S_k := 4.1 \cdot mol \cdot kg^{-1}$	(assumed "effective" solubility to match EQ6 model results - "effective" due to mixture of salts)
Mass of Total Condensed Water at Start of Period 2		$mw_1 := \frac{Mst_{1,0}}{S_1}$	$mw_1 = 1.159 \cdot 10^{-3} \cdot kg$ (assumes accumulated nitrate salts dissolve to solubility)

Fraction of Soluble Salts Dissolved. While NO3 salts are assumed to dissolve completely at the beginning of Period 2, the other salts are assumed to dissolve increasingly as relative humidity increases over time.

Percentages of Salts Dissolved in Period 2

System	Assumptions	Percentage of Salts Dissolved at Start of Period 2	Percentage Salts Dissolved at End of Period 2
K-Na-NO3	NO3 salts are 100% dissolved at all times in Period 2.	$f1_1 := 100 \cdot \%$ $k := 1 .. 2$	$f1_2 := 100 \cdot \%$
K-Na-Cl-SO4-CO3 $j := 1 .. 100$	$ff_j := 10^{\frac{4 \cdot (t_j - t85)}{t85 - t50}}$ Percentage dissolved within reactor assumed to increase exponentially from 0% to 100% within Period 2.		

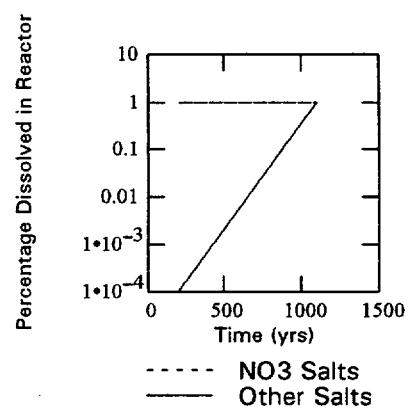

Percentages of Salts Dissolved

		Initial Percentage Dissolved Within Reactor	Percentage Dissolved Within Reactor	
$i := 1 .. 6$				
NO3		$f_{1,0} := 0$	$f_{1,j} := f1_1$	(Na percentage calculated by charge balance later.)
Other Anions	$k := 2 .. 4$	$f_{k,0} := 0$	$f_{k,j} := ff_j$	
K		$f_{6,0} := 0$	$f_{6,j} := f1_1$	

Period 2 Calculations

Incoming Seepage $\quad i := 1..7 \quad j := 1..100$

Moles Added to Reactor in Incoming Seepage During Time Increment $\quad Ms_i := Cs_i \cdot Qs \cdot delt$

Cumulative Moles in Incoming Seepage $\quad Mst_{i,j} := Mst_{i,j-1} + Ms_i$

Reactor Calculations $\quad i := 1..6 \quad k := 1..200$

Moles in Reactor at Each Half *delt* Increment $\quad$ = (previous moles) + (seepage moles) - (runoff moles)

$Mrh_{i,0} := Mst_{i,0}$ (initial moles) $\quad Mrh_{i,k} := Mrh_{i,k-1} + \frac{1}{2} \cdot Ms_i - \frac{1}{2} \cdot Mrh_{i,k-1} \cdot f_{i,floor\left(\frac{k-1}{2}\right)}$

$j := 0..100$

Moles in Reactor at Time t_j $\quad Mr_{i,j} := Mrh_{i,j \cdot 2}$

Moles (Mass) of Dissolved Ions Generated at Time t_j $\quad Md_{i,j} := Mr_{i,j} \cdot f_{i,j}$

Dissolved Mass: $md_{i,j} := Md_{i,j} \cdot W_i$

Mass of Water in Brine Generated at Time t_j (calculated from anions)

$$mw_j := \sum_{i=1}^{4} \frac{Md_{i,j}}{S_i}$$

Dissolved Concentration at Time t_j

$$C_{i,j} := \frac{Md_{i,j}}{mw_j}$$

Na Moles in Reactor (calculated by charge balance, includes charge imbalance error term)

$$Mr_{7,j} := \sum_{i=1}^{4} Mr_{i,j} \cdot z_i - Mr_{6,j} \cdot z_6 + E \cdot \sum_{i=1}^{4} 2 \cdot Mr_{i,j} \cdot z_i \cdot (1 + E)$$

Na Dissolved Concentration (calculated by charge balance, includes charge imbalance error term)

$$C_{7,j} := \sum_{i=1}^{4} C_{i,j} \cdot z_i - C_{6,j} \cdot z_6 + E \cdot \sum_{i=1}^{4} 2 \cdot C_{i,j} \cdot z_i \cdot (1 + E)$$

Dissolved Moles (Mass) of Na in Reactor (calculated by charge balance, includes charge imbalance error term)

$$Md_{7,j} := \sum_{i=1}^{4} Md_{i,j} \cdot z_i - Md_{6,j} \cdot z_6 + E \cdot \sum_{i=1}^{4} 2 \cdot Md_{i,j} \cdot z_i \cdot (1 + E)$$

Percentage Na Dissolved in Reactor $\quad f_{7,j} := \frac{C_{7,j} \cdot mw_j}{Mr_{7,j}}$

Dissolved Mass: $md_{7,j} := Md_{7,j} \cdot W_7$

Cumulative Water Runoff $\quad j := 1..100 \quad mwt_0 := 0 \cdot kg \quad mwt_j := mwt_{j-1} + mw_j$

Cumulative Mass of Total Dissolved Solids Generated at Time tt_j $\quad mdt_0 := 0 \cdot kg \quad mdt_j := mdt_{j-1} + \sum_{i=1}^{4} md_{i,j} + \sum_{i=6}^{7} md_{i,j}$

j

Results i := 1 .. 7 j := 0 .. 100

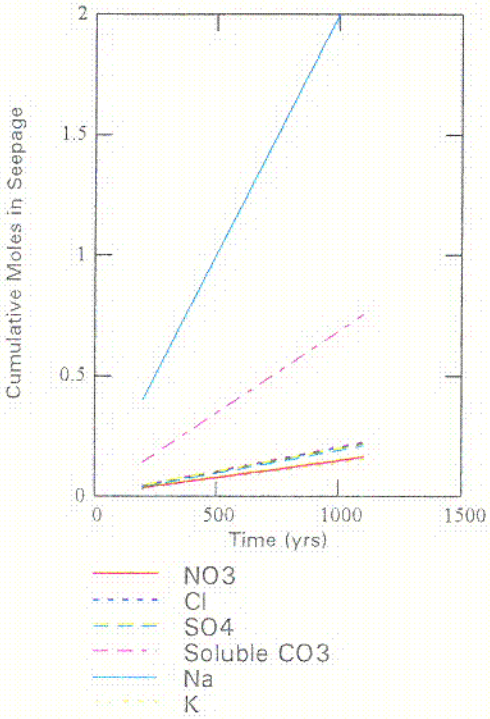

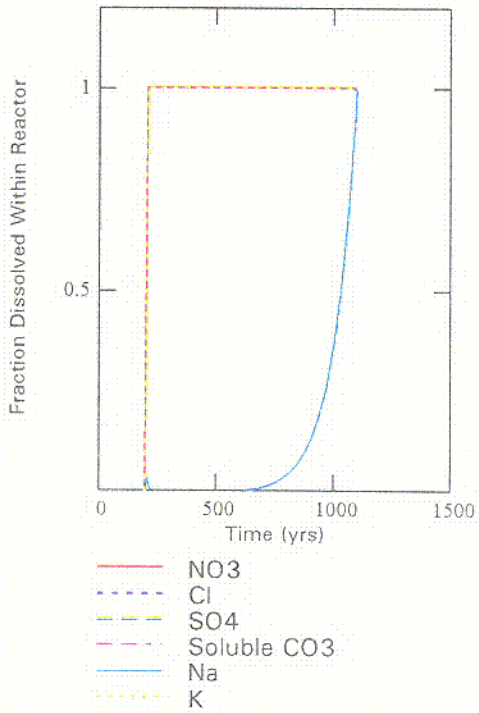

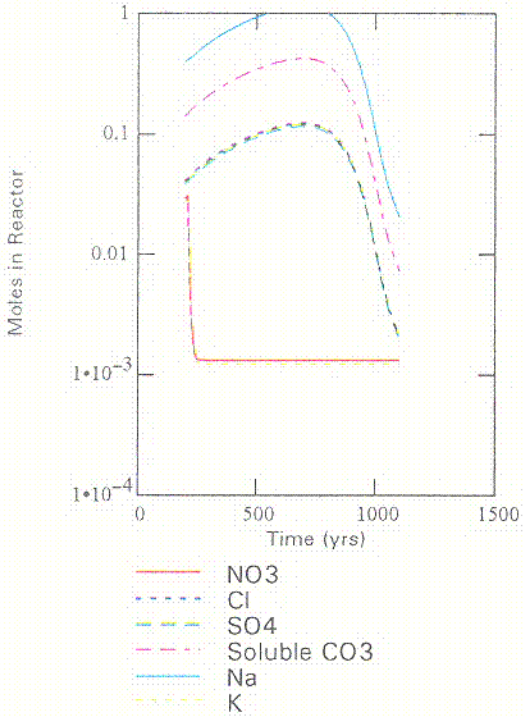

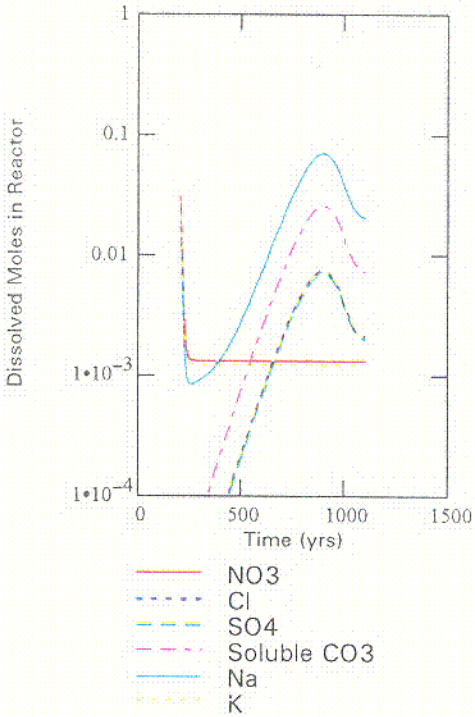

C-1

Solid-Phase (Undissolved)
Moles in Reactor over Time

$$Mu_{i,j} := Mr_{i,j} - Md_{i,j}$$

Note: Mp for NO3 and K is zero when RH exceeds 50%.

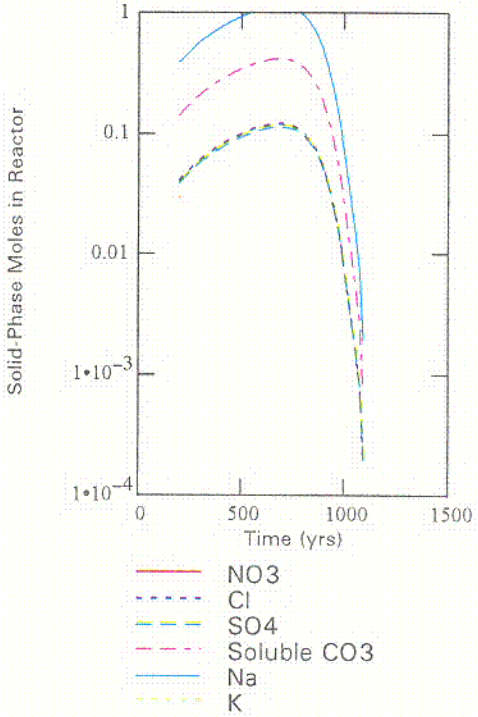

j := 1 .. 100

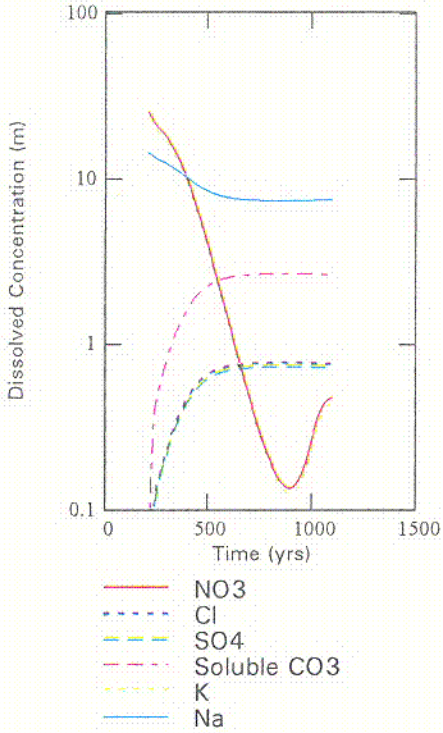

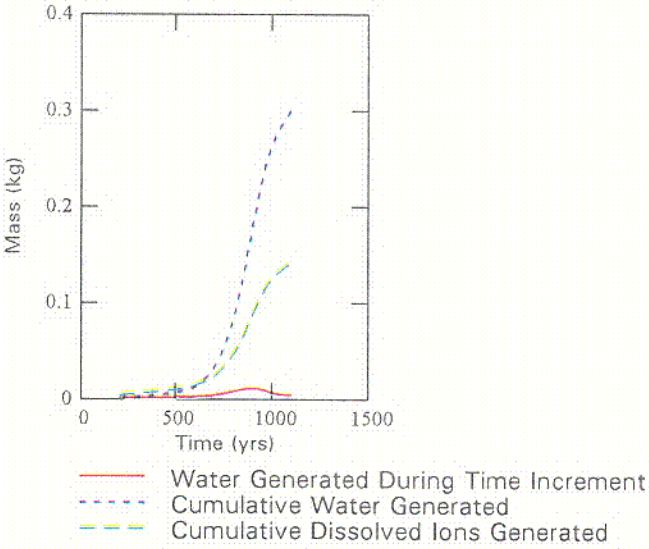

C-2

Summary and Cross-Check

	Concentrations at End of Period 2	Concentrations Calculated by EQ3/6 Model (I = 10 m)	Total Moles in Reactor at End of Period 2
NO3	$C_{1,100} = 0.464 \cdot mol \cdot kg^{-1}$	$0.60 \cdot mol \cdot kg^{-1}$	$Mr_{1,100} = 1.278 \cdot 10^{-3} \cdot mol$
Cl	$C_{2,100} = 0.752 \cdot mol \cdot kg^{-1}$	$0.85 \cdot mol \cdot kg^{-1}$	$Mr_{2,100} = 2.071 \cdot 10^{-3} \cdot mol$
SO4	$C_{3,100} = 0.714 \cdot mol \cdot kg^{-1}$	$0.81 \cdot mol \cdot kg^{-1}$	$Mr_{3,100} = 1.967 \cdot 10^{-3} \cdot mol$
Soluble CO3	$C_{4,100} = 2.556 \cdot mol \cdot kg^{-1}$	$2.47 \cdot mol \cdot kg^{-1}$	$Mr_{4,100} = 7.042 \cdot 10^{-3} \cdot mol$
K	$C_{6,100} = 0.425 \cdot mol \cdot kg^{-1}$	$0.55 \cdot mol \cdot kg^{-1}$	$Mr_{6,100} = 1.17 \cdot 10^{-3} \cdot mol$
Na	$C_{7,100} = 7.362 \cdot mol \cdot kg^{-1}$	$7.3 \cdot mol \cdot kg^{-1}$	$Mr_{7,100} = 0.02 \cdot mol$

Cumulative Mass of Dissolved Solids in Incoming Seepage at End of Period 2

$$\sum_{i=1}^{4} Mst_{i,100} \cdot W_i + \sum_{i=6}^{7} Mst_{i,100} \cdot W_i = 0.139 \cdot kg$$

Cumulative Mass of Dissolved Solids Generated at End of Period 2

$$mdt_{100} = 0.141 \cdot kg$$

Cumulative Mass of Water in Generated Brine at End of Period 2

$$mwt_{100} = 0.300 \cdot kg$$

Cumulative Mass of Brine Generated at End of Period 2

$$mwt_{100} + mdt_{100} = 0.442 \cdot kg$$

Charge Balance Error Maintained Over Time

$j := 1, 10 .. 100$

$$E_j := \frac{\sum_{i=6}^{7} C_{i,j} \cdot z_i - \sum_{i=1}^{4} C_{i,j} \cdot z_i}{\sum_{i=1}^{7} C_{i,j} \cdot z_i}$$

E_j
0.199
0.199
0.199
0.199
0.199
0.199
0.199
0.199
0.199
0.199
0.199
0.199

Response Surface Calculations $j := 0 .. 100$

Relative humidity as a function of time (approximation)

$$RH_j := 0.5 + \left(\frac{t_j - t50}{t85 - t50}\right) \cdot 0.35$$

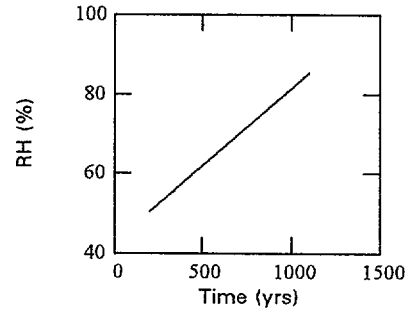

Evaluation points:

$j_1 := 1$ $j_2 := 3$ $j_3 := 9$ $j_4 := 15$ $j_5 := 30$

$j_6 := 45$ $j_7 := 60$ $j_8 := 75$ $j_9 := 90$ $j_{10} := 100$

$k := 1 .. 10$

Lookup Table for Given Seepage Composition

s = "avg. J-13"

$CO_2 = 1 \cdot 10^{-1}$

j_k	RH_{j_k} (Input Parameter: Relative Humidity)	C_{2,j_k} (Output Parameters: Cl Concentration)	$C_{6,j_k} + C_{7,j_k}$ (Output Parameters: Na + K Concentration)
1	0.503	$3.7650 \cdot 10^{-3} \cdot kg^{-1} \cdot mol$	$36.54 \cdot kg^{-1} \cdot mol$
3	0.510	$0.0452 \cdot kg^{-1} \cdot mol$	$34.94 \cdot kg^{-1} \cdot mol$
9	0.531	$0.1865 \cdot kg^{-1} \cdot mol$	$29.51 \cdot kg^{-1} \cdot mol$
15	0.552	$0.3062 \cdot kg^{-1} \cdot mol$	$24.91 \cdot kg^{-1} \cdot mol$
30	0.605	$0.6026 \cdot kg^{-1} \cdot mol$	$13.52 \cdot kg^{-1} \cdot mol$
45	0.657	$0.7262 \cdot kg^{-1} \cdot mol$	$8.77 \cdot kg^{-1} \cdot mol$
60	0.710	$0.7562 \cdot kg^{-1} \cdot mol$	$7.62 \cdot kg^{-1} \cdot mol$
75	0.762	$0.7621 \cdot kg^{-1} \cdot mol$	$7.39 \cdot kg^{-1} \cdot mol$
90	0.815	$0.7576 \cdot kg^{-1} \cdot mol$	$7.56 \cdot kg^{-1} \cdot mol$
100	0.850	$0.7518 \cdot kg^{-1} \cdot mol$	$7.79 \cdot kg^{-1} \cdot mol$

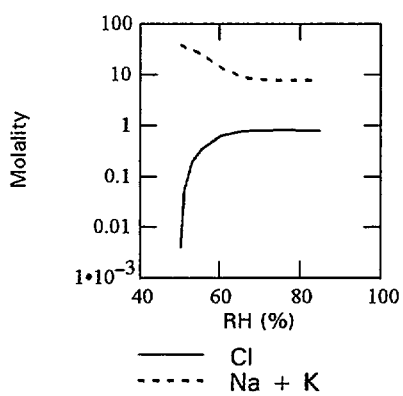

Low Relative Humidity (LRH) Salts Model Calculations
(fco2 = 1e-3)

Conceptual Model. Water seeps into "reactor" (i.e, drip shield or backfill) at a constant rate during the boiling period. In the reactor, seepage water vaporizes and salts accumulate. Salts begin to dissolve when the relative humidity rises above 50%. This model (LRH) approximates the buildup and dissolution of soluble salts in the Na-K-N-S-Cl-C system. All fluid (brine) generated during each time interval flows out of reactor at the end of each time interval; however, mixing is allowed between half time intervals. The end point is designed to be equivalent to the evaporative evolution of seepage water to a stoichiometric ionic strength of 10 molal, as calculated using the EQ3/6 Pitzer model. The LRH salts model is a simplified approximation of salt accumulation and eventual dissolution caused by increasing relative humidity. It maintains mass and charge balance and estimates brine generation as a function of effective solubilities. Its purpose is to provide bounding and scoping calculations for an evaporite system that is has not been deeply studied.

Seepage - Constant rate and constant composition are assumed.

Seepage Name:

$s := \text{"avg. J-13"}$

	Seepage Comp. (molal)	Valency	Seepage Rate
NO3	$Cs_1 := 0.000142 \cdot mol \cdot kg^{-1}$	$z_1 := 1$	$Qs := 1 \cdot \frac{kg}{yr}$
Cl	$Cs_2 := 0.00020 \cdot mol \cdot kg^{-1}$	$z_2 := 1$	
SO4	$Cs_3 := 0.00019 \cdot mol \cdot kg^{-1}$	$z_3 := 2$	
Soluble CO3	$Cs_4 := 0.00062 \cdot mol \cdot kg^{-1}$	$z_4 := 1.33$	Cs_4 is adjusted to achieve a Na:CO_3 ratio equivalent to the final I=10m solution calculated from the EQ3/6 Pitzer model. *Soluble CO_3* represents the CO_3 fraction that precipitates with Na or K.
K	$Cs_6 := 0.00013 \cdot mol \cdot kg^{-1}$	$z_6 := 1$	
Na	$Cs_7 := 0.0020 \cdot mol \cdot kg^{-1}$	$z_7 := 1$	

CO_2 (g) Fugacity:

$CO_2 := 1 \cdot 10^{-3}$

Charge Balance Error

$$E := \frac{\sum_{i=6}^{7} Cs_i \cdot z_i - \sum_{i=1}^{4} Cs_i \cdot z_i}{\sum_{i=1}^{7} Cs_i \cdot z_i}$$

$E = 0.159$
$E = 15.87 \cdot \%$

This charge balance error is maintained for the entire calculation.

Period 1 - Dry Conditions. Salts accumulate. No stable brine is generated. Period ends when relative humidity (RH) rises to level where nitrate salts are no longer stable.

Time Nitrate Salts Become Unstable: $t50 := 200 \cdot yr$ (time when RH exceeds ~50%)

$i := 1 .. 7$

	Total Accumulation in Period 1		Molecular Weight
NO3	$Mst_{i,0} := Cs_i \cdot Qs \cdot t50$	$Mst_{1,0} = 0.028 \cdot mol$	$W_1 := 62 \cdot gm \cdot mol^{-1}$
Cl		$Mst_{2,0} = 0.04 \cdot mol$	$W_2 := 35.5 \cdot gm \cdot mol^{-1}$
SO4		$Mst_{3,0} = 0.038 \cdot mol$	$W_3 := 96 \cdot gm \cdot mol^{-1}$
Soluble CO3		$Mst_{4,0} = 0.124 \cdot mol$	$W_4 := 60 \cdot gm \cdot mol^{-1}$
K		$Mst_{6,0} = 0.026 \cdot mol$	$W_6 := 39 \cdot gm \cdot mol^{-1}$
Na		$Mst_{7,0} = 0.4 \cdot mol$	$W_7 := 23 \cdot gm \cdot mol^{-1}$

Period 2 - Wet Conditions. Nitrate salts are unstable. Water vapor condenses to form nitrate brine. Soluble salts begin to dissolve as RH increases and completely dissolve by the end of the period.

Time Discretization in Period 2

End of Period 2 at 85% RH	$t85 := 1100 \cdot yr$	RH reaches 85% at about 980 years. At RH 85%, soluble salts are dissolved and I = ~10m because the activity of water at I=~10m is approximately 0.85.	
Time Increments in Period 2	$j := 0 .. 100$	Specific Times of Increments	$t_j := t50 + (t85 - t50) \cdot \frac{j}{100}$
Constant Time Increment	$delt := t_1 - t_0$	$delt = 9 \cdot yr$	

Salt Solubilities

		Effective Solubility at 100'C (molal)		
NO3		$S_1 := 24.5 \cdot mol \cdot kg^{-1}$	(pure phase solubility at 100'C for KNO_3)	
Other Salts	$k := 2 .. 4$	$S_k := 3.6 \cdot mol \cdot kg^{-1}$	(assumed "effective" solubility to match EQ6 model results - "effective" due to mixture of salts)	
Mass of Total Condensed Water at Start of Period 2		$mw_1 := \frac{Mst_{1,0}}{S_1}$	$mw_1 = 1.159 \cdot 10^{-3} \cdot kg$	(assumes accumulated nitrate salts dissolve to solubility)

Fraction of Soluble Salts Dissolved. While NO3 salts are assumed to dissolve completely at the beginning of Period 2, the other salts are assumed to dissolve increasingly as relative humidity increases over time.

Percentages of Salts Dissolved in Period 2

System	Assumptions	Percentage of Salts Dissolved at Start of Period 2	Percentage Salts Dissolved at End of Period 2
K-Na-NO3	NO3 salts are 100% dissolved at all times in Period 2.	$f1_1 := 100 \cdot \%$ $k := 1 .. 2$	$f1_2 := 100 \cdot \%$
K-Na-Cl-SO4-CO3 $j := 1 .. 100$	$ff_j := 10^{\frac{4 \cdot (t_j - t85)}{t85 - t50}}$ Percentage dissolved within reactor assumed to increase exponentially from 0% to 100% within Period 2.		

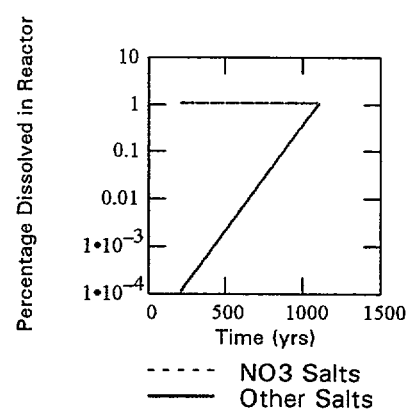

Percentages of Salts Dissolved

		Initial Percentage Dissolved Within Reactor	Percentage Dissolved Within Reactor	
$i := 1 .. 6$				
NO3		$f_{1,0} := 0$	$f_{1,j} := f1_1$	(Na percentage calculated by charge balance later.)
Other Anions	$k := 2 .. 4$	$f_{k,0} := 0$	$f_{k,j} := ff_j$	
K		$f_{6,0} := 0$	$f_{6,j} := f1_1$	

Period 2 Calculations

Incoming Seepage $\quad i := 1..7 \quad j := 1..100$

Moles Added to Reactor in Incoming Seepage During Time Increment $\quad Ms_i := Cs_i \cdot Qs \cdot delt$

Cumulative Moles in Incoming Seepage $\quad Mst_{i,j} := Mst_{i,j-1} + Ms_i$

Reactor Calculations $\quad i := 1..6 \quad k := 1..200$

Moles in Reactor at Each Half *delt* Increment = (previous moles) + (seepage moles) - (runoff moles)

$Mrh_{i,0} := Mst_{i,0}$(initial moles) $\quad Mrh_{i,k} := Mrh_{i,k-1} + \frac{1}{2} \cdot Ms_i - \frac{1}{2} \cdot Mrh_{i,k-1} \cdot f_{i,floor\left(\frac{k-1}{2}\right)}$

$j := 0..100$

Moles in Reactor at Time t_j $\quad Mr_{i,j} := Mrh_{i,j \cdot 2}$

Moles (Mass) of Dissolved Ions Generated at Time t_j $\quad Md_{i,j} := Mr_{i,j} \cdot f_{i,j}$

Dissolved Mass: $md_{i,j} := Md_{i,j} \cdot W_i$

Mass of Water in Brine Generated at Time t_j (calculated from anions)

$$mw_j := \sum_{i=1}^{4} \frac{Md_{i,j}}{S_i}$$

Dissolved Concentration at Time t_j

$$C_{i,j} := \frac{Md_{i,j}}{mw_j}$$

Na Moles in Reactor (calculated by charge balance, includes charge imbalance error term)

$$Mr_{7,j} := \sum_{i=1}^{4} Mr_{i,j} \cdot z_i - Mr_{6,j} \cdot z_6 + E \cdot \sum_{i=1}^{4} 2 \cdot Mr_{i,j} \cdot z_i \cdot (1 + E)$$

Na Dissolved Concentration (calculated by charge balance, includes charge imbalance error term)

$$C_{7,j} := \sum_{i=1}^{4} C_{i,j} \cdot z_i - C_{6,j} \cdot z_6 + E \cdot \sum_{i=1}^{4} 2 \cdot C_{i,j} \cdot z_i \cdot (1 + E)$$

Dissolved Moles (Mass) of Na in Reactor (calculated by charge balance, includes charge imbalance error term)

$$Md_{7,j} := \sum_{i=1}^{4} Md_{i,j} \cdot z_i - Md_{6,j} \cdot z_6 + E \cdot \sum_{i=1}^{4} 2 \cdot Md_{i,j} \cdot z_i \cdot (1 + E)$$

Percentage Na Dissolved in Reactor $\quad f_{7,j} := \frac{C_{7,j} \cdot mw_j}{Mr_{7,j}}$

Dissolved Mass: $md_{7,j} := Md_{7,j} \cdot W_7$

Cumulative Water Runoff $\quad j := 1..100 \quad mwt_0 := 0 \cdot kg \quad mwt_j := mwt_{j-1} + mw_j$

Cumulative Mass of Total Dissolved Solids Generated at Time tt_j $\quad mdt_0 := 0 \cdot kg \quad mdt_j := mdt_{j-1} + \sum_{i=1}^{4} md_{i,j} + \sum_{i=6}^{7} md_{i,j}$

j

Results i := 1 .. 7 j := 0 .. 100

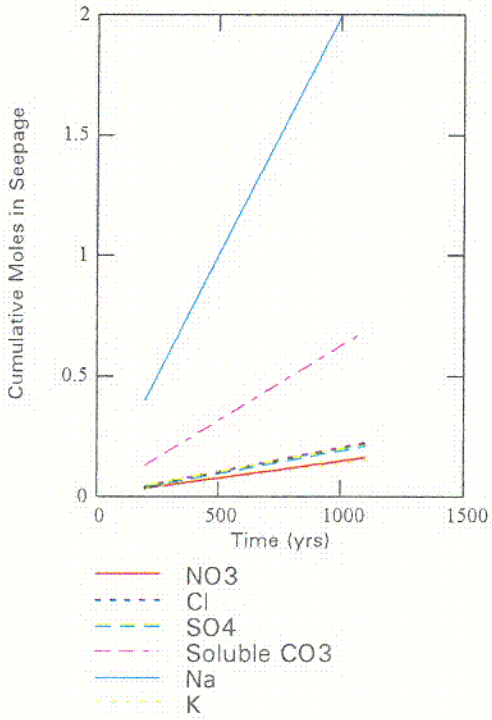

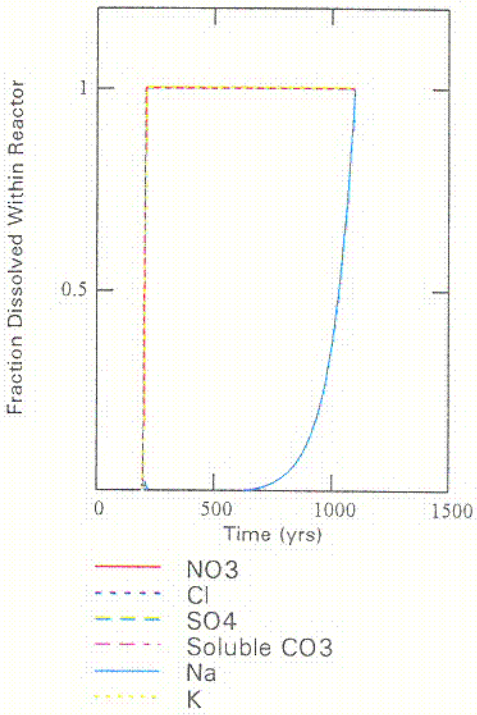

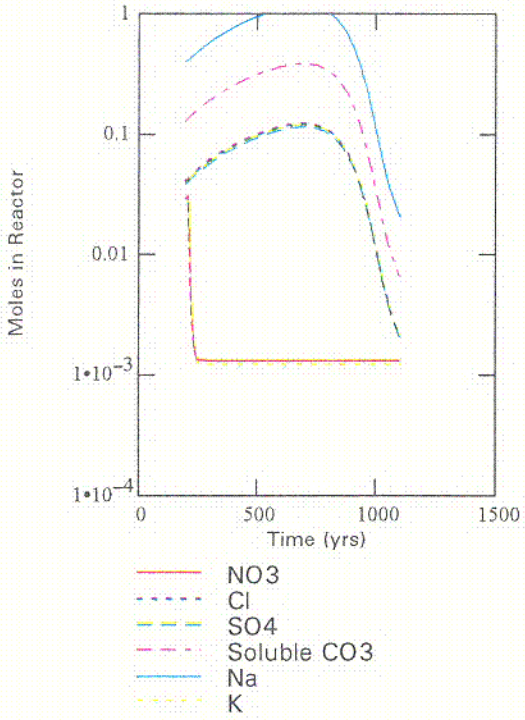

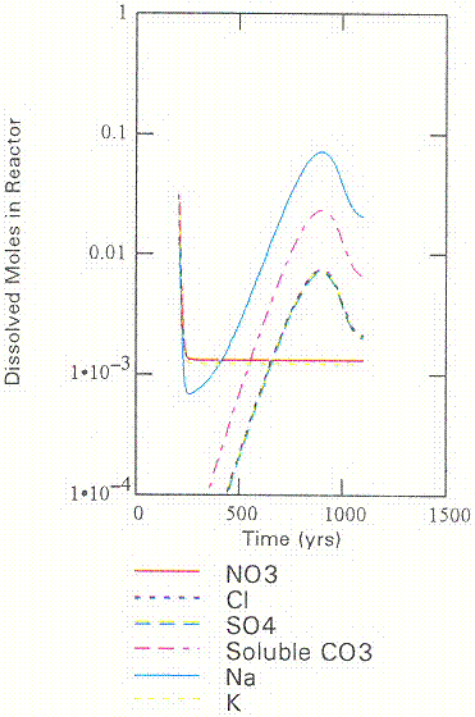

C-3

Solid-Phase (Undissolved)
Moles in Reactor over Time

$$Mu_{i,j} := Mr_{i,j} - Md_{i,j}$$

Note: Mp for NO3 and K is zero when RH exceeds 50%.

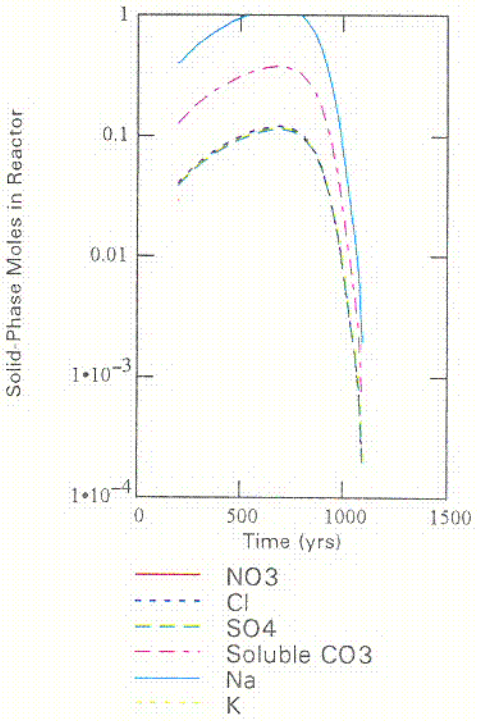

$j := 1 .. 100$

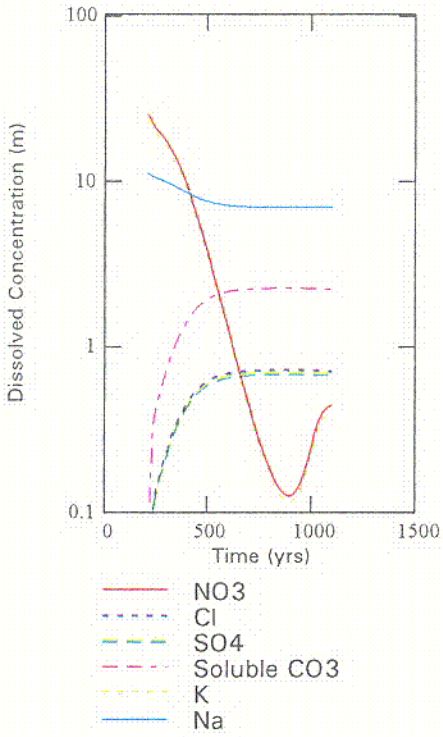

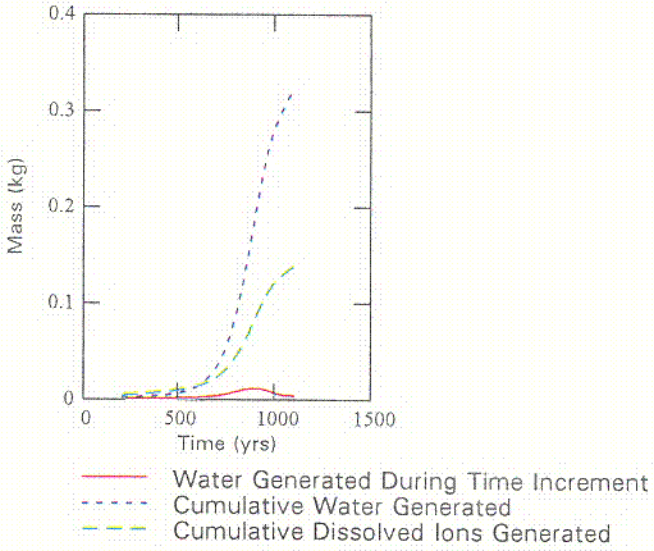

C-4

Summary and Cross-Check

	Concentrations at End of Period 2	Concentrations Calculated by EQ3/6 Model (I = 10 m)	Total Moles in Reactor at End of Period 2
NO3	$C_{1,100} = 0.432 \cdot mol \cdot kg^{-1}$	$0.50 \cdot mol \cdot kg^{-1}$	$Mr_{1,100} = 1.278 \cdot 10^{-3} \cdot mol$
Cl	$C_{2,100} = 0.7 \cdot mol \cdot kg^{-1}$	$0.71 \cdot mol \cdot kg^{-1}$	$Mr_{2,100} = 2.071 \cdot 10^{-3} \cdot mol$
SO4	$C_{3,100} = 0.665 \cdot mol \cdot kg^{-1}$	$0.68 \cdot mol \cdot kg^{-1}$	$Mr_{3,100} = 1.967 \cdot 10^{-3} \cdot mol$
Soluble CO3	$C_{4,100} = 2.171 \cdot mol \cdot kg^{-1}$	$2.23 \cdot mol \cdot kg^{-1}$	$Mr_{4,100} = 6.42 \cdot 10^{-3} \cdot mol$
K	$C_{6,100} = 0.396 \cdot mol \cdot kg^{-1}$	$0.46 \cdot mol \cdot kg^{-1}$	$Mr_{6,100} = 1.17 \cdot 10^{-3} \cdot mol$
Na	$C_{7,100} = 6.922 \cdot mol \cdot kg^{-1}$	$7.0 \cdot mol \cdot kg^{-1}$	$Mr_{7,100} = 0.02 \cdot mol$

Cumulative Mass of Dissolved Solids in Incoming Seepage at End of Period 2

$$\sum_{i=1}^{4} Mst_{i,100} \cdot W_i + \sum_{i=6}^{7} Mst_{i,100} \cdot W_i = 0.135 \cdot kg$$

Cumulative Mass of Dissolved Solids Generated at End of Period 2

$$mdt_{100} = 0.138 \cdot kg$$

Cumulative Mass of Water in Generated Brine at End of Period 2

$$mwt_{100} = 0.322 \cdot kg$$

Cumulative Mass of Brine Generated at End of Period 2

$$mwt_{100} + mdt_{100} = 0.46 \cdot kg$$

Charge Balance Error Maintained Over Time

$j := 1, 10 .. 100$

$$E_j := \frac{\sum_{i=6}^{7} C_{i,j} \cdot z_i - \sum_{i=1}^{4} C_{i,j} \cdot z_i}{\sum_{i=1}^{7} C_{i,j} \cdot z_i}$$

E_j
0.155
0.155
0.155
0.155
0.155
0.155
0.155
0.155
0.155
0.155
0.155
0.155

Output Files:

C:\..\lrh_t.xls	C:\..\lrh_c.xls	C:\..\lrh_mwt.xls	C:\..\lrh_mw.xls	C:\..\lrh_mdt.xls
$\frac{t}{yr}$	$C \cdot \frac{kg}{mol}$	$\frac{mwt}{kg}$	$\frac{mw}{kg}$	$\frac{mdt}{kg}$

C:\..\lrh_Mst.xls	C:\..\lrh_f.xls	C:\..\lrh_Mr.xls	C:\..\lrh_Md.xls	C:\..\lrh_Mu.xls
$\frac{Mst}{mol}$	f	$\frac{Mr}{mol}$	$\frac{Md}{mol}$	$\frac{Mu}{mol}$

Response Surface Calculations $j := 0 .. 100$

Relative humidity as a function of time (approximation)

$$RH_j := 0.5 + \left(\frac{t_j - t50}{t85 - t50}\right) \cdot 0.35$$

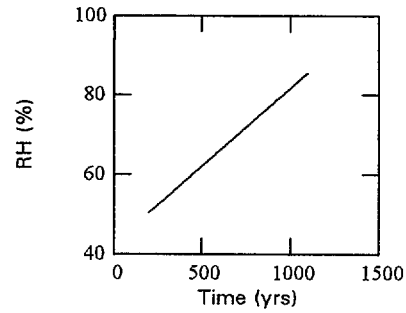

Evaluation points:

$j_1 := 1$ $j_2 := 3$ $j_3 := 9$ $j_4 := 15$ $j_5 := 30$

$j_6 := 45$ $j_7 := 60$ $j_8 := 75$ $j_9 := 90$ $j_{10} := 100$

$k := 1 .. 10$

Lookup Table for Given Seepage Composition

s = "avg. J-13"

$CO_2 = 1 \cdot 10^{-3}$

Input Parameter		Output Parameters	
	Relative Humidity	Cl Concentration	Na + K Concentration
j_k	RH_{j_k}	C_{2,j_k}	$C_{6,j_k} + C_{7,j_k}$
1	0.503	$3.7636 \cdot 10^{-3} \cdot kg^{-1} \cdot mol$	$33.37 \cdot kg^{-1} \cdot mol$
3	0.510	$0.0450 \cdot kg^{-1} \cdot mol$	$31.83 \cdot kg^{-1} \cdot mol$
9	0.531	$0.1831 \cdot kg^{-1} \cdot mol$	$26.66 \cdot kg^{-1} \cdot mol$
15	0.552	$0.2973 \cdot kg^{-1} \cdot mol$	$22.39 \cdot kg^{-1} \cdot mol$
30	0.605	$0.5690 \cdot kg^{-1} \cdot mol$	$12.23 \cdot kg^{-1} \cdot mol$
45	0.657	$0.6780 \cdot kg^{-1} \cdot mol$	$8.15 \cdot kg^{-1} \cdot mol$
60	0.710	$0.7041 \cdot kg^{-1} \cdot mol$	$7.18 \cdot kg^{-1} \cdot mol$
75	0.762	$0.7092 \cdot kg^{-1} \cdot mol$	$6.99 \cdot kg^{-1} \cdot mol$
90	0.815	$0.7053 \cdot kg^{-1} \cdot mol$	$7.13 \cdot kg^{-1} \cdot mol$
100	0.850	$0.7003 \cdot kg^{-1} \cdot mol$	$7.32 \cdot kg^{-1} \cdot mol$

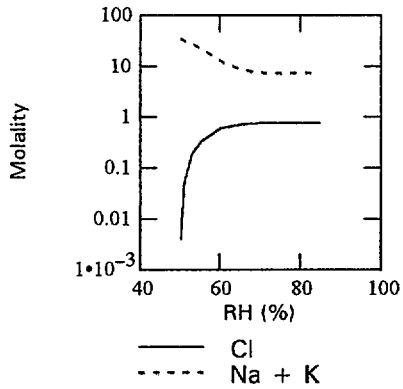

Low Relative Humidity (LRH) Salts Model Calculations
(fco2 = 1e-6)

Conceptual Model. Water seeps into "reactor" (i.e, drip shield or backfill) at a constant rate during the boiling period. In the reactor, seepage water vaporizes and salts accumulate. Salts begin to dissolve when the relative humidity rises above 50%. This model (LRH) approximates the buildup and dissolution of soluble salts in the Na-K-N-S-Cl-C system. All fluid (brine) generated during each time interval flows out of reactor at the end of each time interval; however, mixing is allowed between half time intervals. The end point is designed to be equivalent to the evaporative evolution of seepage water to a stoichiometric ionic strength of 10 molal, as calculated using the EQ3/6 Pitzer model. The LRH salts model is a simplified approximation of salt accumulation and eventual dissolution caused by increasing relative humidity. It maintains mass and charge balance and estimates brine generation as a function of effective solubilities. Its purpose is to provide bounding and scoping calculations for an evaporite system that is has not been deeply studied.

Seepage - Constant rate and constant composition are assumed.

Seepage Name:

$s := \text{"avg. J-13"}$

CO_2 (g) Fugacity:

$CO_2 := 1 \cdot 10^{-6}$

	Seepage Comp. (molal)	Valency	Seepage Rate
NO3	$Cs_1 := 0.000142 \cdot mol \cdot kg^{-1}$	$z_1 := 1$	$Qs := 1 \cdot \frac{kg}{yr}$
Cl	$Cs_2 := 0.00020 \cdot mol \cdot kg^{-1}$	$z_2 := 1$	
SO4	$Cs_3 := 0.00019 \cdot mol \cdot kg^{-1}$	$z_3 := 2$	
Soluble CO3	$Cs_4 := 0.00058 \cdot mol \cdot kg^{-1}$	$z_4 := 2$	
K	$Cs_6 := 0.00013 \cdot mol \cdot kg^{-1}$	$z_6 := 1$	
Na	$Cs_7 := 0.0020 \cdot mol \cdot kg^{-1}$	$z_7 := 1$	

Cs_4 is adjusted to achieve a Na:CO_3 ratio equivalent to the final I=10m solution calculated from the EQ3/6 Pitzer model. *Soluble CO_3* represents the CO_3 fraction that precipitates with Na or K.

Charge Balance Error

$$E := \frac{\sum_{i=6}^{7} Cs_i \cdot z_i - \sum_{i=1}^{4} Cs_i \cdot z_i}{\sum_{i=1}^{7} Cs_i \cdot z_i}$$

$E = 0.062$
$E = 6.18 \cdot \%$

This charge balance error is maintained for the entire calculation.

Period 1 - Dry Conditions. Salts accumulate. No stable brine is generated. Period ends when relative humidity (RH) rises to level where nitrate salts are no longer stable.

Time Nitrate Salts Become Unstable: $t50 := 200 \cdot yr$ (time when RH exceeds ~50%)

$i := 1..7$	Total Accumulation in Period 1		Molecular Weight
NO3	$Mst_{i,0} := Cs_i \cdot Qs \cdot t50$	$Mst_{1,0} = 0.028 \cdot mol$	$W_1 := 62 \cdot gm \cdot mol^{-1}$
Cl		$Mst_{2,0} = 0.04 \cdot mol$	$W_2 := 35.5 \cdot gm \cdot mol^{-1}$
SO4		$Mst_{3,0} = 0.038 \cdot mol$	$W_3 := 96 \cdot gm \cdot mol^{-1}$
Soluble CO3		$Mst_{4,0} = 0.116 \cdot mol$	$W_4 := 60 \cdot gm \cdot mol^{-1}$
K		$Mst_{6,0} = 0.026 \cdot mol$	$W_6 := 39 \cdot gm \cdot mol^{-1}$
Na		$Mst_{7,0} = 0.4 \cdot mol$	$W_7 := 23 \cdot gm \cdot mol^{-1}$

Period 2 - Wet Conditions. Nitrate salts are unstable. Water vapor condenses to form nitrate brine. Soluble salts begin to dissolve as RH increases and completely dissolve by the end of the period.

Time Discretization in Period 2

End of Period 2 at 85% RH	$t85 := 1100 \cdot yr$	RH reaches 85% at about 980 years. At RH 85%, soluble salts are dissolved and I = ~10m because the activity of water at I=~10m is approximately 0.85.	
Time Increments in Period 2	$j := 0 .. 100$	Specific Times of Increments	$t_j := t50 + (t85 - t50) \cdot \frac{j}{100}$
Constant Time Increment	$delt := t_1 - t_0$	$delt = 9 \cdot yr$	

Salt Solubilities

		Effective Solubility at 100'C (molal)	
NO3		$S_1 := 24.5 \cdot mol \cdot kg^{-1}$	(pure phase solubility at 100'C for KNO_3)
Other Salts	$k := 2 .. 4$	$S_k := 3.6 \cdot mol \cdot kg^{-1}$	(assumed "effective" solubility to match EQ6 model results - "effective" due to mixture of salts)
Mass of Total Condensed Water at Start of Period 2		$mw_1 := \frac{Mst_{1,0}}{S_1}$	$mw_1 = 1.159 \cdot 10^{-3} \cdot kg$ (assumes accumulated nitrate salts dissolve to solubility)

Fraction of Soluble Salts Dissolved. While NO3 salts are assumed to dissolve completely at the beginning of Period 2, the other salts are assumed to dissolve increasingly as relative humidity increases over time.

Percentages of Salts Dissolved in Period 2

System	Assumptions	Percentage of Salts Dissolved at Start of Period 2	Percentage Salts Dissolved at End of Period 2
K-Na-NO3	NO3 salts are 100% dissolved at all times in Period 2.	$f1_1 := 100 \cdot \%$ $k := 1 .. 2$	$f1_2 := 100 \cdot \%$
K-Na-Cl-SO4-CO3 $j := 1 .. 100$	$ff_j := 10^{\frac{4 \cdot (t_j - t85)}{t85 - t50}}$ Percentage dissolved within reactor assumed to increase exponentially from 0% to 100% within Period 2.		

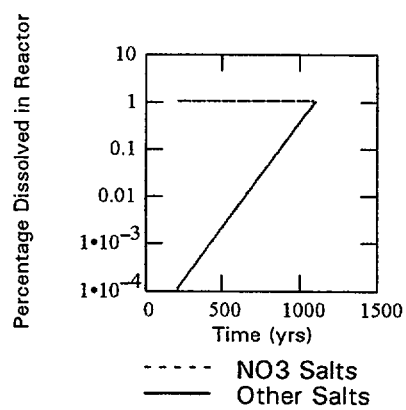

Percentages of Salts Dissolved

		Initial Percentage Dissolved Within Reactor	Percentage Dissolved Within Reactor	
$i := 1 .. 6$				
NO3		$f_{1,0} := 0$	$f_{1,j} := f1_1$	(Na percentage calculated by charge balance later.)
Other Anions	$k := 2 .. 4$	$f_{k,0} := 0$	$f_{k,j} := ff_j$	
K		$f_{6,0} := 0$	$f_{6,j} := f1_1$	

Period 2 Calculations

Incoming Seepage $i := 1..7$ $j := 1..100$

Moles Added to Reactor in Incoming Seepage During Time Increment $Ms_i := Cs_i \cdot Qs \cdot delt$

Cumulative Moles in Incoming Seepage $Mst_{i,j} := Mst_{i,j-1} + Ms_i$

Reactor Calculations $i := 1..6$ $k := 1..200$

Moles in Reactor at Each Half *delt* Increment = (previous moles) + (seepage moles) - (runoff moles)

$Mrh_{i,0} := Mst_{i,0}$(initial moles) $Mrh_{i,k} := Mrh_{i,k-1} + \frac{1}{2} \cdot Ms_i - \frac{1}{2} \cdot Mrh_{i,k-1} \cdot f_{i,floor\left(\frac{k-1}{2}\right)}$

$j := 0..100$

Moles in Reactor at Time t_j $Mr_{i,j} := Mrh_{i,j \cdot 2}$

Moles (Mass) of Dissolved Ions Generated at Time t_j $Md_{i,j} := Mr_{i,j} \cdot f_{i,j}$

Dissolved Mass: $md_{i,j} := Md_{i,j} \cdot W_i$

Mass of Water in Brine Generated at Time t_j (calculated from anions)

$$mw_j := \sum_{i=1}^{4} \frac{Md_{i,j}}{S_i}$$

Dissolved Concentration at Time t_j

$$C_{i,j} := \frac{Md_{i,j}}{mw_j}$$

Na Moles in Reactor (calculated by charge balance, includes charge imbalance error term)

$$Mr_{7,j} := \sum_{i=1}^{4} Mr_{i,j} \cdot z_i - Mr_{6,j} \cdot z_6 + E \cdot \sum_{i=1}^{4} 2 \cdot Mr_{i,j} \cdot z_i \cdot (1 + E)$$

Na Dissolved Concentration (calculated by charge balance, includes charge imbalance error term)

$$C_{7,j} := \sum_{i=1}^{4} C_{i,j} \cdot z_i - C_{6,j} \cdot z_6 + E \cdot \sum_{i=1}^{4} 2 \cdot C_{i,j} \cdot z_i \cdot (1 + E)$$

Dissolved Moles (Mass) of Na in Reactor (calculated by charge balance, includes charge imbalance error term)

$$Md_{7,j} := \sum_{i=1}^{4} Md_{i,j} \cdot z_i - Md_{6,j} \cdot z_6 + E \cdot \sum_{i=1}^{4} 2 \cdot Md_{i,j} \cdot z_i \cdot (1 + E)$$

Percentage Na Dissolved in Reactor

$$f_{7,j} := \frac{C_{7,j} \cdot mw_j}{Mr_{7,j}}$$

Dissolved Mass: $md_{7,j} := Md_{7,j} \cdot W_7$

Cumulative Water Runoff $j := 1..100$ $mwt_0 := 0 \cdot kg$ $mwt_j := mwt_{j-1} + mw_j$

Cumulative Mass of Total Dissolved Solids Generated at Time tt_j $mdt_0 := 0 \cdot kg$

$$mdt_j := mdt_{j-1} + \sum_{i=1}^{4} md_{i,j} + \sum_{i=6}^{7} md_{i,j}$$

j

Results i := 1.. 7 j := 0.. 100

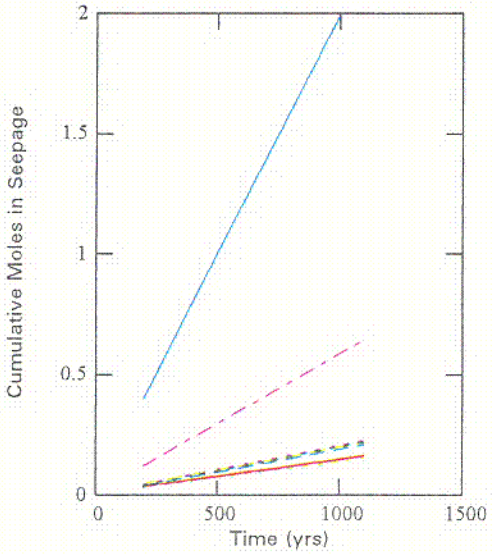

NO3
Cl
SO4
Soluble CO3
Na
K

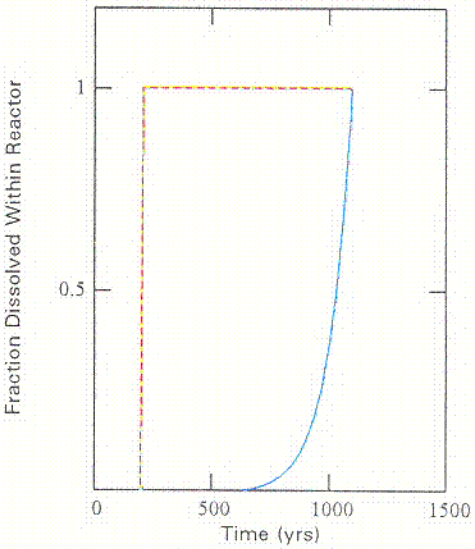

NO3
Cl
SO4
Soluble CO3
Na
K

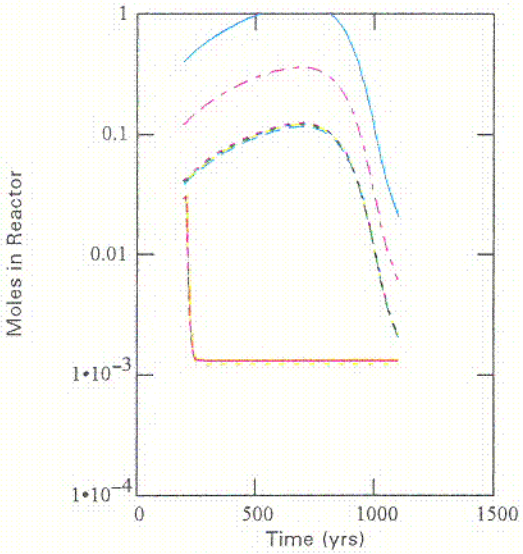

NO3
Cl
SO4
Soluble CO3
Na
K

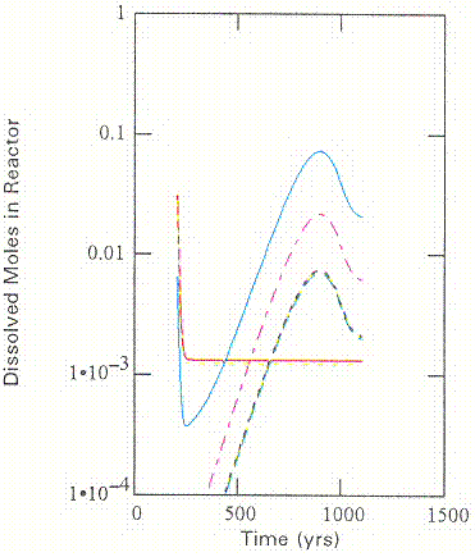

NO3
Cl
SO4
Soluble CO3
Na
K

C-5

Solid-Phase (Undissolved)
Moles in Reactor over Time

$$Mu_{i,j} := Mr_{i,j} - Md_{i,j}$$

Note: Mp for NO3 and K is zero when RH exceeds 50%.

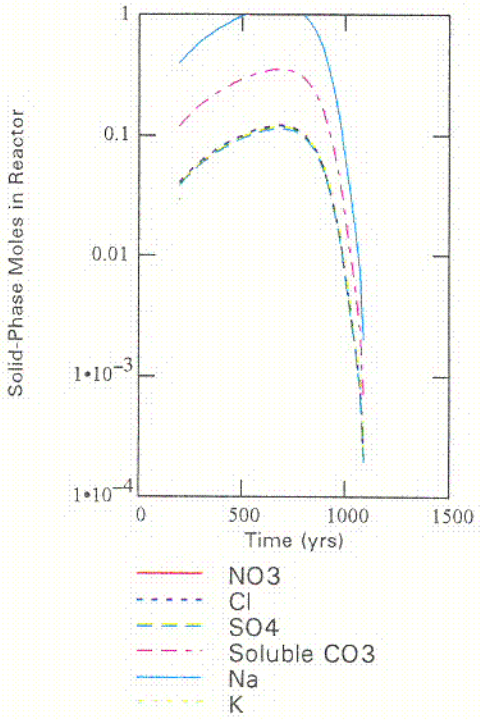

j := 1 .. 100

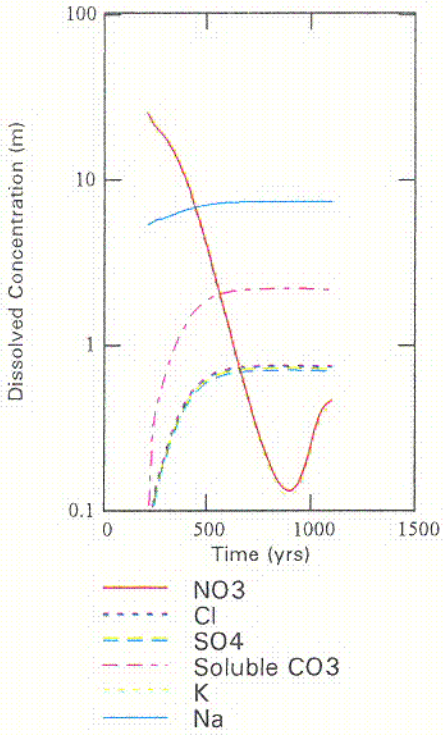

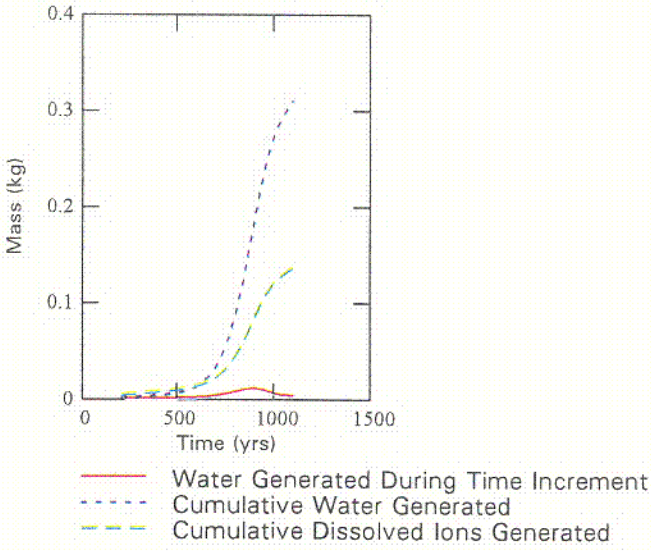

C-6

Summary and Cross-Check

	Concentrations at End of Period 2	Concentrations Calculated by EQ3/6 Model (I = 10 m)	Total Moles in Reactor at End of Period 2
NO3	$C_{1,100} = 0.45 \cdot mol \cdot kg^{-1}$	$0..50 \cdot mol \cdot kg^{-1}$	$Mr_{1,100} = 1.278 \cdot 10^{-3} \cdot mol$
Cl	$C_{2,100} = 0.729 \cdot mol \cdot kg^{-1}$	$0.71 \cdot mol \cdot kg^{-1}$	$Mr_{2,100} = 2.071 \cdot 10^{-3} \cdot mol$
SO4	$C_{3,100} = 0.692 \cdot mol \cdot kg^{-1}$	$0.68 \cdot mol \cdot kg^{-1}$	$Mr_{3,100} = 1.967 \cdot 10^{-3} \cdot mol$
Soluble CO3	$C_{4,100} = 2.113 \cdot mol \cdot kg^{-1}$	$2.02 \cdot mol \cdot kg^{-1}$	$Mr_{4,100} = 6.006 \cdot 10^{-3} \cdot mol$
K	$C_{6,100} = 0.412 \cdot mol \cdot kg^{-1}$	$0.46 \cdot mol \cdot kg^{-1}$	$Mr_{6,100} = 1.17 \cdot 10^{-3} \cdot mol$
Na	$C_{7,100} = 7.268 \cdot mol \cdot kg^{-1}$	$7.0 \cdot mol \cdot kg^{-1}$	$Mr_{7,100} = 0.021 \cdot mol$

Cumulative Mass of Dissolved Solids in Incoming Seepage at End of Period 2

$$\sum_{i=1}^{4} Mst_{i,100} \cdot W_i + \sum_{i=6}^{7} Mst_{i,100} \cdot W_i = 0.132 \cdot kg$$

Cumulative Mass of Dissolved Solids Generated at End of Period 2

$$mdt_{100} = 0.135 \cdot kg$$

Cumulative Mass of Water in Generated Brine at End of Period 2

$$mwt_{100} = 0.310 \cdot kg$$

Cumulative Mass of Brine Generated at End of Period 2

$$mwt_{100} + mdt_{100} = 0.445 \cdot kg$$

Charge Balance Error Maintained Over Time

$j := 1, 10 .. 100$

$$E_j := \frac{\sum_{i=6}^{7} C_{i,j} \cdot z_i - \sum_{i=1}^{4} C_{i,j} \cdot z_i}{\sum_{i=1}^{7} C_{i,j} \cdot z_i}$$

E_j
0.062
0.062
0.062
0.062
0.062
0.062
0.062
0.062
0.062
0.062
0.062
0.062

Response Surface Calculations $j := 0 .. 100$

Relative humidity as a function of time (approximation)

$$RH_j := 0.5 + \left(\frac{t_j - t50}{t85 - t50}\right) \cdot 0.35$$

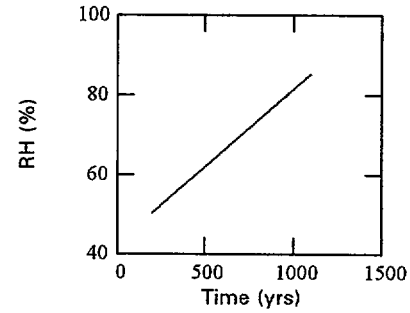

Evaluation points:

$j_1 := 1$ $j_2 := 3$ $j_3 := 9$ $j_4 := 15$ $j_5 := 30$

$j_6 := 45$ $j_7 := 60$ $j_8 := 75$ $j_9 := 90$ $j_{10} := 100$

$k := 1 .. 10$

Lookup Table for Given Seepage Composition

s = "avg. J-13"

$CO_2 = 1 \cdot 10^{-6}$
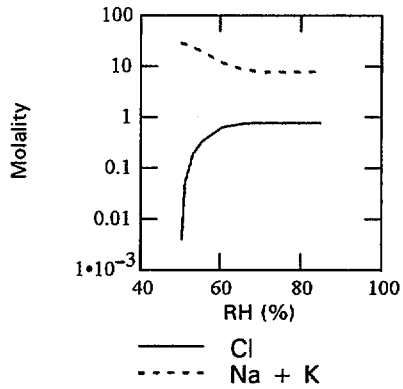
Input Parameter		Output Parameters	
	Relative Humidity	Cl Concentration	Na + K Concentration
j_k	RH_{j_k}	C_{2,j_k}	$C_{6,j_k} + C_{7,j_k}$
1	0.503	$3.7644 \cdot 10^{-3} \cdot kg^{-1} \cdot mol$	$27.61 \cdot kg^{-1} \cdot mol$
3	0.510	$0.0451 \cdot kg^{-1} \cdot mol$	$26.48 \cdot kg^{-1} \cdot mol$
9	0.531	$0.1850 \cdot kg^{-1} \cdot mol$	$22.63 \cdot kg^{-1} \cdot mol$
15	0.552	$0.3023 \cdot kg^{-1} \cdot mol$	$19.40 \cdot kg^{-1} \cdot mol$
30	0.605	$0.5876 \cdot kg^{-1} \cdot mol$	$11.56 \cdot kg^{-1} \cdot mol$
45	0.657	$0.7045 \cdot kg^{-1} \cdot mol$	$8.34 \cdot kg^{-1} \cdot mol$
60	0.710	$0.7327 \cdot kg^{-1} \cdot mol$	$7.57 \cdot kg^{-1} \cdot mol$
75	0.762	$0.7383 \cdot kg^{-1} \cdot mol$	$7.42 \cdot kg^{-1} \cdot mol$
90	0.815	$0.7341 \cdot kg^{-1} \cdot mol$	$7.53 \cdot kg^{-1} \cdot mol$
100	0.850	$0.7286 \cdot kg^{-1} \cdot mol$	$7.68 \cdot kg^{-1} \cdot mol$